The role of DNA methylation in the regulation of depot-specific gene expression in human adipose tissue

Nathan Denton

Brasenose College

MSc (by research) in Clinical Medicine

Trinity term 2013

The role of DNA methylation in the regulation of depot-specific gene expression in human subcutaneous adipose tissue

Nathan Denton, Brasenose College, MSc (by research) in Clinical Medicine

Adipose tissue is not homogenous as individual fat depots display regional variation in their physiological properties. It follows that body fat distribution is increasingly being recognised as a major determinant of metabolic disease risk. At the cellular level, depot-specific properties are exhibited by adipocyte precursors during *in vitro* culture and persist for many generations, suggesting these cells retain an 'intrinsic memory' of their anatomical origin which is epigenetic in nature. A primary aim was to identify depot-specific genes whose expression may be regulated by DNA methylation in adipose precursors.

Using two paired preadipocyte cell lines derived from human subcutaneous abdominal and gluteal adipose tissue - to represent upper and lower body fat with their opposing associations with cardiovascular disease and diabetes respectively - depot-specific gene expression and DNA methylation profiles were detected. Furthermore, the expression of certain genes in preadipocytes was found to change in response to treatment with the DNA demethylating agent 5-azacytidine, which suggests DNA methylation may regulate depot-specific gene expression. A secondary aim was to investigate whether glucocorticoids – which are important determinants of body fat distribution – exert their effects through DNA methylation. The synthetic glucocorticoid dexamethasone was found to modulate the expression of some of the differentially expressed genes in preadipocytes, with this effect possibly being mediated by DNA methylation. It has been postulated that depot-specific phenotypes in adipose tissue may arise from developmental differences. Several genes were found to be expressed in a depot-specific fashion during a differentiation time course, suggesting regional variation in adipogenesis may contribute to the generation of depot-specific phenotypes.

Overall, the data presented suggests regional variation within subcutaneous white adipose tissue exists and supports the notion that DNA methylation patterns can, in part, determine adipose tissue heterogeneity.

Contents

Figures

Tables

1 Introduction

Introduction

1.1 Introduction

Adipose tissue plays a critical role in energy homeostasis and is far more than just a passive repository for excess energy. Furthermore, adipose tissue is heterogeneous, with individual fat depots displaying regional variation in their physiological properties. In support of this regional heterogeneity, depot-specific gene expression profiles have been observed at the tissue and cellular level. There is mounting evidence to suggest epigenetic modifications, such as DNA methylation, are involved in regulating regional gene expression as well as the development of functionally distinct adipose tissue depots. Understanding the regional properties of adipose tissue is important as body fat distribution is being increasingly recognised as a major determinant of metabolic health.

In this chapter, the functional biology of adipose tissue and its development will be discussed before body fat distribution and the epidemiological evidence indicating the protective role that lower body fat accumulation exerts on metabolic disease risk are considered. The regional properties of adipose tissue, in addition to the factors which influence body fat distribution, are then discussed. Finally, the various epigenetic mechanisms involved in regulating gene expression, with a focus on DNA methylation, and their contribution to body fat distribution are also explored.

1.2 Adipose tissue biology

The adipose tissue pool in mammals comprises at least two functionally and morphologically distinct types of fat - white and brown – that together form the 'adipose organ' (Cinti, S. *et al* 2001). White adipose tissue (WAT) plays a key role in regulating energy homeostasis; it primarily acts as a long-term store of energy (in the form of energy-

dense triglycerides) but is also a source of many hormones (so-called adipokines) and cytokines that modulate whole body metabolism, appetite, and insulin sensitivity (Rosen, E. D. *et al* 2006). WAT can also provide mechanical protection for soft organs as well as thermal insulation (Trayhurn, P. 2007). Brown adipose tissue is highly specialised for heat production through the process of non-shivering thermogenesis (Hassan, K. *et al* 2012).

1.2.1 Composition of white adipose tissue

White adipose tissue is a type of loose connective tissue in which lipid-laden adipocytes are held in a network of collagen fibres. Several cell types reside within WAT in addition to adipocytes which are known collectively as stromovascular cells. These include fibroblasts, endothelial cells, infiltrated leukocytes and macrophages, multipotent stem cells, and preadipocytes; the latter are committed to the adipose lineage but are yet to be recruited for differentiation and lipid accumulation. Most stromovascular cells - except preadipocytes - do not participate in the lipid handling activities of WAT but some can secrete bioactive peptides and contribute to its endocrine role (Galic, S. e*t al* 2010).

An important component of WAT is the extracellular matrix (ECM) which is a collagenous network that provides mechanical strength to adipose tissue by acting as an external scaffold to protect the lipid droplet from disruption by physical forces (Mariman, E. C. *et al* 2010). There is mounting evidence suggesting the ECM plays an important role in co-ordinating preadipocyte differentiation (i.e. adipogenesis) as well as cellular turnover and vascularisation of WAT (Divoux, A. *et al* 2011). Therefore, ECM composition and structure in adipose tissue may contribute to metabolic health.

1.2.2 Regional white adipose tissue depots

White adipose tissue is located throughout the body; under the skin (subcutaneous), around internal organs (visceral), in bone marrow (yellow bone marrow), and in breast tissue. In a healthy individual approximately 80 – 90% of total body fat is stored just underneath the skin surrounding the abdominal (waist), sub-scapular (upper back), gluteal (buttock), and femoral (thigh) areas. Visceral fat, on the other hand, accounts for 6 – 20% of total body fat and comprises the omental and mesenteric depots that surround the digestive organs (Gesta, S. *et al* 2007). The various fat depots are depicted in figure 1.1.

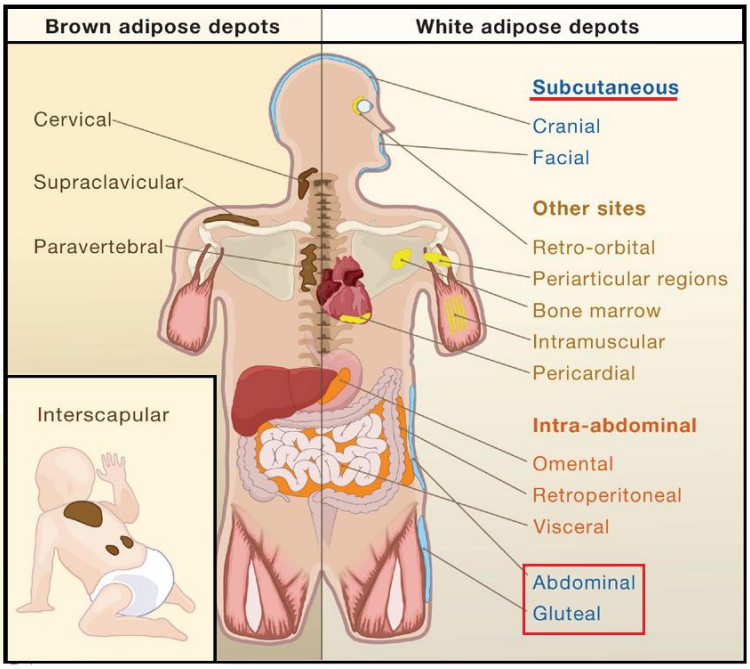

Figure 1.1 – *Fat distribution in humans.* The fat depots important to this project, principally subcutaneous abdominal and gluteal adipose tissue, are highlighted by the red box. Diagram adapted from Gesta, S. *et al* 2007

A key anatomical consideration regarding visceral fat is that its blood supply drains into the portal vein, meaning the liver is directly exposed to products released by these depots (i.e. non-esterified fatty acids and adipokines) which haven't undergone prior 'dilution' by the systemic circulation. This means adipokines derived from this depot may exert a

disproportionate influence on hepatic function; this idea and its (patho)physiological implications are somewhat controversial though (Frayn, K. 2000).

1.2.3 White adipose tissue function: fatty acid metabolism

The major metabolic role of WAT is the controlled storage and release of fat, which is stored in adipocytes as triglyceride (TAG) and released into the systemic circulation as non-esterified fatty acids (NEFAs). Both are multi-step processes which are tightly regulated and highly co-ordinated so the body's energy requirements can be met efficiently. Metabolic flux can range from fatty acid storage in the post-prandial state to fatty acid mobilisation during fasting. It is generally thought that subcutaneous (abdominal) WAT acts as a buffer against the daily influx of dietary lipids to protect extra-adipose tissues from lipid overflow and the deleterious effects of 'lipotoxicity' (Frayn, K. 2002); this function is analogous to the role of the liver in glucose homeostasis.

As TAGs are hydrophobic they are transported in lipoprotein particles. These particles are too large to escape from the capillaries into the interstitial fluid so adipocytes cannot take their lipid load up directly. Adipocytes therefore rely on lipoprotein lipase (LPL) to hydrolyse circulating lipoprotein-TAG and take up liberated NEFAs which enter the interstitial fluid. Locally produced NEFAs generate a concentration gradient which favours their entry into adipocytes (Frayn, K. *et al* 1994), although not all are taken up; some enter the systemic circulation and are referred to as 'spillover fatty acids' (Frayn, K. *et al* 1995).

Once the NEFAs enter the interstitial fluid and are taken up by the adipocyte, they are 'trapped' by the formation of an acyl-CoA derivative before undergoing re-esterification with glycerol-3-phosphate (generated by glycolysis). This process reforms TAGs which join the lipid droplet for storage (Frayn, K. *et al* 2003). During the post-prandial period, insulin secretion increases and stimulates the activity (and expression) of LPL (Frayn, K.

et al 1994) and the enzymes involved in re-esterification (Coleman, R. A. *et al* 2004) whilst simultaneously suppressing TAG hydrolysis (Coppack, S. W. *et al* 1989). Together, insulin's actions shift fatty acid flux in favour of storage.

Stored fat can be mobilised by hydrolysis (lipolysis) of TAGs by the sequential action of several lipases. The liberated NEFAs are released into the circulation and carried in the plasma bound to albumin. A single TAG is hydrolysed to generate diacylglycerol (DAG) plus one NEFA by adipose triacylglycerol lipase (Zimmermann, R. *et al* 2004). A second NEFA is released by hormone-sensitive lipase acting on the DAG, whose activity can be stimulated by catabolic hormones such as epinephrine (Rizack, M. 1961) and corticotropin (Hollenburg, C. H. *et al* 1961). The last fatty acid is liberated from the remaining monoacylglycerol (MAG) by MAG lipase (Watt, M. J. *et al* 2008).

1.2.4 White adipose tissue as an endocrine organ: bioactive peptide secretion

In addition to releasing NEFAs, white adipocytes secrete adipokines involved in regulating appetite, lipid metabolism, glucose homeostasis, angiogenesis, vascular haemostasis, and immune system activity. The idea that a circulating 'factor' could convey information regarding peripheral energy status to the central nervous system was first proposed after the results of parabiosis studies performed in the 1970s (Coleman, D. L. 1973). However, it took several decades to identify the molecule responsible for the intriguing results of the parabiosis studies; leptin was discovered after positional cloning of the same inbred strains of mice predisposed to extreme obesity and / or type 2 diabetes mellitus (T2DM) used by Coleman in the 1970s (Zhang, Y. *et al* 1994).

A host of other bioactive peptides in addition to leptin are secreted by WAT (Raucci, R. *et al* 2013). For instance, WAT can secrete various pro-inflammatory cytokines such as

interleukin-6 (McGuinness, O. P. 2007) and monocyte chemoattractant protein-1 (Kanda, H. *et al* 2006), both of which have been associated with metabolic disease.

WAT also secretes adiponectin, a molecule which exerts insulin-sensitising effects (Maeda, N. *et al* 2002) and may provide a mechanistic link between lower body fat accumulation and higher insulin sensitivity (Buemann, B. *et al* 2005). Furthermore, secreted frizzled-related protein 5 (Sfrp5) is an anti-inflammatory adipokine whose expression and secretion has been found to be perturbed in mouse models of obesity and T2DM (Ouchi, N. *et al* 2010).

1.2.5 White adipose tissue as an endocrine organ: steroid hormone metabolism

WAT also possesses the full complement of enzymes required for the activation, interconversion, and inactivation of sex steroid hormones (Meseguer, A. *et al* 2002). This property has been known for several decades (Siiteri, P. K. 1987) and predates the identification of any bioactive peptides. The contribution made by adipose tissue to whole body sex steroid metabolism can be significant. For instance, most of the circulating oestrogen in post-menopausal women is produced in peripheral tissues, principally WAT (Grodin, J. M. *et al* 1973). The role that sex steroids play in influencing the distribution of fat throughout the body will be discussed in greater detail in section 1.6.1.

Adipose tissue is also a key site of glucocorticoid metabolism. WAT expresses 11β-hydroxysteroid dehydrogenase 1 (11β-HSD1), an enzyme which catalyses the conversion of biologically inactive cortisone (in humans) into biologically active cortisol (in humans). However, cortisol generated within WAT by 11β-HSD1 only acts locally and does not contribute significantly to the general circulation. Dysregulation of 11β-HSD1 has been associated with a variety of metabolic disturbances such as obesity, T2DM, hypertension, dyslipidaemia, and polycystic ovary syndrome (Pereira, C. D. *et al* 2012). Selective

inhibitors of 11β-HSD1 are currently under development as a treatment for metabolic diseases like T2DM (Wang, M. 2011). Glucocorticoids are important regulators of body fat distribution and metabolic health and are discussed further in section 1.6.2.

1.3 Development of white adipose tissue

The first lobules of fat start to develop between weeks 14 to 16 of gestation in humans, with fat being detected at all predicted subcutaneous and visceral WAT depots by week 28 (Poissonnet, C. M. *et al* 1984). White adipocytes are generally thought to be mesodermal in origin (Gesta, S. *et al* 2007), although this is most likely an oversimplification; a subset of white adipocytes which developed from neural crest stem cells have been identified in mice (Billon, N. *et al* 2007).

1.3.1 Commitment to the adipose lineage

Adipocyte progenitors derive from mesenchymal stem cells (MSCs); such cells are devoid of lipid but are committed to the adipocyte lineage and so are regarded as 'preadipocytes' (Gesta, S. *et al* 2007). MSCs are multipotent cells that reside in the mesoderm of the developing embryo and are capable of differentiating into adipocytes, myocytes, osteoblasts, or chondrocytes.

Substantial progress has been made in the past few years with regards to understanding the process of commitment to the adipose lineage. For instance, several molecular markers were discovered that permitted the identification of preadipocytes within the stromovascular fraction of adipose tissue (Rodeheffer, M. S. *et al* 2008). Indeed, this cell population displayed an adipogenic capability as functional adipose tissue developed when it was infused into lipodystrophic A-Zip mice (i.e. they lack adipose tissue).

Mounting evidence suggests the committed preadipocyte population derives from the vasculature supplying the adipose tissue, with preadipocytes probably being endothelial in nature. Indeed, when a transgenic mouse was engineered to irreversibly express a reporter gene under control of the peroxisome proliferator-activated receptor gamma (PPARγ) promoter - which is necessary and sufficient for adipogenesis (Rosen, E. D. *et al* 1999) - it was found that most adipocytes derived from a pool of proliferating progenitor cells residing in the adipose tissue vasculature (Tang, W. *et al* 2008).

A recent series of papers has implicated *Zfp423*, a zinc finger transcription factor, as a molecular component involved in determining the fate of adipose progenitors. It has been reported that preadipocytes, but not primary muscle tissue (another mesenchymal cell type), highly express this gene. Furthermore, ectopic expression of *Zfp423* in non-adipogenic NIH 3T3 fibroblasts resulted in robust expression of *PPARγ* (indicating it acts upstream of *PPARγ*) and rendered such cells able to undergo adipogenesis. In addition, white and brown adipogenesis were markedly impaired in *Zfp423* knockout mice (Gupta, R. K. *et al* 2010).

By driving green fluorescent protein (GFP) expression under the control of the *Zfp423* promoter in transgenic mice Gupta *et al* identified a population of perivascular cells within subcutaneous and visceral fat depots which could undergo robust adipogenesis *in vitro* (Gupta, R. K. *et al* 2012). Tran *et al* also identified a subset of vascular endothelial cells of human adipose tissue capillaries which expressed *Zfp423*; activation of PPARγ in these cells resulted in loss of their endothelial phenotype followed by the formation of mature adipocytes which accumulated lipid (Tran, K. V. *et al* 2012).

The evidence concerning the role of *Zfp423* also provides insight into the potential mechanisms involved in adipose expansion. As adipocyte progenitors appear to reside in

the vasculature, this suggests adipogenesis and angiogenesis are intimately linked which provides a neat mechanism that may explain how expanding adipose tissue is vascularised.

Other data has indicated that *in utero* expression of *Zfp423* is regulated by epigenetic mechanisms which can be modulated by maternal obesity. Maternal obesity predisposes offspring to the development of obesity and T2DM (Heerwagen, M. *et al* 2010). Using a rat model of maternal obesity it has been found that *Zfp423* expression is enhanced in foetal tissue obtained from obese dams, which was associated with decreased methylation of the *Zfp423* promoter (Borengasser S. J. *et al* 2013). These results have been replicated in a mouse model of maternal obesity (Yang, Q. Y. *et al* 2013). Such findings implicate epigenetic mechanisms as a crucial link between the (intrauterine) environment and the developing foetus; these are discussed in more detail in section 1.7.

Many other factors have been found to promote or inhibit the conversion of pluripotent stem cells into committed preadipocytes. These include members of the bone morphogenic protein (BMP), wingless (Wnt), and hedgehog (Hh) families of signalling pathways (Tang, Q. Q. *et al* 2012). For example, BMP4 has been found to promote adipose commitment (Bowers, R. R. *et al* 2006), whereas Hh signalling has an inhibitory effect (Zehentner, B. K. *et al* 2000). Different members of the Wnt signalling family exert diverse effects on adipogenesis; some promote commitment (Bowers, R. R. *et al* 2008) whereas others inhibit differentiation (Ross, S. E. *et al* 2000).

Amidst the complex network of interactions between the various signalling pathways involved in commitment to the adipose lineage, it is possible that there is regional heterogeneity which may contribute to the depot-specific phenotypes observed *in vivo*. Indeed, it has been suggested that different adipose depots have distinct developmental

origins (Gesta, S. *et al* 2007), and after considering the data regarding *Zfp423*, it is likely that epigenetic mechanisms are involved (see section 1.7).

1.3.2 Transcriptional regulation of white adipogenesis

In order to become mature functional adipocytes, committed preadipocytes must become terminally differentiated. This process involves a temporally co-ordinated transcriptional cascade regulated by a number of transcription factors, with PPARγ and the C/EBPs being the most extensively studied. Furthermore, the dynamic changes in gene expression that occur during adipogenesis probably involve epigenetic modifications such as DNA methylation and histone modifications; these are discussed in section 1.7.

PPARγ is regarded as the 'master regulator' of adipogenesis as its expression is both necessary and sufficient for adipogenesis (Rosen, E. D. *et al* 1999); ectopic expression of *PPARγ* in (non-adipogenic) fibroblasts is sufficient to induce them to develop into mature adipocytes (Tontonoz, P. *et al* 1994). *PPARγ* expression is also required to maintain the differentiated state, as introduction of a dominant negative PPARγ isoform into mature murine 3T3-L1 adipocytes precipitates 'de-differentiation' where any accumulated lipid is lost and the expression of adipogenic markers decreases (Tamori, Y. *et al* 2002).

The importance of PPARγ in adipogenesis is further exemplified by the discovery that mutations in this gene are associated with familial partial lipodystrophy. For instance, patients with the R425C or P467L mutations display a marked lack of subcutaneous WAT in their extremities in conjunction with insulin resistance, T2DM, and dyslipidaemia (Agarwal, A. K. *et al* 2002; Savage, D. B. *et al* 2003). The inherited lipodystrophies will be discussed in more detail in section 1.6.4.

Members of the C/EBP transcription factor family also participate in adipogenesis; expression of C/EBPβ and C/EBPδ is induced early in adipogenesis (Tang, Q. Q. *et al* 1999), with these proteins activating the expression of *C/EBPα* (Farmer, S. R. 2006). Once *C/EBPα* is expressed, it maintains its own expression in an autoregulatory fashion (Timchenko, N. *et al* 1995) and also activates *PPARγ* expression (Elberg, G. *et al* 2000). Despite their importance, however, C/EBPs cannot drive adipogenesis in the absence of PPARγ (Rosen, E. D. *et al* 2002). It has been proposed that terminal differentiation involves a positive feedback loop between these transcription factors so adipogenesis proceeds in an irreversible manner, with the same mechanisms also maintaining the mature adipocyte phenotype (Park, B. O. *et al* 2012).

Many other proteins are involved in regulating adipogenesis. For instance, sterol regulatory element binding protein 1c (SREBP1c) is a transcription factor responsible for activating the expression of lipogenic genes (Tang, Q. Q. *et al* 2012) whilst different members of the Krüppel-like factor (KLF) family of transcription factors can promote or inhibit adipogenesis (Rosen, E. D. *et al* 2006).

Overall, adipogenesis is a complex process that occurs throughout life due to considerable cellular turnover. Indeed, approximately 10% of white fat cells are renewed each year (Spalding, K. L. *et al* 2008) with preadipocytes being recruited to replace old, damaged, or dead adipocytes, or during the process of adipose expansion.

1.4 Adipose tissue and metabolic health

Despite the beneficial functions that WAT fulfils in the healthy state, excessive amounts and / or dysfunction of this tissue has been linked with metabolic disease (Hassan, M. *et al* 2012). Indeed, overweight (BMI 25-29.9) and obese (BMI >30) patients who possess excessive amounts of fat are at high risk of developing cardiovascular disease and T2DM

(Willet, W. C. *et al* 2004). The link between adiposity and metabolic disease risk is not straightforward. However, there is mounting evidence suggesting the distribution of fat throughout the body, rather than amount of fat, is a major determinant of metabolic health (Manolopoulos, K. N. *et al* 2010).

1.4.1 Relationship of obesity to health

An epidemic of obesity has been sweeping the world since the 1970s, with the upward trend of overweight (BMI 25 – 29.9) and obesity (BMI >30) showing little sign of abating in the foreseeable future (Kelly, T. *et al* 2008). This is not just a public health problem but also an economic one; vast amounts of money could be saved if the prevalence of overweight and obesity were curtailed even slightly (Finkelstein E. A. *et al* 2012). As excessive adiposity is a major risk factor in the development of metabolic disease, it is perhaps unsurprising that T2DM is also reaching epidemic proportions across the world (King, H. *et al* 1998).

The progressive nature of T2DM involves deterioration of multiple organs and systems which principally manifests as macrovascular complications (cardiovascular disease - coronary artery disease, myocardial infarction, stroke, congestive heart failure), renal failure (diabetic nephropathy), and blindness (diabetic retinopathy). These complications arise from prolonged periods of dysregulated glucose and lipid metabolism which are accompanied and promoted by inappropriate activation of the immune system. Together, this comprises the 'metabolic syndrome' (Dixon, J. B. 2010).

There is strong evidence that BMI is a good predictor of all-cause mortality (Whitlock, G. *et al* 2009). However, it is only a crude anthropometric index of adiposity. There are many different ways of measuring both body fat content and its distribution that vary in their level of sophistication, usefulness, and cost. The most commonly used techniques are

outlined in Table 1.1. These techniques, as well as their advantages and disadvantages, have also been reviewed (Lee, S. Y *et al* 2008; Wang, J. *et al* 2000).

Table 1.1 Methods for measuring body composition and fat distribution

Technique	**Description**
Body mass index (BMI)	BMI is defined as Weight (kg) / [Height (m)]^2, with both measures being made using inexpensive, readily available equipment (e.g. tape measure). BMI only provides a rough estimate of adiposity and provides no information on body fat distribution. Several categories have been devised: <18.5 underweight; 18.5-24.9 normal weight, 25-29.9 overweight; >30 obese.
Waist-to-hip ratio (WHR)	WHR is defined as waist circumference (cm) / hip circumference (cm), with both measures being made using a tape measure. This index provides a measure of fat distribution, specifically abdominal obesity. Due to the sexual dimorphism of body shape, WHR categories are gender–specific: for males, WHR >0.9 is defined as (abdominally) obese; for female, WHR >0.85 is (abdominally) obese.
Skin-fold thickness	Callipers are used to measure the thickness of skin folds at specific parts of the body, with the measurements being used in a series of equations that can provide an estimate of body composition and body fat distribution (Jackson, A. S. *et al* 1978; Jackson, A. S. *et al* 1980).
Dual energy X-ray absorptiometry (DEXA)	DEXA can be used to directly measure fat mass based on a multi-compartment model, with the underlying principle that adipose, bone and non-adipose soft tissue attenuate X-ray energy in a tissue specific manner. Modern software can be used to analyse regional body composition, meaning DEXA can be used to provide a good measure of body fat distribution (Mazess, R. B. *et al* 1990). Also, the latest versions of GE/LunariDXA can give accurate estimates of visceral fat content.
Magnetic resonance imaging (MRI)	MRI can be used to accurately measure the volume of internal tissues. It is probably the best tool currently available, but its costs are potentially prohibitive due to the high costs of scan acquisition and data processing. MRI scans often use a single slice measurement over the visceral area which restricts the accurate estimation of subcutaneous fat volume.

Before considering the epidemiological data regarding the relationship between body fat distribution and metabolic health, however, the various patterns of body fat distribution will first be considered in section 1.4.2.

1.4.2 Body fat distribution and its relationship with metabolic health

There is marked sexual dimorphism in both body composition and shape in humans; for the same BMI, women typically present with ~10% absolute higher body fat content compared to men (Jackson, A. S. *et al* 2002). Although adiposity increases with age, dimorphism in body composition persists throughout life (Gallagher, D. *et al* 1996). Gender-specific body shapes arise from different patterns of fat distribution; the male / android shape is characterised by upper body fat accumulation, whereas the female / gynoid shape is defined by lower body fat accumulation, particularly in the hips and thighs (Karastergiou, K. *et al* 2012). Such patterns are also modulated by ethnicity. For example, in contrast to Caucasians, African men and women have a similar fat content at higher BMIs (Camhi, S. M. *et al* 2011).

Sexual dimorphism in fat distribution is also observed between individuals at a comparable level of adiposity. Women have more subcutaneous fat in both the abdominal (Schreiner, P. J. *et al* 1996) and gluteofemoral areas (Yim, J. E. *et al* 2008) compared to males. At the same time, females accumulate less fat in the intra-abdominal / visceral depots than males (Schreiner, P. J. *et al* 1996).

As mentioned in section 1.4.2, BMI is a good predictor of all-cause mortality (Whitlock, G. *et al* 2009) but provides only a rough measure of adiposity. The relationship between adiposity and metabolic health is not straightforward or universal, as some seemingly paradoxical clinical situations exist. Indeed, some obese individuals maintain their metabolic health whereas other people can develop metabolic disease at normal BMIs (Beck, E. *et al* 2009). However, body fat distribution is being increasingly recognised as a crucial determinant of metabolic health.

The link between body fat distribution and metabolic disease was originally made in the 1940s and 1950s (Vague, J. 1947; Vague, J. 1956). In a pair of seminal studies it was highlighted that upper body / central obesity (i.e. the android fat distribution pattern) was associated with diabetes and atherosclerosis, whereas these diseases had a very low incidence in patients exhibiting lower body fat accumulation (i.e. the gynoid fat distribution pattern). These initial findings have been supported and extended in numerous epidemiological studies which are discussed in section 1.4.3.

1.4.3 Epidemiological evidence for gluteofemoral fat protecting against metabolic disease

There is much evidence to suggest the metabolic complications that typically accompany obesity depend on the accumulation of abdominal fat; increased waist circumference is a strong independent predictor of T2DM risk (Langenburg, C. *et al* 2012) and is associated with hypertension and raised levels of circulating TAGs (Canoy, D. *et al* 2004). Both adiposity and central obesity contribute to metabolic disease risk, which can be most effectively predicted when a combination of anthropometric indices are used (Hou, X. *et al* 2013). The increased risk of developing metabolic disease conferred by central obesity is modified by fat partitioning between subcutaneous abdominal and visceral depots (Taksali, S. E. *et al* 2008). Despite this, it is unclear whether increased visceral adiposity is a cause or effect of metabolic dysfunction (Frayn, K. 2000).

In marked contrast to central obesity, there is substantial evidence indicating lower body (i.e. gluteofemoral) fat accumulation exerts a striking protective role against the development of metabolic and cardiovascular disease. The protective effect of gluteofemoral fat was clearly demonstrated in the INTERHEART study which included 27,000 participants from around the world (Yusuf, S. *et al* 2005); it was found that the risk

of myocardial infarction decreased with increasing hip circumference, independently of BMI.

These observations have been replicated in other studies of large populations. For instance, a larger hip circumference was associated with a lower prevalence of undiagnosed diabetes and dyslipidaemia in the AusDiab study (Snijder, M. B. *et al* 2004). Increased hip circumference was associated with a reduced risk of developing coronary heart disease in the EPIC study (Canoy, D. *et al* 2007) while increased hip and thigh circumference were independently associated with lower incidence of T2DM in the Hoorn study (Snijder, M. B. *et al* 2003).

Lower body fat accumulation is also independently associated with a beneficial metabolic profile in both men and women. Indeed, increased hip circumference has been associated with lower fasting insulin levels and TAGs (Seidell, J. C. *et al* 2001). Conversely, a reduced amount of gluteofemoral fat was independently associated with a less favourable glucose and lipid profile in the Health ABC study (Snijder, M. B. *et al* 2005).

Although the beneficial effects of gluteofemoral fat on metabolic health are evident, the mechanisms underlying this phenomenon are currently unclear. However, it has been postulated that gluteofemoral fat acts as a 'metabolic sink' which traps fatty acids and safely stores them for extended periods of time (Lemieux, I. 2004); see section 1.5.

1.5 Depot-specific white adipose tissue physiology

In line with the different associations of body fat distribution with metabolic disease, there is mounting evidence suggesting different adipose depots exhibit distinct physiological properties and should be treated as distinct 'mini-organs' (Caserta, F. *et al* 2001). Regional variation in the rates of lipolysis, (post-prandial) fatty acid uptake, and blood flow may

potentially explain the beneficial effects on metabolic health exerted by gluteofemoral fat depots (Manolopoulos, K. N. *et al* 2010).

There are two important distinctions to make regarding WAT. Firstly, subcutaneous abdominal and visceral fat are intrinsically different (Tchkonia, T. *et al* 2013), with subcutaneous adipose tissue exhibiting higher sensitivity to the adipogenic effects of PPARγ agonists in comparison to omental (visceral) preadipocytes (Adams, M. *et al* 1997; Mori, Y. *et al* 1999). In addition, heterogeneity within visceral adipose tissue has been observed, with mesenteric and omental adipose tissue displaying depot-specific characteristics despite their close proximity (Tchkonia, T. *et al* 2005).

Secondly, there is heterogeneity within subcutaneous WAT, most notably between abdominal (upper body) and gluteofemoral (lower body) depots. For instance, abdominal subcutaneous fat is more lipolytically active and contributes the majority of NEFAs in the circulation (Martin, M. L. *et al* 1991). Abdominal subcutaneous WAT is also more active during the post-prandial period, during which time it avidly traps meal-derived TAGs in comparison to the gluteofemoral depot (Koutsari, C. *et al* 2008).

Consistent with the idea that gluteofemoral fat acts as a 'metabolic sink', this tissue may preferentially accumulate fatty acids recycled in the circulation as NEFAs and very low-density lipoproteins - as opposed to meal-derived chylomicrons - and trap them for long-term storage (McQuaid, S. E. *et al* 2010; Koutsari, C. *et al* 2008). Gluteofemoral fat is also less sensitive to adrenaline-stimulated lipolysis as measured by palmitate release (Guo, Z. *et al* 1997), microdialysis of glycerol (Horowitz, J. F. *et al* 2000) or arteriovenous difference of stable isotope tracers (Manolopoulos, K.M. *et al* 2012) . Further, the gluteofemoral adipose depot remains metabolically silent during fasting, with abdominal fat predominantly mobilising its fat stores during such periods (Tan, G. D. *et al* 2004).

Adipose tissue blood flow also varies between upper and lower body subcutaneous depots; the gluteofemoral depot has a lower basal blood flow in comparison to abdominal fat (Dowling, H. J. *et al* 1995). Furthermore, blood flow in the post-prandial period increases in both abdominal and femoral depots in women, but only in abdominal fat in men (Koutsari, C. *et al* 2008). Together, these properties may contribute to regional fat accumulation and sexual dimorphism in body shape.

Overall, it appears that upper and lower body fat exhibit depot-specific physiological properties that presumably reflect their distinct roles in energy regulation. It follows that depot-specific dysfunction of adipose tissue could precipitate metabolic disturbances of varying severity, depending on the type of tissue affected (Tchkonia, T. *et al* 2013). The field of regional differences in fatty acid handling is large and complex, and is further complicated by sex differences. However, the current state of these areas has been reviewed recently (Manolopoulos, K. N. *et al* 2010; Karastergiou, K. *et al* 2012).

1.5.1 Cell autonomous properties of white adipose tissue

Several cellular and molecular mechanisms have been identified during *in vitro* experiments of adipose tissue that may underlie the regional behaviour of adipose tissue observed *in vivo*. Interestingly, it appears that the depot-specific phenotypes of adipose tissue are 'cell autonomous' to a large extent. Indeed, many studies have reported that isolated preadipocytes retain the characteristics of the depot from which they derive *in vitro*. This has prompted the suggestion that these cells have an 'intrinsic memory' of their anatomical origin which has been reported to persist for many generations (Tchkonia, T. *et al* 2006).

To complicate matters further, heterogeneity has been observed within (abdominal) subcutaneous and visceral adipose depots; Tchkonia *et al* identified two preadipocyte

'subtypes' which exhibited different replication rates and adipogenic potential (Tchkonia, T. *et al* 2005). The relative abundance of these preadipocyte subtypes varied between depots, with the behaviour of a depot likely reflecting the aggregate behaviour of its component cells.

In general, subcutaneous preadipocytes tend to exhibit a greater ability to undergo adipogenesis *in vitro* (as assessed by lipid accumulation and adipogenic marker expression) in comparison to those from visceral depots (Tchkonia, T. *et al* 2002). These depot-specific differences in adipogenic potential have been reported on numerous occasions (Adams, M. *et al* 1997; Hauner, H. *et al* 1988; and Hocking, S. *et al* 2010), but not all (Van Harmelen, V. *et al* 2004; Tchoukalova, Y. *et al* 2010). Such discrepancies may arise from variation in the donor population, culture conditions, and / or the way differentiation was assessed.

Regional differences in the manner in which different adipose depots expand during positive energy balance have also been observed; it has been reported that subcutaneous abdominal tissue expanded by hypertrophy whereas the subcutaneous femoral depot expanded via hyperplasia in healthy adults on an 8-week overfeeding program (Tchoukalova, Y. D. *et al* 2010). Similar to the abdominal subcutaneous depot, visceral adipose tissue seems to preferentially expand through hypertrophy (Joe, A. *et al* 2009).

To support the notion that depot-specific differences in preadipocyte behaviour are intrinsic, it has been reported that regional phenotypes persist *ex vivo* even after *in vivo* hormonal manipulations such as hypophysectomy (Kirkland, J. *et al* 1992) or ovariectomy (Lacasa, D. *et al* 1997). Overall, it appears that preadipocytes exhibit depot-specific characteristics which are retained during *in vitro* culture.

1.5.2 Depot-specific gene expression in white adipose tissue

Genome-wide analyses of gene expression in whole adipose tissue, mature adipocytes, and preadipocytes have identified depot-specific gene expression profiles, which may contribute to depot-specific phenotypes and are likely regulated by epigenetic modifications (see section 1.7). Regional gene expression profiles have been described for subcutaneous and visceral preadipocytes in human and murine adipose tissue (Tchkonia, T. *et al* 2007). Developmental regulators constitute a substantial proportion (~25%) of differentially expressed genes between depots. In addition, the expression of certain genes has been associated with anthropometric indices such as BMI (Gesta, S. *et al* 2006).

Distinct gene expression patterns have also been reported for upper and lower body subcutaneous adipose tissue (Karastergiou, K. *et al* 2013; Rehrer, C.W. *et al* 2012). Again, the most well represented group of differentially expressed genes were developmental regulators, especially members of the *HOX* family. The expression of adipogenic genes, like certain *C/EBP*s, may be regulated by a network of HOX transcription factors (Huang, Y. *et al* 2012). Most importantly, the expression of certain developmental regulatory genes in preadipocytes can have functional consequences. For example, over-expression of *T-box 15* (*TBX15*) has been found to inhibit differentiation in murine 3T3-L1 preadipocytes (Gesta, S. *et al* 2011).

1.6 Determinants of body fat distribution

Body fat distribution is influenced by many factors. The final pattern is the integrated output of a complex interplay between hormonal, environmental, and genetic factors.

1.6.1 Regulation of body fat distribution by sex steroids

Gender-specific fat distribution patterns are heavily influenced by sex steroids, with differences in body shape emerging during puberty. Body mass increases in both genders during puberty; in males this is primarily driven by an increase in lean mass, whereas females experience a greater increase in adiposity (Maynard, L. *et al* 2001). These differences in body composition persist for life (Wells, J. C. 2007).

It has been postulated that oestrogens are responsible for driving and maintaining the metabolically favourable gynoid fat distribution pattern. This is because the menopause is accompanied by fat redistribution to a more central / android pattern (Toth, M. J. *et al* 2000) with a concomitant increase in visceral fat accumulation (Lovejoy, J. C. *et al* 2008). On the other hand, the age-related decline in testosterone levels in men is associated with an increase in visceral adiposity (Allan, C. A. *et al* 2008).

The power of sex hormones in regulating body fat redistribution is truly exemplified by their effect in transgendered individuals. Testosterone administered to female-to-male transsexuals reduces the amount of subcutaneous fat throughout the body whilst increasing visceral adipose mass. Conversely, oestradiol treatment in male-to-female transsexuals is accompanied by a general increase in subcutaneous adiposity (Elbers, J. M. *et al* 1999).

The importance of these hormones in determining body fat distribution is evident but the cellular and molecular mechanisms employed are incompletely understood. However, it is known that both adipocytes and preadipocytes express sex steroid receptors (Dieudonne,

M. N. *et al* 1998), and testosterone has been reported to suppress LPL activity in femoral adipose tissue *in vivo* (Ramirez, M. E. *et al* 1997). The latter could contribute to abdominal fat accumulation and the android pattern of fat distribution. It is possible that manipulating sex steroid action may offer an alternative approach to modulate fat distribution and metabolic disease risk.

It is important to note that sex differences observed *in vivo* may not be carried over to the *in vitro* setting. For example, it has been reported that no gender-specific differences in the adipogenic capacity of preadipocytes were observed *in vitro* despite female tissue being found to contain a greater number of preadipocytes in the early differentiated state (Tchoukalova, Y. D. *et al* 2010). Therefore, the local microenvironment, rather than inherent differences in preadipocyte properties, may be responsible for mediating gender-specific properties.

1.6.2 Regulation of body fat distribution by glucocorticoids

Glucocorticoids released by the adrenal gland also influence body fat distribution. These hormones are catabolic and act to mobilise energy stores during times of stress. There are many conflicting reports on the effects of glucocorticoids in adipose tissue metabolism suggesting their mechanism of action is not straightforward (Peckett, A. J. *et al* 2011). The current state of knowledge regarding the complex regulation of lipid metabolism by glucocorticoids has been reviewed recently (Lee, M. J. *et al* 2013).

Cushing's syndrome patients - who experience chronically high levels of glucocorticoids - exhibit central obesity in conjunction with wasting of peripheral (subcutaneous) fat, particularly in the gluteofemoral depot (Geer, E. B. *et al* 2010; Rockall; A. G. *et al* 2003). These patients also present with an insulin-resistant phenotype similar to T2DM. Together

these observations support the notion that the gluteofemoral depot exerts a protective effect against the development of metabolic disease.

Glucocorticoid action in adipose tissue is modulated by local (pre-receptor) metabolism. Indeed, the amount of biologically active glucocorticoids is locally amplified within adipose tissue by 11β-HSD1. Over-expression of *11β-HSD1* within adipose tissue in transgenic mice produces an insulin-resistant, obese phenotype characterised by preferential expansion of visceral adipose depots accompanied by derangements of glucose and lipid metabolism (Masuzaki, H. *et al* 2001). On the contrary, genetic inactivation of this enzyme has been associated with a lean, insulin-sensitive phenotype (Kotelevtsev, Y. *et al* 1997; Kershaw, E. E. *et al* 2005). Such results have spurred an interest in developing inhibitors of this enzyme as a potential anti-diabetic therapy (Hollis, G. *et al* 2011).

1.6.3 Environmental influences regulating body fat distribution

The advent of highly active anti-retroviral therapy (HAART) for the treatment of HIV/AIDS has transpired to be a double-edged sword. These drugs have greatly reduced the mortality rates in HIV/AIDS patients, which is a substantial achievement. Unfortunately, these drugs can precipitate HAART-associated lipodystrophy syndrome (HALS) in which the gluteal and femoral adipose depots waste away (Shlay, J. C. *et al* 2009) whilst abdominal depots expand (Behrens, G. M. 2005).

This syndrome puts patients at risk of developing insulin resistance, T2DM, dyslipidaemia, and cardiovascular disease (Blumer, R. M. *et al* 2008) and may be partly driven by compromised fatty acid storage. Indeed, HAART drugs inhibit adipogenic gene expression (Pacenti, M. *et al* 2006) and suppress the lipogenic pathway (El Hadri, K. *et al* 2004). However, it is currently unclear why adipose tissue exhibits regional sensitivity to certain HAART regimes.

1.6.4 Genetic regulation of body fat distribution

In addition to hormonal and environmental influences, genetics plays a key role in determining body fat distribution. The importance of this genetic component is exemplified by the phenotype exhibited by patients who suffer from the various types of inherited monogenic lipodystrophy. The lipodystrophies can be subdivided into generalised (near-total lack of adipose tissue) or partial (selective loss of adipose tissue).

There are two types of congenital generalised lipodystrophy (CGL) – or Berardinelli-Seip syndrome - classified on the type of genetic mutation and associated phenotype. Both are rare, autosomal recessive diseases associated with T2DM, hypertriglyceridaemia, hepatic steatosis, and cirrhosis (Fiorenza, C. G. *et al* 2011). CGL1 is associated with mutations within the *AGPAT2* gene on chromosome 9q34 (Agarwal, A. K. *et al* 2002), which encodes an enzyme that catalyses the formation of phosphatidic acid, an intracellular signalling molecule required for normal adipocyte function and TAG synthesis (Simha, V. *et al* 2003). Interestingly, this mutation predominantly affects metabolically important adipose depots but leaves mechanically important fat unaffected.

CGL2 is associated with mutations in *BSCL2* on chromosome 11q13 (Magre, J. *et al* 2001), which encodes the protein seipin. This molecule has been localised to the endoplasmic reticulum (Szymanski, K. M. *et al* 2007) and has been implicated in adipogenesis (Payne, V. *et al* 2008) and lipid droplet formation (Boutet, E. *et al* 2009). CGL2 patients lack both metabolically and mechanically important adipose tissue.

The importance of anatomically distinct adipose depots in maintaining metabolic health (as opposed to adipose tissue in general) is perhaps better illustrated by the inherited partial lipodystrophies. There are many types of familial partial lipodystrophy (FPLD), although most are exceedingly rare. The most common form is FPLD2 or Dunnigan-type familial

partial lipodystrophy which is inherited in an autosomal dominant fashion and results from mutations in the *LMNA* gene located on chromosome 1q21-22 (Cao, H. *et al* 2000; Speckman, R. A. *et al* 2000).

LMNA encodes the lamin A and C nuclear envelope proteins which provide structural integrity to the nucleus. These proteins have been implicated in insulin and PPARγ signalling as well as adipogenesis (Boguslavsky, R. L. *et al* 2006). FPLD2 develops during puberty and involves fat-redistribution from peripheral subcutaneous adipose tissue to intra-abdominal depots, thereby generating a Cushingoid appearance (Garg, A. 2004). Furthermore, mutations in *PPARγ* can precipitate FPLD syndromes and the associated metabolic derangements (Agarwal, A. K. *et al* 2002; Hegele, R. A. *et al* 2002; Barroso, I. *et al* 1999; Savage, D. B. *et al* 2003).

These rare conditions provide useful insight into the genetic regulation of adipose tissue development and distribution as well as the relationship between metabolic health and body fat distribution. It is interesting when only certain WAT depots are affected after a fundamental component of adipose differentiation like PPARγ is disrupted, but this suggests regional variation in adipogenesis exists. This further supports the notion that different fat depots should be treated as distinct mini-organs. Despite these insights, this knowledge does not help explain common variation in body fat distribution in the general population.

To address this issue, genome-wide association studies (GWAS) have been performed. There is evidence suggesting individual variation in WHR is heritable, even after accounting for BMI (Mills, G. W. *et al* 2004; Souren, N. Y. *et al* 2007), with heritability estimates for WHR ranging from 22 – 61% (Rose, K. *et al* 1998; Selby, J. V. *et al* 1990). A recent meta-analysis has identified 14 genomic loci associated with WHR (Heid, I. *et al*

2010). Furthermore, a locus near to the *LYPLAL1* gene has been found to be associated with WHR independent of BMI, which suggests genetic control over body fat distribution distinct from that over general adiposity exists (Lindgren, C. M. *et al* 2009).

Although it is generally agreed that obesity and body fat distribution are highly heritable, the currently identified common risk variants only account for ~5% of the variation in BMI, for example (Hebebrand, J. *et al* 2013), which is a trivial contribution. It is possible, however, that epigenetic modifications may account for at least part of this 'missing heritability'.

Epigenetic modifications also provide a mechanistic link between maternal nutrition and the intra-uterine environment; it is well-established that maternal obesity is associated with increased adiposity in offspring (Heerwagen, J. R. *et al* 2010). It follows that adipose tissue development may also be regulated by epigenetics (as mentioned in section 1.3.2) with these same mechanisms possibly contributing to the depot-specific gene expression profile exhibited by preadipocytes; see section 1.7.

1.7 Epigenetic regulation of body fat distribution

Superimposed on the genetic code is a layer of heritable epigenetic modifications, which store information as chemical modifications of cytosine bases (i.e. DNA methylation) and to the histone proteins around which DNA is coiled (i.e. histone modifications). Unique profiles of gene expression can be generated in different stages of development, tissue types, and in disease states by modifying the structure of chromatin, which thereby regulate the accessibility of DNA to transcriptional machinery (Bernstein, B. E. *et al* 2007). Gene expression can also be regulated at the post-transcriptional stage by microRNAs. The various epigenetic mechanisms are summarised in figure 1.2.

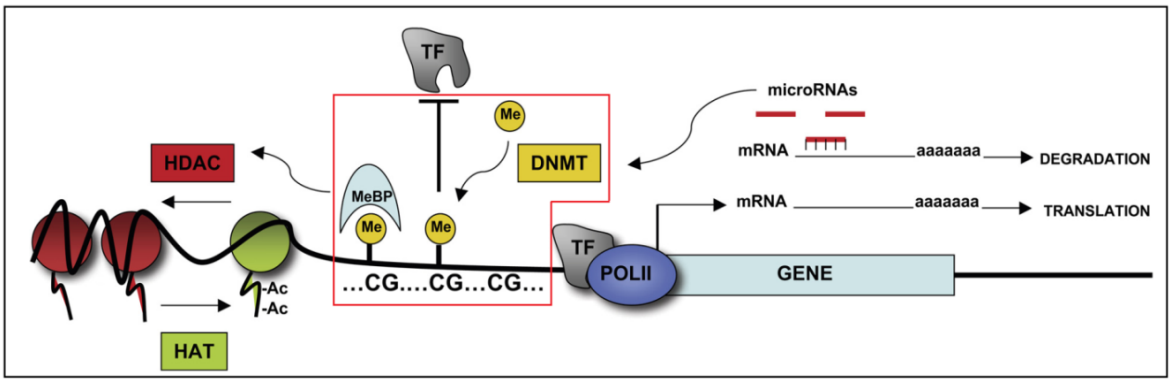

Figure 1.2 – *Overview of epigenetic mechanisms regulating gene expression*. Epigenetic mechanisms alter gene expression independent of gene sequence and principally involve the methylation of DNA and covalent modification of chromatin structure. DNA methylation is catalysed by a DNA methyltransferase (DNMT). Methylation of cytosine residues within cytosine-guanine (CpG) dinucleotides in the 5' promoter region of genes is associated with transcriptional repression. This is achieved both by blocking the binding of transcription factors and the recruitment of transcriptional co-repressors and / or histone modifying complexes. The tails of histone proteins can be covalently modified in many ways, although acetylation and deacetylation, catalysed by a histone acetyl-transferase (HAT) and histone deacetylase (HDAC) respectively, are the most extensively studied. Histone tail acetylation promotes an open-chromatin conformation, and is associated with transcriptional activation, whereas histone tail deacetylation promotes a closed-chromatin conformation and is associated with transcriptional repression. Also, microRNAs have recently been shown to regulate DNA methylation as well. MeBP, methyl-CpG binding protein; TF, transcription factor; Pol II, DNA polymerase II. Diagram adapted from Heerwagen, M. *et al* 2010.

1.7.1 Histone modifications

The fundamental unit of chromatin is the nucleosome which comprises 147bp of DNA wrapped around an octomer of histone proteins that constitute two copies of H2A, H2B, H3 and H4 (Intine, R. V. *et al* 2012). The tails of histone proteins can be modified by the addition or removal of functional groups, with the list of known histone modifications currently standing at over 100 (Rando, O. J. 2012). Although certain modifications have been associated with different effects on gene expression it is important to appreciate that they do not exist singly or in isolation. Several modifications will be present at a given locus so the 'meaning' of a histone mark is likely influenced by the presence of other

epigenetic marks at the same locus; the term 'histone code' has been coined to describe this hypothetical phenomenon (Rando, O. J. 2012).

Significant changes in gene expression occur during the process of adipogenesis (section 1.3) and these are accompanied by dynamic changes in epigenetic modifications. Indeed, distinct and dynamic patterns of histone modifications at specific genes in murine 3T3-L1 preadipocytes undergoing adipogenesis have been documented (Zhang, Q. *et al* 2012). As expected, increased expression of adipogenic regulatory markers was accompanied by a decrease in repressive histone marks and / or the recruitment of activating marks. For example, *PPARG2* and *aP2* both acquired H3 and H4 acetylation during adipogenesis; these marks are associated with transcriptional activation.

1.7.2 MicroRNAs

MicroRNAs (miRNAs) are a group of non-coding RNA molecules of ~22 nucleotides in length that regulate gene expression at the post-transcriptional level (Romao, J. M. *et al* 2011). They bind to complementary sites present in the 3' untranslated region of their target mRNA molecules to cause the direct repression of translation or degradation of the bound mRNA molecule (Yekta, S. *et al* 2004). Certain miRNAs can regulate the expression of hundreds of genes (Lim, L. P. *et al* 2005), with computational predictions suggesting that over 45,000 putative miRNA binding sites exist in protein-coding genes in humans (Friedman, R. C. *et al* 2009), although most await experimental validation.

These molecules may contribute to depot-specific gene expression profiles; regional variation in miRNA expression has been detected between subcutaneous abdominal and gluteal adipose tissue (Drong, A. W. *et al* 2011) as well as between subcutaneous abdominal and omental (visceral) adipose tissue in humans (Kloting, N. *et al* 2009). MicroRNAs also present themselves as attractive therapeutic targets in the treatment of

metabolic disease; anti-sense oligonucleotides which neutralise specific miRNAs to elicit therapeutic effects are currently under development (Alexander, R. *et al* 2011).

1.7.3 DNA methylation

DNA methylation involves the covalent addition of a methyl group derived from the universal methyl donor s-adenosyl L-methionine to the 5' carbon atom of a cytosine ring (Illingworth, R. S. *et al* 2009). This happens on cytosine residues adjacent to a guanine base (so-called CpG dinucleotides). Approximately 70 – 80% of all cytosine residues within the mammalian genome are methylated (Lister, R. *et al* 2009). In addition, DNA methylation patterns are heritable (Bird, A. 2002).

Cytosine methylation is catalysed by DNA methyltransferases (DNMTs), with the ability of DNA methylation patterns to be passed down generations being conferred by DNMT1, the 'maintenance' DNMT. During cellular replication a fully methylated parent DNA molecule separates with each strand acting as a template for DNA synthesis. The nascent DNA strand will be unmethylated; DNMT1 recognises hemi-methylated CpG dinucleotides and methylates the nascent strand, thereby rendering the molecule fully methylated (Goll, M. G. *et al* 2005).

It is important to consider that methylation is an epigenetic modification which is acquired. The DNA of early embryos is hypomethylated but methylation patterns are established during embryogenesis and early postnatal life by DNMT3a and DNMT3b. Further increases in methylation are associated with organogenesis and differentiation (Laurent, L. *et al* 2010).

The mammalian genome is relatively CpG-poor owing to the mutagenic nature of 5'-methylcytosine, which can spontaneously deaminate to thymine; this is the most common

cause of C to T transition mutations in somatic cells (Rideout, W. M. *et al* 1990). However, the genome is punctuated with regions known as CpG islands which are ~1 kb regions with an elevated GC content and are often hypomethylated. About 70% of all annotated promoters are associated with a CpG island (Saxonov, S. *et al* 2006). These sites are key regions for gene expression regulation (Deaton, A. M. *et al* 2011); RNA polymerase II has been found localised to CpG island promoters (Maunakea, A. K. *et al* 2010) and RNA sequence analysis has identified transcripts which originate from these genomic regions (Bird, A. 2002).

1.7.4 Regulation of gene expression by DNA methylation

DNA methylation is classically associated with transcriptional repression; the information contained within this epigenetic mark is translated by DNA binding proteins which recognise methylated cytosine residues and generate a repressive chromatin structure to inhibit gene expression (Klose, R. J. *et al* 2006). Promoter methylation is classically associated with transcriptional repression whereas gene body methylation and expression have been positively correlated (Hellman, A. *et al* 2007). Such observations suggest the effect of a specific 5-methylcytosine residue on gene expression is determined by its genomic (and nucleosomal) context (Jones, P. A. *et al* 2012).

There are three main types of DNA sequence whose expression is repressed by DNA methylation in normal cells (Prokhortchouk, E. *et al* 2008), the first of which are parentally imprinted genes. Imprinted genes are differentially expressed from the maternal or paternal chromosome and tend to be key regulators of embryonic development (Delaval, K. *et al* 2006); the inactivated allele is typically hypermethylated so loss of methylation results in bi-allelic expression (Feinberg, A. P. 2007). Secondly, transposons and other repetitive sequences that constitute a substantial portion of the human genome are typically

hypermethylated to repress their expression. Thirdly, a number of genes are methylated in a tissue-specific fashion (Illingworth, R. *et al* 2008).

Gene expression can be regulated by DNA methylation in a variety of ways. For instance, CpG dinucleotides often feature in the recognition site of transcription factors - such as Sp1 and CREB (Mancini, D. N. *et al* 1999) - with methylation of these sites inhibiting their binding to DNA and preventing transcriptional activation. Alternatively, transcriptional repression can be mediated by proteins which are attracted to, rather than repelled by, methylated DNA. The family of proteins containing the methyl-binding domain of MeCP2 can mediate this effect (Bird, A. P. *et al* 1999). Genetic disruption of MeCP2 precipitates Rett syndrome, an X-linked neurodevelopmental disorder characterised by microcephaly, autism, ataxia and seizures (Amir, R. E. *et al* 1999). This condition highlights the importance of reading DNA methylation patterns correctly so normal (neurological) development can occur.

Another family of proteins which contain the zinc finger (ZF)-CxxC DNA binding domain has also been identified (Long, H. K. *et al* 2013). These proteins specifically bind non-methylated CpG dinucleotides and exhibit histone modifying capabilities (Lee, J. H. *et al* 2005). As such, these proteins provide a potential link between DNA methylation and histone modifications in the regulation of gene expression (Fuks, F. 2005).

Although DNA methylation is classically associated with transcriptional repression, it can also promote gene expression. The key example concerns the imprinting of *IGF2* by CTCF. The maternal copy of *IGF2* is transcriptionally silent in mammals owing to the binding of CTCF, a DNA binding protein which 'insulates' the *IGF2* promoter from its downstream enhancer. However, CpG sites on the paternal chromosome are methylated

which prevents the binding of CTCF and so permits the downstream enhancer to promote *IGF2* expression (Bell, A. C. *et al* 2000).

1.7.5 DNA methylation in white adipose tissue

Dynamic changes in DNA methylation patterns have been detected during the process of adipogenesis, much in the same way that histone modification profiles change (Zhang, Q. *et al* 2012). Indeed, global methylation profiles have been reported to change in preadipocytes during adipogenesis (Sakamoto, H. *et al* 2008). Furthermore, there is mounting evidence suggesting the expression of several genes crucial to adipose function is regulated by DNA methylation. For instance, CpG sites present in the promoters of *leptin* (Yokomori, N. *et al* 2002) and *GLUT4* (Yokomori, N. *et al* 1999) have been reported to become demethylated during adipogenesis in 3T3-L1 preadipocytes, which correlates with their increased expression.

It is important to remember that progenitor cells must have committed to the adipose lineage before they can undergo adipogenesis (section 1.3.1). DNA methylation has been implicated in the process of commitment (Boquest, B. C. *et al* 2006), as manipulation of the global DNA methylation profile of adipose progenitors can permit them to follow other mesenchymal lineages under the appropriate culture conditions (Cifarelli, R. *et al* 2012).

Expression of the 'master regulator' of adipogenesis is regulated by DNA methylation patterns that may be modulated by deleterious environmental factors like overnutrition. Indeed, it has been reported that visceral preadipocytes obtained from two mouse models of T2DM (including diet-induced obesity) exhibit decreased *PPARγ* expression in conjunction with hypermethylation of the *PPARγ* promoter (Fujiki, K. *et al* 2009). Given this, it was postulated that reduced expression of *PPARγ* might compromise effective fat storage, thereby promoting metabolic dysfunction in these mice.

DNA methylation patterns can also change in response to beneficial environmental influences. For instance, a six-month exercise program was found to significantly alter the global DNA methylation profile of whole adipose tissue from the subcutaneous femoral depot in humans. The methylation status of CpG sites within 18 obesity and 21 T2DM risk genes changed with altered expression being documented for 6 of these genes (Rönn, T. *et al* 2013).

As mentioned in section 1.3.1, there is mounting evidence that the intrauterine environment has a significant and long-lasting influence over the long-term metabolic health of the developing foetus (Heerwagen, M. *et al* 2010; Seki, Y. *et al* 2012). Furthermore, epigenetic modifications provide a mechanistic link between the intrauterine environment and changes in gene expression in the developing foetus that may underlie the increased susceptibility to, or even pathogenesis of, obesity and metabolic disease.

In a rat model of maternal overnutrition, it was reported that the offspring of obese dams displayed increased *in vivo* expression of adipogenic regulators (*PPARγ*, *C/EBPα*, and *C/EBPβ*), with stromovascular cells from subcutaneous WAT exhibiting a greater adipogenic potential compared to those from normal weight controls, suggesting such offspring were 'programmed' for obesity (Borengasser S. J. *et al* 2013).

When considering the data indicating the promoters of certain adipogenic markers (e.g. *leptin* and *GLUT4*) become demethylated during differentiation, it is not clear whether this dynamic process can be modified by environmental influences or simply proceeds autonomously. Such a feature may be gene-specific, and depending on the gene, this may have important functional implications. It is currently unclear what determines a gene's ability to be modified by a particular environmental factor. Despite this, it is known that *PPARγ* expression is regulated by DNA methylation, with increased methylation of its

promoter and reduced expression in visceral preadipocytes having been associated with diet-induced obesity and T2DM in mice (Fujiki, K. *et al* 2009).

Given this gene's crucial role in adipose function and its apparently modifiable nature, it follows that *PPARγ* may represent an intersection point between the environment and metabolic health. Whether it's dynamic expression (and epigenetic) profile during adipogenesis can be altered by environmental factors is currently unclear, possibly in a depot-specific manner, but perturbation of these during differentiation may underlie the insulin-resistant phenotype exhibited by mature adipocytes from diabetic individuals.

In addition, it may be the case that the 'plasticity' of certain genes varies over time, which may have wide-ranging functional consequences. For example, if a gene relevant to adipose tissue function can be predominantly modified during development but this property diminishes during adulthood, long term metabolic health may essentially be irreversibly programmed during early life experiences. Overall, epigenetic modifications, such as DNA methylation, can translate environmental factors into biochemical signals which may influence adipose tissue function and long-term metabolic health.

1.7.6 Pharmacological manipulation of DNA methylation by 5-azacytidine

Cytosine methylation is a reversible epigenetic mark as DNA demethylation has been observed in non-dividing cells types like differentiating preadipocytes (Sakamoto, H. *et al* 2008; Yokomori, N. *et al* 1999; and Yokomori, N. *et al* 2002). This means DNA methylation is potentially open to pharmacological manipulation for therapeutic benefit. 5-azacytidine is a cytidine nucleoside analogue which is incorporated into newly synthesised DNA where it forms a covalent bond with DNMT1 (Santi, D. *et al* 1984). This sequesters the enzyme and leads to the passive demethylation of DNA during cell proliferation. 5-azacytidine has been used to treat certain myelodysplastic syndromes (Issa, J. P. 2005)

with some degree of success (Blum, W. *et al* 2010). Despite its cytotoxic effects, this drug can also be used to probe the role of DNA methylation in normal cellular physiology.

5-azacytidine has been used to confirm *PPARγ* expression is regulated by DNA methylation. Indeed, *PPARγ* expression in 3T3-L1 preadipocytes can be increased by treatment with 5-azacytidine, whereas expression of a reporter gene under control of the *PPARγ* promoter is reduced when the transfected construct is *in vitro* methylated (Fujiki, K. *et al* 2009).

This drug has also been used in many studies investigating the role of DNA methylation in cellular differentiation and lineage commitment (Jones, P. A. *et al* 1980). Perhaps unsurprisingly, DNA methylation has been found to contribute to these processes in adipose tissue. For example, human preadipocytes treated with 5-azacytidine have been reported to revert to a 'less differentiated' state characterised by increased expression of stem cell markers such as *Oct4* and *Nanog* (Cifarelli, R. A. *et al* 2012). Indeed, such drug-treated preadipocytes were able to differentiate into other mesodermal lineages (such as bone, cartilage and muscle) when cultured in the appropriate inductive media. This effect has not been consistently observed, however (Zych, J. *et al* 2013). In addition, adipogenesis can be inhibited in a stage-dependent manner by 5-azacytidine, with early exposure to the drug being the most effective (Sakamoto, H. *et al* 2008). Overall, this suggests that formation of an accurate DNA methylation profile is necessary for proper differentiation.

However, it must be appreciated that the effects of 5-azacytidine are not mediated through straightforward mechanisms, which may complicate the interpretation of results. It has been noted that 5-azacytidine exerted distinct and reproducible gene- and cell-type specific effects in two different cancer cell lines (Hagemann, S. *et al* 2011). Interestingly, a

substantial number of CpG sites were resistant to drug-induced demethylation although this could be overcome by knockout of DNMT1 and DNMT3a. It is possible that resistance to drug-induced demethylation is determined (at least in part) by the underlying chromatin. In support of this, 5-azacytidine-resistant CpG sites were found to be associated with Polycomb repressor complex 2 (PRC2) components, suggesting they may be readily remethylated (Hagemann, S. *et al* 2011).

1.7.7 Pharmacological manipulation of DNA methylation by glucocorticoids

Although DNA demethylating agents such as 5-azacytidine are useful tools, there is evidence suggesting DNA methylation can be modified by more physiologically relevant molecules, namely glucocorticoids, which are also important determinants of body fat distribution (see section 1.6.2).

Glucocorticoids down-regulate corticotropin-releasing hormone (*CRH*) expression in hypothalamic neurons in a negative feedback loop within the hypothalamic-pituitary-adrenal axis (Buckingham, J. C. 2006) although the mechanism(s) underlying this process are not well understood. There is data suggesting dexamethasone can repress *CRH* expression by stimulating the recruitment of a transcriptional repressor complex comprising MeCP2, DNMT3b and histone deacetylase 1 to the *CRH* promoter under the direction of activated glucocorticoid receptors (Sharma, D. *et al* 2012). Occupancy of the promoter by this complex was associated with increased methylation of specific CpG sites in the *CRH* promoter.

Dexamethasone increases the expression of *FKBP5*, a co-chaperone protein which regulates the sensitivity of the glucocorticoid receptor (GR) (Binder, E. B. 2009). FKBP5 reduces both the affinity of GRs for cortisol and the efficiency of nuclear translocation of activated receptors (Wochnik, G. M. *et al* 2005). Indeed, increased expression of *FKBP5*

can generate glucocorticoid-resistance (Scammell, J. G. *et al* 2001). Hypothalamic and hippocampal *FKBP5* expression was increased in mice treated with dexamethasone for 4 weeks (Lee, R. S. *et al* 2010) and this was accompanied by a reduction in the methylation status of specific CpG sites within two intronic regions of *FKBP5* in the same tissues. This dexamethasone-induced demethylation also occurred in whole blood DNA (Lee, R. S. *et al* 2011).

Glucocorticoids are also potent immunosuppressants which inhibit the expression of cytokines and chemokines, which is why they are used to control chronic inflammatory diseases like asthma (Barnes, P. J. 2010). Granulocyte/macrophage colony stimulating factor (GM-CSF) was released from A549 cells in a dose-dependent fashion upon administration of IL-1β, but this was inhibited by co-administration of the glucocorticoid mometasone furoate (Kagoshima, M. *et al* 2001). However, when the glucocorticoid was administered in the presence of 5-azacytidine, its suppressive effect on IL-1β – induced GM-CSF release was attenuated. This suggests that glucocorticoid-mediated suppression of GM-CSF release involves DNA methylation. Overall, it appears that glucocorticoids may modulate DNA methylation in a variety of cell types and target genes.

1.8 Aims

There are several aims in this project which will involve using human subcutaneous preadipocyte cell lines derived from abdominal and gluteal depots to represent upper and lower body fat respectively.

- Analyse and verify the depot-specific expression of a select group of candidate genes identified in a previous microarray investigation in untreated preadipocytes.
- Analyse the expression profile of these candidate genes during the process of adipogenesis over a 14 day differentiation time course.

- Analyse and verify the DNA methylation status of CpG islands indicated to be differentially methylated between these depots in a previous differential methylation hybridisation array investigation using bisulfite-pyrosequencing.
- Investigate whether the expression of any candidate genes is regulated by DNA methylation using the DNA demethylating agent 5-azacytidine as a screening tool.
- Investigate whether the expression of any candidate genes is sensitive to glucocorticoid action due to the influential role of these hormones in body fat distribution.
- Investigate whether any changes in candidate gene expression upon drug treatment are accompanied by changes in DNA methylation status within the previously identified differentially methylated regions.

2 Methods

Methods

2.1 Cell culture of human preadipocyte cell lines

2.1.1 Maintenance of human preadipocyte cell lines

Human male and female paired preadipocyte cell lines derived from the stromovascular fraction of subcutaneous abdominal and gluteal adipose tissue were used in this project to represent upper and lower body fat respectively. Primary human preadipocytes have a low proliferative capacity and their ability to undergo adipogenesis declines during sub-culturing; it is for these reasons that immortalised human preadipocytes were used. Experimental variation is also minimised by using cell lines as this avoids the inter-individual differences encountered when using primary tissue. Together, these properties make the preadipocyte cell lines ideal to use for preliminary experiments before attempting to replicate any initial findings within primary tissue.

The paired preadipocyte cell lines were originally derived from the stromovascular fraction of subcutaneous abdominal and gluteal adipose tissue obtained from an individual male and female subject. Using a modified version of the protocol used by Darimont *et al*, these cells were transduced with lentiviral particles carrying the human telomerase-reverse transcriptase (hTERT) to extend their lifespan. Immortalisation was achieved by co-expression of the E7 oncoprotein of the human papilloma virus (HPV-E7); transformed cells also express a blasticidin-resistance gene to permit the selection of clones. The immortalised preadipocytes exhibit an extended lifespan and a preserved adipogenic potential (Darimont, C. *et al* 2003).

These cell lines were cultured in Dulbecco's modified Eagle's medium / Nutrient F-12 Ham (v/v, 1:1; Sigma-Aldrich; Gillingham, UK) supplemented with 10% foetal bovine

serum (Gibco; Paisley, UK); 2mM L-glutamine (Invitrogen; Paisley, UK); 100 units/ml penicillin and 100µg/ml streptomycin (Invitrogen; Paisley, UK); 0.25ng/ml fibroblast growth factor (Sigma-Aldrich; Gillingham, UK); and 10mg/ml blasticidin (Invitrogen; Paisley, UK) - this solution will now be referred to as 'growth medium'. The preadipocytes were seeded into T175 tissue culture flasks (Sarstedt; Leicester, UK) and maintained in a humidified atmosphere at 37°C in a 5% CO_2 incubator. Paired preadipocytes of passage 8 – 16 were used for gene expression, DNA methylation, and differentiation experiments.

2.1.2 Administration of dexamethasone and / or 5-azacytidine

To analyse the effects of azacytidine and dexamethasone, alone or in combination, on preadipocyte gene expression and DNA methylation, preadipocytes were plated and cultured in growth medium for 24 hr followed by drug treatment. For this, preadipocytes were cultured in growth medium supplemented with the respective compound(s) for 48 hr which was followed by cell harvesting. Untreated cells were included as controls; such cells were cultured in parallel but were only exposed to growth medium throughout the 72 hr duration.

For gene expression analysis the preadipocytes were seeded onto a 6 well tissue culture plate (Sarstedt; Leicester, UK) at a density of 7.5×10^4 cells per well (per experimental condition). For DNA methylation analysis, 4×10^5 cells were seeded into a single T75 tissue culture flask (Sarstedt; Leicester, UK) in 13ml growth medium (per experimental condition).

Due to the instability of 5-azacytidine (Sigma-Aldrich; Gillingham, UK) fresh solutions were made on the day of drug administration. A 491µM stock solution was made in phosphate-buffered saline (PBS), with this being diluted in growth medium to give a 5-

azacytidine solution at a final concentration of 15µM. This was then administered to the preadipocytes for 48 hr. This concentration was chosen because previous work has found it exerts detectable effects on gene expression (Zych, J. *et al* 2013), DNA methylation status (Hagemann, S. *et al* 2011) as well as the phenotype and behaviour of human preadipocytes (Cifarelli, R. A *et al* 2012) whilst having an acceptable effect on cell viability (Hagemann, S. *et al* 2011).

Dexamethasone solutions were made on the day of administration from a 4.14mM stock solution (Sigma-Aldrich; Gillingham, UK) which was stored at -20°C. A 250µM working stock solution was made from this in growth medium. This was then used to make 10nM, 100nM and 1000nM dexamethasone-growth medium solutions which were subsequently administered to the preadipocytes.

Finally, some experiments involved treating cells with a combination of dexamethasone (100nM) and 5-azacytidine (15µM). This solution was made by adding 5-azacytidine to the 100nM dexamethasone-growth medium solution before administration to the preadipocytes.

2.1.3 Differentiation of human preadipocytes

Preadipocytes were seeded onto 6 well plates at a density of 2 x 10^5 cells / well and allowed to grow to 100% confluence for 48 hr before the administration of standard differentiation medium adapted from a previous protocol (Hauner, H. *et al* 2001).

Differentiation medium consisted of Dulbecco's modified Eagle's medium / Nutrient F-12 Ham (v/v, 1:1; Sigma-Aldrich; Gillingham, UK-Aldrich;) containing 2mM L-glutamine (Invitrogen; Paisley, UK); 17µM pantothenate (Sigma-Aldrich; Gillingham, UK); 100nM human insulin (Invitrogen; Paisley, UK); 1nM triiodo-L-thyronine (Sigma-Aldrich;

Gillingham, UK); 33µM biotin (Sigma-Aldrich; Gillingham, UK); 10µg/ml transferrin (Sigma-Aldrich; Gillingham, UK); and 1µM dexamethasone. For the first 4 days the differentiation medium was supplemented with 250µM 3-isobutyl-1-methylxanthine (Sigma-Aldrich; Gillingham, UK) and 2µM troglitazone (Sigma-Aldrich; Gillingham, UK).

Differentiation was carried out for 14 days with cells being harvested for RNA (see section 2.3) on days 0, 2, 4, 7, and 14 post-induction of adipogenesis. Note that adipogenesis occurred in the absence of exogenous lipids. Adipogenesis and lipid accumulation can still proceed in a normal fashion despite their absence (Collins, J. M. *et al* 2011), as glucose present in the differentiation medium can be used as the primary carbon source for *de novo* lipogenesis (DNL). The subsequent modification of lipids synthesised by DNL generates a range of different saturated and unsaturated fatty acids that are consistent with proper adipogenesis, adipocyte maturation, and lipid accumulation.

2.2 Gene expression analysis

2.2.1 RNA extraction

For RNA extraction, cells were washed twice with PBS and 500µl Tri-reagent (Ambion; Paisley, UK) was added to each well. The cells were scraped and homogenised before the cell lysate was transferred to a 2ml PhaseLock gel Eppendorf tube (Eppendorf; Stevenage, UK) before 100µl chloroform was added. Samples were then shaken by hand and incubated at room temperature for 2 - 3 min before centrifugation at 12,000 x *g* for 15 min. The clear aqueous RNA-containing supernatant was transferred to a clean tube before an equal volume of isopropanol was added along with 2µl GlycoBlue reagent (Invitrogen; Paisley, UK); the latter reagent makes visual identification of the RNA pellet easier. The samples were then precipitated at -30°C overnight.

RNA was collected by centrifugation at 12,000 x *g* for 20 min at 4°C. Isopropanol was aspirated off and the pellets were washed in 0.5ml of 70% ethanol. The pellets were then collected again by centrifugation at 12,000 x *g* for 20 min at 4°C, with this step being repeated once more. After the second wash, the 70% ethanol was aspirated off and the pellets allowed to air-dry for 5 - 10 min at room temperature. Once the pellet was dry, the RNA was resuspended in 11µl of RNase-free dH_2O.

The concentration of RNA was determined using a NanoDrop spectrophotometer (Thermo Scientific; Hemel Hempstead, UK). Only 1µl of each sample is required to determine its concentration, with the sample purity being assessed by the ratio of sample absorbance at 260 and 280nm. A ratio between 1.8 and 2.0 is generally accepted as 'pure' for RNA, with such samples being used for further analysis of gene expression. If the ratio was appreciably lower than 2.0, this indicated the presence of contaminants such as phenol or protein, with such samples being discarded.

2.2.2 Complementary DNA synthesis

Double stranded complementary DNA (cDNA) was synthesised from 500-1000ng RNA (made up to 10µl with dH_2O) in a 20µl reaction using the High Capacity cDNA Reverse Transcriptase (RT) kit (Invitrogen; Paisley, UK). Reaction volumes are listed in table 2.1.

Table 2.1 Composition of reverse transcription reaction mix

Reagent	Volume per reaction (µl)
10x RT Buffer	2.0
25x dNTP mix (100mM)	0.8
10x RT Random primers	2.0
Multiscribe™ Reverse transcriptase (50U/µl)	1.0
Nuclease-free dH2O	4.2

A no-template control containing dH_2O instead of RNA was run in parallel with the experimental samples to act as a quality control measure (i.e. to act as an indicator of sample contamination by foreign RNA during cDNA synthesis).

Each reaction was mixed thoroughly and placed on a thermal cycler. The cycling parameters were as follows; 25°C for 10 min, 37°C for 120 min, 85°C for 5 min followed by incubation at 4°C. The synthesised cDNA was then stored at -80°C. All of the experimental cDNA samples were diluted 1/40 in 10mM Tris (pH 8.0), plated in triplicate on 384 well plates, and stored at -80°C.

2.2.3 Quantitative real-time PCR – principles and calculations

Gene expression was analysed using the technique of quantitative real time-PCR with Taqman chemistry. This method relies on a DNA-based probe with a fluorescent reporter attached at one end and a quencher at the opposite end. The close proximity of the quencher to the fluorescent reporter prevents the emission and subsequent detection of any fluorescence. However, degradation of the probe by the 5' – 3' exonuclease activity of the Taq polymerase during the extension phase of the PCR cycle breaks the reporter-quencher proximity, thereby permitting the emission of fluorescence from the reporter. This fluorescence can be detected after excitation by a laser. An increase in the amount of product amplified with each subsequent PCR cycle therefore causes a proportional increase in the amount of fluorescence due to further probe breakdown and release of the fluorescent reporter.

To quantify gene expression, detected fluorescence is plotted against the number of cycles on a logarithmic scale. A threshold for detection was set above background, with the cycle at which fluorescence exceeded this threshold being known as the threshold cycle (Ct). This threshold was manually set within the exponential amplification phase of PCR,

during which the number of target DNA molecules (theoretically) doubles with each PCR cycle. In practice, however, the efficiency of amplification can vary between probes and samples so it is necessary to correct the data for this.

The efficiency of PCR amplification was assessed in a titration experiment in which a serially diluted DNA standard was used to create a standard curve of the change in Ct at each dilution. A cDNA standard comprising a pool of each sample was serially diluted 1/10, 1/20, 1/40, 1/80, 1/160, and 1/320 in 10mM Tris (pH 8.0), with this dilution series being used to assess the efficiency of the PCR reaction during real-time PCR.

The slope of the linear regression line can then be used to determine the efficiency (E) of amplification using the following calculation; $E = 10^{[-1/slope]}$. A reaction is 100% efficient if a dilution of 1:2 generates a difference in Ct of 1.

The data generated from real time PCR was analysed using the SDS 2.3 program (Applied Biosystems; Warrington, UK) and was used to quantify gene expression using the relative quantification method. Relative quantification of gene expression is based upon comparing a target gene with that of an internal reference gene so a fold difference in expression can be calculated.

Such normalised gene expression was calculated for each target gene using the Δ/ΔCt calculation (Pfaffl, M. W. 2001). This involved calculating the ΔCt of each sample using the following calculation (with the previously calculated efficiency value);

$$\Delta Ct = E^{[minCT-sampleCT]}.$$

The Δ/ΔCt for each target gene was then calculated by dividing the ΔCt of the target gene by the ΔCt of the stable internal reference gene. The average of the Δ/ΔCt was then calculated for each data point.

As the changes in target gene expression are normalised to that of an internal reference gene, it is critical such a gene is expressed uniformly across all experimental conditions as this allows pipetting or experimental error to be corrected for when calculating the Δ/ΔCt. Indeed, this important issue has been addressed in the context of quantifying gene expression in adipose tissue in a recent paper (Neville, M. J. *et al* 2011).

Given this, different reference genes were used that were found to be the most stable for each experiment. A variety of reference genes were analysed for each experiment, with their Ct values being assessed for each experimental condition. Only the most stable genes were used in the Δ/ΔCt calculation, with 'stable' being defined as a variation of less than 1.5 cycles between experimental conditions. Finding reference genes that fulfilled this criterion was fairly difficult given the broad-acting nature of azacytidine and dexamethasone, alone or in combination. Such investigation meant *GAPDH*, *PGK1*, *RPL4* and *PPIC* were discounted from any further calculations due to their substantial responses to these drugs.

PPIA and *18s* were used as reference genes in the dexamethasone-azacytidine co-administration experiments in male and female preadipocytes. *UBC* and *18s* were used to normalise gene expression in differentiation time-course experiments in both male and female preadipocytes, as well as the dexamethasone dose-response experiment performed in male preadipocytes.

2.2.4 Quantitative real-time PCR – equipment, gene expression assays, and reaction volumes

Messenger RNA levels were analysed by quantitative real time PCR using "Assays on Demand" gene expression assays (Life Technologies; Paisley, UK) with KlearKall 2x Master mix with standard ROX (LGC Genomics; Middlesex, UK). These reactions were

run on an Applied Biosystems 7900HT real time PCR machine (Applied Biosystems; Warrington, UK) in a final volume of 6µl; each well contained 2.7µl of cDNA; 3µl KlearKall 2x Master mix with standard ROX; and 0.3µl of the specific gene expression assay. Details of the specific gene expression assays are listed in table 2.2. The cycle parameters for real-time PCR were as follows; 95°C for 10 min followed by 40 cycles of 95°C for 15 sec and 60°C for 1 min.

In addition to the experimental samples and serially diluted cDNA pool being analysed, a no-template control (see section 2.3.2) and blank (10mM Tris, pH 8.0) were also included in triplicate to act as quality control measures to indicate possible contamination by foreign nucleic acids.

Table 2.2 Gene expression assays

Gene	Abbreviation	Assay ID
Eukaryotic 18s ribosomal subunit (rRNA)	*18s*	Hs99999901_s1
Peptidylprolyl isomerase A (cyclophilin)	*PPIA*	Hs99999904_m1
Peptidylprolyl isomerase C (cyclophilin)	*PPIC*	Hs00181460_m1
Glyceraldehyde-3-phosphate dehydrogenase	*GAPDH*	Hs02758991_g1
Phosphoglycerate kinase 1	*PGK1*	Hs99999906_m1
Ubiquitin C	*UBC*	Hs00824723_m1
60s Ribosomal protein L4	*RPL4*	Hs01939407_m1
T-box 5	*TBX5*	Hs01052567_m1
T-box 15	*TBX15*	Hs00537087_m1
Single-minded homologue 1	*SIM1*	Hs00231914_m1
Cartilage oligomeric matrix protein	*COMP*	Hs00164359_m1
Homeobox A5	*HOXA5*	Hs00430339_m1
Homeobox C8	*HOXC8*	Hs00224073_m1
Fatty acid synthase	*FASN*	Hs00188012_m1
Peroxisome proliferator-activated receptor gamma*	*PPARG*	Hs00234592_m1
Leptin	*LEP*	Hs0017877_m1
Fatty acid synthase	*FASN*	Hs00188012_m1
DNA methyltransferase 1	*DNMT1*	Hs00945899_m1
DNA methyltransferase 3a	*DNMT3A*	Hs00602456_m1
DNA methyltransferase 3b	*DNMT3B*	Hs01003405_m1
R-Spondin 3	*RSPO3*	Hs00262176_m1
HOX antisense transcript	*HOTAIR*	Hs03296631_m1
Tryptophanyl tRNA synthetase 2 (mitochondrial)	*WARS2*	Hs00210571_m1

* Note that the *PPARG* assay does not discriminate between the PPARγ1 and PPARγ2 isoforms.

2.3 Analysis of DNA methylation status

In this project, the methylation status of DNA was analysed using *bisulfite-pyrosequencing*. An overview of the pyrosequencing process is presented in figure 2.1.

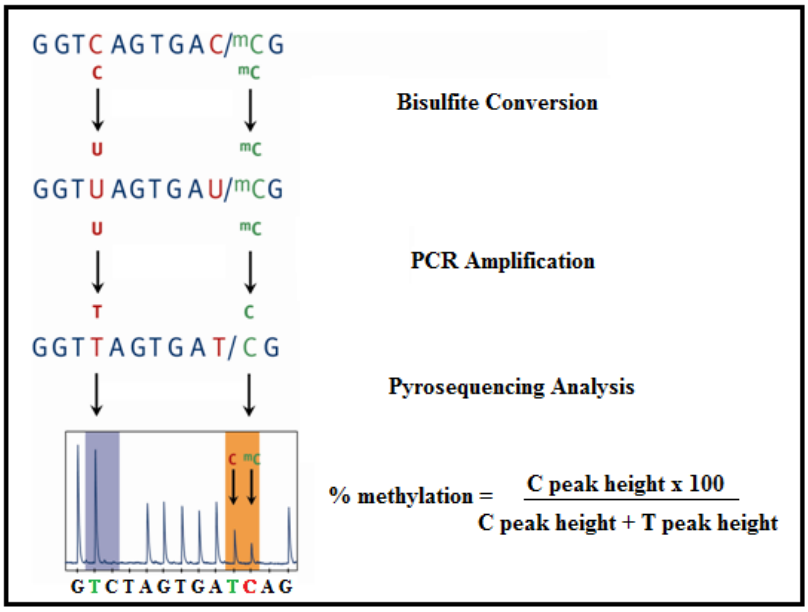

Figure 2.1 - *Overview of bisulfite-pyrosequencing technique*. Bisulfite conversion of DNA (in which unmethylated cytosine residues are converted to uracil residues) is outlined in section 2.3.2. The region of interest to be sequenced undergoes amplification by bisulfite PCR (sections 2.3.3 - 2.3.5) before pyrosequencing, a technique which can analyse the methylation status of CpG dinucleotides (sections 2.3.6 – 2.3.11).

2.3.1 DNA extraction

For DNA extraction, the growth medium was removed from the preadipocytes before they were washed in PBS. The cells were then trypsinised and the pellet was collected and stored in a clean 1.5ml tube at -80°C before further processing. Genomic DNA was extracted from the cell pellets using the GenElute Mammalian Genomic DNA Miniprep kit (Sigma-Aldrich; Gillingham, UK) according to the manufacturer's protocol. This process involved initially lysing the cell pellet in a chaotropic salt solution that ensures thorough denaturation of macromolecules in the presence of proteinase K (to degrade the nucleosomal proteins that the DNA is wrapped around), with unwanted RNA being degraded by the addition of RNase A. The cell lysate mixture was then heated at 70°C for 10 min before being added to a MiniPrep column; the addition of ethanol causes the DNA to bind when the lysate is spun through a silica membrane in a micro-centrifuge tube. Contaminants were then washed away from the column before the genomic DNA was eluted in 100µl Tris-EDTA solution (10mM Tris-HCl, 0.5mM EDTA, pH 9.0).

The concentration of DNA was determined using a NanoDrop spectrophotometer (Thermo Scientific; Hemel Hempstead, UK). Only 1µl of each sample is required to determine its concentration, with the sample purity being assessed by the ratio of sample absorbance at 260 and 280nm. DNA purified from the kit had an A_{260} / A_{280} ratio between 1.6 – 1.9, which is generally accepted as 'pure' for DNA. Between 3 - 15µg DNA can be obtained from 1 x T75 seeded with 4 x 10^5 cells (depending on the experimental condition).

2.3.2 Bisulfite conversion of purified genomic DNA

Bisulfite conversion is the most commonly used technique to detect and quantify the methylation status of genomic DNA (Frommer, M. *et al* 1992). This technique involves (methylated) genomic DNA undergoing a coupled heat denaturation and sodium bisulfite treatment, which converts non-methylated cytosine residues into uracil but leaves methylated cytosine residues unaltered. The uracil residues present in the template DNA are replaced with thymine residues during the subsequent process of PCR amplification. This means the methylation profile of the genomic DNA can be deduced by pyrosequencing the bisulfite PCR product (see figure 2.1).

Bisulfite conversion of genomic DNA was achieved using the EZ DNA Methylation-Gold kit (Zymo Research; Cambridge, UK) according to a slightly modified version of the manufacturer's protocol. For each conversion reaction 400ng of genomic DNA was used. CT conversion reagent (supplied with the kit) was added to the genomic DNA and the sample was mixed thoroughly. The mixed samples were placed on a thermal cycler and heated to 98°C for 10 min followed by 64°C for 12 hr. The converted DNA was then washed and desulphonated in a spin column before being eluted in 10µl Tris-EDTA solution. PCR amplification of the converted DNA was performed straight after the bisulfite conversion process, with any excess bisulfite-treated DNA being stored at -80°C.

2.3.3 Bisulfite PCR primer design

To measure the methylation status in a region of DNA of interest, the region must first be amplified by PCR, a technique which involves using a pair of primers (forward and reverse) that encompass the region of interest. The design of these primers involved the use of several different programs. Firstly, the genomic nucleotide sequence of a CpG island of interest (plus an additional 100bp up- and downstream) was obtained from the University of California, Santa Cruz, (UCSC) genome browser at the following web address;

http://genome-euro.ucsc.edu/

This sequence information was then used in the freely available MethylPrimer program (Applied Biosystems; Warrington, UK) to design bisulfite-specific PCR primers. This software can simulate the bisulfite modification of the DNA sequence and design pairs of primers that encompass a region of interest within a given CpG island. As PCR products of approximately 200 – 400bp are of the optimal length for pyrosequencing (Tost, J. *et al* 2007), this influenced the choice of pre-designed primer pairs. It also meant that certain larger CpG islands were subdivided into several PCR products that could be analysed in separate reactions so good coverage could be achieved. Furthermore, certain regions within some CpG islands did not lend themselves to the placement of primers. This could be due to a high density of CpG dinucleotides (which may or may not get converted during bisulfite conversion) or long homopolymeric runs of a certain nucleotide, both of which make primer design difficult.

The program predicts the annealing temperature for each primer it designs using a formula that takes the GC content (ideally 40 – 60%) and primer length (18 - 30bp) into account; primer pairs with very similar / identical predicted annealing temperatures were chosen.

Primers were synthesised (Sigma-Aldrich; Gillingham, UK) as a desalt oligonucleotide that was resuspended in Tris-EDTA solution to obtain a 100µM stock which was stored at -30°C.

2.3.4 Bisulfite PCR

Once the primers were designed, the optimal reaction conditions had to be determined so that a good PCR product was generated in preparation for bisulfite-pyrosequencing. For this process, the optimal annealing temperature for the primer pair had to be identified; the predicted annealing temperature is a good reference point but can be (very) different from what temperature works in practice. To identify the optimal annealing temperature, a series of identical PCR reactions were set up and placed on a MJ Research PTC-225 thermal cycler (GMI; Minnesota, USA) with a temperature gradient that spanned the predicted annealing temperature (this was typically from 55°C to 65°C) being performed at the annealing stage of the PCR cycle.

A great deal of molecular genetics research has highlighted that PCR amplification of GC-rich sequences can be difficult due to the formation of secondary structures and mis-priming. This has prompted a search for ways to enhance reaction efficiency for such sequences, with the use of certain additives to the bisulfite PCR reaction being one such method. In addition to the series of no-additive bisulfite PCR reactions, two other series of bisulfite PCR reactions were run in parallel; one containing 1M betaine (Sigma-Aldrich; Gillingham, UK) and the other 1% dimethyl sulfoxide (DMSO - Sigma-Aldrich; Gillingham, UK). These organic reagents were chosen as they have previously been found to be effective for amplifying GC-rich regions (Jensen, M. A. *et al* 2010). The bisulfite PCR reactions containing additives were also ran across a temperature gradient at the annealing stage.

If no PCR product was generated under any of these conditions, the temperature gradient was repeated with another series of bisulfite PCR reactions containing an increased concentration of betaine or DMSO until a PCR product was generated. Betaine was found to be the most effective additive overall.

Each bisulfite-PCR reaction was 50µl in total; 2µl of bisulfite converted DNA was used (80ng) along with 48µl bisulfite PCR master mix. Titanium Taq buffer (Clontech; Saint-Germain-en-Laye, France), Titanium Taq polymerase (Clontech; Saint-Germain-en-Laye, France), and a 10mM deoxynucleotide mix (Thermo Scientific; Hemel Hempstead, UK) were used in the bisulfite PCR reactions.

Note that the forward and reverse primers were used at a concentration of 10µM (i.e. the 100µM primer stocks were diluted 1:10 in Tris-EDTA solution). A no template control (in which 2µl dH_2O was added to 48µl bisulfite PCR master mix) was included for each reaction type to act as a negative control which could be used to indicate the presence of any contamination by foreign nucleic acids. In addition, a positive control was ran in parallel which involved using a set of primers known to work and 2µl of bisulfite-converted DNA from the same batch of recently bisulfite-converted DNA.

Reagent volumes per reaction are listed in table 2.3 whereas the thermal cycling parameters are listed in table 2.4. Thermal cycling was performed 48 times in an attempt to completely exhaust any primers in the reaction mix so they would not interfere with the pyrosequencing. A representative example of the process of primer optimisation (both temperature gradient and the use of PCR additives) is depicted in figure 2.2 in which the primer set for the *COMP_1* amplicon was used.

Table 2.3 Composition of bisulfite PCR reactions

Reagent	No additive (µl)	1% DMSO (µl)	1M Betaine (µl)	2M Betaine (µl)
dH2O	38.5	37.5	27.5	17.5
10x Titanium Taq Buffer	5.0	5.0	5.0	5.0
dNTPs (10mM)	1.0	1.0	1.0	1.0
Forward Primer (10µM)	1.5	1.5	1.5	1.5
Reverse Primer (10µM)	1.5	1.5	1.5	1.5
50x Titanium Taq	0.5	0.5	0.5	0.5
5M Betaine	/	/	10	20
100% DMSO	/	1.0	/	/

Table 2.4 Thermal cycling parameters for bisulfite PCR

Step 1	95°C for 1 min
Step 2	95°C for 30secs - *Denaturation*
Step 3	Primer-specific temperature or temperature gradient for 30secs – *Annealing*
Step 4	72°C for 30secs - *Extension*
Step 5	Go to **step 2** 47 times
Step 6	Incubate at 4°C

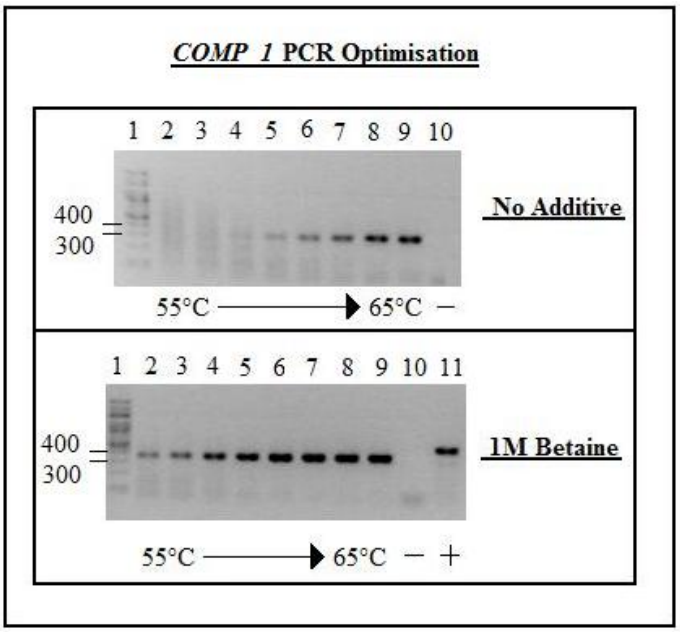

Figure 2.2 - *Optimisation of COMP_1 primers.* A 100bp DNA ladder was run in lane 1, with bisulfite PCR reactions performed across a temperature gradient run in lanes 2 – 9; the COMP_1 amplicon is 376bp in length. No-template control reactions (indicated by the '-' sign) were run in lane 10, whereas a positive control (indicated by the '+' sign; the *COMP_2* amplicon, 418bp) was run in lane 11. The 2% agarose gel was run for 25 mins at 110V and the PCR products were visualised with ethidium bromide.

Once the optimal conditions for a given primer set had been deduced, a 5'-biotinylated reverse primer was synthesised (Sigma-Aldrich; Gillingham, UK) as a desalt oligonucleotide. This was resuspended in Tris-EDTA solution to generate a 100µM stock solution, with a 10µM primer solution being used in the bisulfite PCR reaction (see table 2.3). The PCR primers and their optimal reaction conditions are listed in table 2.5.

Table 2.5 Bisulfite PCR primers and their optimal conditions

Amplicon	Forward Primer	Reverse (biotinylated) Primer	Amplicon size (bp)	Annealing temp (°C)	Additive
COMP_1	GTGTTGGGATTATAGGAGTGAA	AAACACCCACTTACACTCTCC	376	63	1M betaine
COMP_2	GGAGAGTGTAAGTGGGTGTTT	AACCTCTAAATTCCCCTCCC	418	64	1M betaine
COMP_3	GGAGAGGAGAGGAGAGTTGTT	CCCAACCCAAAAACCATCCC	300	62	2M betaine
SIM1_2	TTGGTTGTTTAGTAGGGGTTG	CTCCAATTCATAATCCAAAAAAA	337	59	1M betaine
TBX5_1	TTTTAGAAGAAAGGGTTTTAAAGAAT	ACAAACTAATACAACAACCTAAAC	269	59	1M betaine
TBX5_2	GGGAGTAGTGGGTATTGAGTAG	ATACACATCCTAATAAAAAATAA	248	56	1M betaine
TBX5_5	TAGTTTAAGGTTGGTTTGTGGT	TAAAAAATTCCCTCCTCTCC	388	63	1M betaine
TBX15_1	TTGTATTTAATATGGATTTTTAAGGAA	TAAACCCCCTAACCTAAACTTT	378	56	1M betaine

Experimental bisulfite-converted genomic DNA samples were amplified using normal forward and biotinylated reverse primers so that the resultant PCR product could be bound by sepharose beads and subsequently picked up by the vacuum station tool in preparation for bisulfite-pyrosequencing.

2.3.5 Detection of PCR products by agarose gel electrophoresis

After amplifying the region of interest using PCR, the presence of a PCR product was confirmed before proceeding with bisulfite-pyrosequencing. This process involved

performing agarose gel electrophoresis in which negatively charged DNA molecules are moved through an agarose gel matrix towards the positive electrode upon application of an electrical field. Note that this technique can be used to separate a mix of DNA fragments on the basis of length (in which smaller fragments migrate faster than larger ones), but in this instance it was simply used to identify the presence of a PCR product of the correct size. The separated DNA can be visualised with ethidium bromide, which fluoresces under UV light.

A 2% agarose gel was used as it provides good resolution for small DNA fragments of approximately 200 – 1000bp. These 2% gels were made by dissolving agarose powder (VWR International; Lutterworth, UK) in 1x Tris/Borate/EDTA (TBE) buffer (0.089M Tris-Borate, pH 8.3 plus 2mM Na_2EDTA – Geneflow Limited; Lichfield, UK); this solution was heated in a microwave to completely dissolve the agarose. It was then allowed to cool, at which point 2µl ethidium bromide (Sigma-Aldrich; Gillingham, UK) was added per 100ml gel and mixed. The gel was poured into a mould with combs in place (to make wells for loading DNA) and allowed to set. The combs were then removed and the set gel was subsequently placed in a gel electrophoresis tank and submerged in 1x TBE buffer before the DNA samples were loaded. A further 5µl ethidium bromide was added per litre of TBE buffer near the positive electrode.

5µl of the 50µl biotinylated bisulfite PCR product was mixed with 5µl loading buffer (30% glycerol and orange G dye); the remaining 45µl was stored at -30°C before bisulfite-pyrosequencing. The loading buffer contains a dense compound (i.e. glycerol) which raises the density of the DNA sample so that it sinks to the bottom of the well in the gel. A 100bp molecular weight ladder (New England Biolabs; Hitchin, UK) was run in parallel with the experimental PCR products so that their size could be assessed visually. The samples were electrophoresed through the agarose gel at 110V for 25 min. After running a gel the

samples were visualised using a Gel Doc 2000 scanner (Bio-Rad; Hemel Hempstead, UK) under UV light with the images captured using the Quantity One program (Bio-Rad; Hemel Hempstead, UK). Only samples that generated a single strong PCR band were taken forward for bisulfite-pyrosequencing.

2.3.6 Bisulfite-pyrosequencing primer design

Before the bisulfite PCR products underwent pyrosequencing, sequencing primers were designed. These are short oligonucleotides (10 - 25bp) that anneal to the single stranded PCR product at a specific site. Pyrosequencing utilises the principle of 'sequencing by synthesis' (this is discussed in more detail in section 2.4.8), with the 3' end of the sequencing primer acting as the start site for nucleotide incorporation and therefore synthesis.

Optimal placement of a sequencing primer within a PCR product requires the consideration of several factors. Firstly, a primer must not be placed across any CpG dinucleotides (as these sites may have been altered during the bisulfite conversion – this would depend on their unknown methylation status). Secondly, the primer must contain a sequence that is unique within the PCR product to prevent it annealing to multiple sites. To meet the high degree of specificity required for accurate pyrosequencing, homopolymeric runs of certain nucleotides must be avoided; this can be more difficult than initially thought, as long homopolymeric runs of Ts can be generated after the bisulfite conversion of DNA.

The free-to-use online MethMarker program (Max Planck Institute) was used to assist in the process of primer design.

http://methmarker.mpi-inf.mpg.de/

The optimal length of a single pyrosequencing run ranges from 30 - 120 nucleotides from the 3' end of the sequencing primer (Tost, J. *et al* 2007). This means that complete coverage of a 300 - 400bp PCR product typically required 3 sequencing primers which annealled at different sites. Although the single stranded PCR product can be recaptured, annealed to another sequencing primer and re-sequenced from a different starting position, potential degradation of the template DNA can occur that may negatively influence the quality of sequencing that can be performed. As a result of this, separate PCR products were used for each sequencing primer for a given region of interest. The details for each sequencing primer are listed in table 2.6.

Table 2.6 Sequencing primers for bisulfite-pyrosequencing

Amplicon	Sequencing primer 1	Sequencing primer 2	Sequencing primer 3
COMP_1	GTAGATTTATTTTTTTATTGGGGAT	GTTGGGTATAGTTA	GTTTAGGTTAGTG
COMP_2	GTTTTAAGTTTAGTT	GTATTGGAAGGAGTTTTG	GTATTGGAAGGAGTTTTG
COMP_3	GTATTTTTAGTAGAGGGGGGTAGGGGT	GTTTTTTGGTTGTGGAAGG	AGGAGGGTAGTTGGG
SIM1_2	GTTAGGTTAATAGGT	GGTTTTTTTTATATTAT	GGGGTTGTTGGG
TBX5_1 *	TTTYGATGGTTGGTTAG	GTTAAATTTYGGGAAGTAG	TYGTAYGGAAAGTAGAAGG
TBX5_2 *	TTGTYGGGAGAAAGATGTT	TTAYGGGTATTAAAATGG	RTAGTTTGTTTTTTATAGT
TBX5_5	TAAAGAGGTAATTAGG	GTTTGGTTGGGGGGTAG	GGGAATAAATAAAG
TBX15_1	GAGTGTAGAGAAAG	GGTTTAGATATAGTT	GGAAAGAGTTGGGTT

* Note that R denotes A or G whereas Y denotes C or T.

The sequencing primers were synthesised (Sigma-Aldrich; Gillingham, UK) as desalt oligonucleotides and resuspended in Tris-EDTA solution to generate a 100µM stock solution. These stocks were then stored at -30°C.

2.3.7 Preparation of bisulfite PCR products for pyrosequencing

Once the presence of a bisulfite PCR product had been confirmed using agarose gel electrophoresis (i.e. a single strong band was detected – see section 2.3.5), the remaining 45µl of biotinylated bisulfite PCR product was taken forward for pyrosequencing. Before the biotinylated (double-stranded) bisulfite PCR products could be pyrosequenced the strands were first separated. The biotinylated single-stranded PCR products were then annealed to their respective sequencing primer before bisulfite-pyrosequencing.

To prepare a biotinylated bisulfite PCR product for processing on the vacuum preparation station (Qiagen; Manchester, UK), a binding buffer (Qiagen; Manchester, UK) and streptavidin-coated sepharose beads (GE Healthcare; Hatfield, UK) solution was made (for 1 x 96 well plate - 2ml ddH2O, 3.7ml binding buffer; and 0.3ml sepharose beads) and 40µl was added to each PCR product. This mixture was then shaken at room temperature on a plate shaker at 1050rpm for 15 min; this physical agitation allowed the streptavidin-coated beads to interact and bind with the biotinylated PCR product so the PCR product can be picked up by the vacuum station tool for further processing.

During the process of mixing the PCR product with the beads, the PSQ96 low read plate (Qiagen; Manchester, UK) on which the pyrosequencing reaction will occur was prepared. The sequencing primers were first diluted from their stock solutions; for one 96-well plate, 8µl of 100µM sequencing primer was dissolved in 1992µl annealing buffer (Qiagen; Manchester, UK). After mixing thoroughly, 40µl of this diluted sequencing primer solution was added to the appropriate well of the low read plate in preparation for bisulfite-pyrosequencing.

After mixing the biotinylated PCR product with streptavidin-coated sepharose beads, the 96-well PCR plate was then placed onto the vacuum tool station. The vacuum tool was

turned on and lowered onto the PCR plate to pick up the sepharose bead-bound PCR product. The bead-bound PCR product was then washed in 70% ethanol solution before being placed into denaturation solution (Qiagen; Manchester, UK); this solution denatures the double stranded PCR product to leave a single stranded DNA strand (i.e. the strand which has incorporated the biotinylated reverse primer). The bead-bound single-stranded PCR product was then cleaned in wash buffer (Qiagen; Manchester, UK) and then washed in ddH_2O. After this, the vacuum station tool was turned off, placed onto the low read plate and manoeuvred so that the bead-bound single stranded PCR product was released into the sequencing primer-annealing buffer solution.

In order to capture as much PCR product as possible, 50µl of a binding buffer solution (for 1 x 96-well plate – 3ml ddH2O, 3ml binding buffer) was added to each well that previously contained bisulfite PCR product (and consequently the sepharose bead solution). Any remaining beads were resuspended by shaking the 96-well PCR plate back on the plate shaker for 10 min, with the vacuum tool procedure described in the paragraph above being repeated in a bid to deposit the maximal amount of PCR product in the low read plate in preparation for pyrosequencing.

After the vacuum tool stage, the processed low read plate was then placed on a sample preparation heat block set at 80°C for 2 min on a thermal cycler. Once this time had elapsed, the low read plate (still placed on the heat block) was allowed to cool to room temperature. The gradual cooling of the heat block (and therefore low read plate) provided a temperature gradient to permit the sequencing primer to anneal to the template DNA (i.e. the single stranded PCR product) at its optimal temperature, thereby preparing the sample for pyrosequencing.

2.3.8 Principle of bisulfite-pyrosequencing

Bisulfite-pyrosequencing is a sequencing-by-synthesis method that relies on the sequential addition and consequent incorporation of a nucleotide into a nascent oligonucleotide in a primer-directed polymerase-catalysed reaction. The DNA polymerase is exonuclease-deficient to prevent primer degradation. An added nucleotide will only be incorporated into the nascent oligonucleotide if it is complementary to the template DNA; if successful, this event is accompanied by the emission of light which can be monitored in real-time (Tost, J. *et al* 2007; Ronaghi, M. 2001). The intensity of the light signal generated is proportional to the number of nucleotides incorporated. This technique allows the accurate quantification of the degree of methylation of several CpG dinucleotides in close proximity with high resolution. Pyrosequencing utilises a four enzyme system and the pyrophosphate (PPi) released upon nucleotide incorporation to an oligonucleotide to generate a bioluminometric signal that can be subsequently detected. The basic chemistry is presented in figure 2.3.

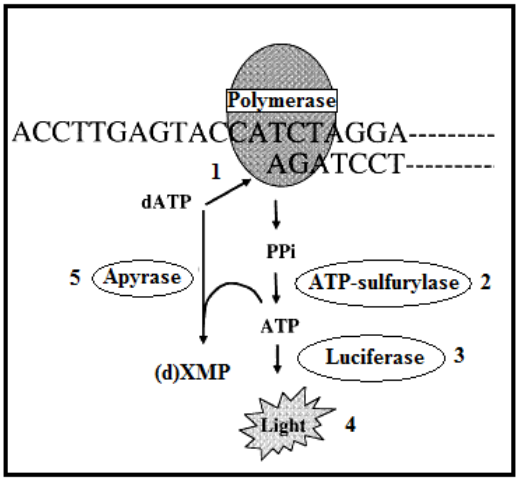

Figure 2.3 - *Chemistry of pyrosequencing*. When a complementary nucleotide (denoted by d(XMP)) is incorporated into the nascent oligonucleotide by a DNA polymerase (step 1), PPi is released and converted into ATP by ATP sulfurylase (step 2). This ATP then drives the luciferase-mediated oxidation of luciferin to oxyluciferin (step 3) which is generated in an excited state but subsequently relaxes to its ground state. During this relaxation a photon (λ = 560 nm) is emitted and detected by a charge-coupled device (CCD) camera (step 4). Unincorporated nucleotides (including excess ATP which can act as a substrate for the DNA polymerase) are degraded by apyrase (5) before the next nucleotide is added to the reaction mix according to dispensation order. Diagram adapted from Ronaghi, M. 2001.

2.3.9 Programming the Q-CpG software (version 1.0.9)

Before any single stranded bisulfite PCR product underwent pyrosequencing, the software - namely the Q-CpG program (Qiagen; Manchester, UK) – was first programmed. Note that for each sequencing primer a different region of the bisulfite PCR product was analysed, meaning that a different sequence of nucleotides was required in each respective well. The Q-CpG software generated a dispensation order for each pyrosequencing reaction (as defined by the sequencing primer used and the number of downstream nucleotides sequenced) when the nucleotide sequence to be analysed was input to the program. Each CpG dinucleotide was detected and designated as C / T (so C and T were sequentially dispensed at these sites). The methylation status of a CpG dinucleotide was then calculated using the following formula;

% methylation = C peak height x 100 / (C peak height + T peak height).

The program also included several negative control steps (in which a different nucleotide to the one expected is injected into the well and so should not be incorporated into a non-contaminated sample) by default. Each pyrosequencing assay also included an internal positive control step to assess the efficiency of the bisulfite conversion stage. This involved analysing the C / T ratio of a cytosine residue known to be converted to a thymine during the bisulfite conversion stage (i.e. a non-CpG cytosine residue); the C / T conversion rate should be 100% for efficient bisulfite treatment. Incomplete bisulfite conversion can lead to overestimation of the methylation status of any CpG dinucleotides analysed.

A table outlining the dispensation order for each sequencing primer and PCR product is listed in table 2.7.

Table 2.7 Dispensation orders for pyrosequencing reactions

Amplicon	Sequencing Primer	Dispensation order
COMP_1	1	ATCTGTTCAGTCGCTGATCGTATCGTATGTCAGTTCGATGTGATCTGTC
	2	ATCGCTAGTGTTGGTCGTATAGAGTGTGAGGTCTGTCGTATGATGTTC
	3	GTCTGTTCAGTTCGTTATATTGATCGCTATAGTCGTTGTATGTCGTATGTTCAGTCGATGTC
COMP_2	1	ATCTGTCGCTATATGATCGTGATCGTATCAGTCGAGTGATCTGTCGTTAGTATCGT
	2	ATCGTGCTGATCGTAGTCGATGTCAGTCGGTAGATGTCGTGTAGTCTGTCAGTCGTGTAGTGTATC
	3	ATCTGTCGATGTCAGTCGAGTATGTCGCTATGTCAGTCTGTCAGTCGTTGATTCTGTC
COMP_3	1	GTCTGTCGGTCGTAGTCGTAGTCTGTCGTAGTCGGTAGTCGTAGTCGCTT
	2	TGTCGTGATAGTCGATTAGTCTGTCGAGAGCTAGTGGTCGA
	3	TGTCGACTATTAGTCGTGAGATGTCAGTCGGAGTCTGTCG
SIM1_2	1	AGTCTGTCAGTCTGTCGACTATGTTCGTATGTTCGGTGATGTCAGTCTGTC
	2	GTCTGTCGAGTAGTCGGCT
	3	GTCTGTCAGTCGGTCGTTGTTATATTAGTTACTATGTCGTAGATGTTCGGTC
TBX5_1	1	ATCTGTCAGTCGCTATAGTCGTATGTGATTCGAG
	2	ATCTGTCGAGAGCTG
	3	GTCGAGTGTAGTGTTAGTTCGTTATGTTCGTAGTCGTGAGTGATCTGTCAGTCGCTA
TBX5_2	1	AGTCGTTGCTATGTCGTGATCAGTCGTTAATTATGTCG
	2	ATCGAGCTGATCGTT
	3	TATCGTGATCGTAGTCGCTAGATATATATATATATATGATCGTATGATCGATATATATGATC
TBX5_5	1	ATCGATATGTCGATATTATATGTCGTGTATATAGATGAGTATCGTGATCGAGTGATCGCTGATCAGTCTGTCAGTCGTGTGATC
	2	GTCTGTCGAGTGATTCAGTTCGTATAGTAGTCGTAGTCGTAGTACTATGTTCGTATCGTTAGTTC
TBX15_1	1	ATGATCGCTATGTCGATGTCGTTAGTAGTGAATCAGTTCGTATTCAGTCGATATGTC
	2	GTCGATTAGCTTAGTGTTAGTCGAGTATCGTT
	3	ATCGGTCGGACTAGATGAGAGTAGTAGTATGTCGTGTATCGAT

2.3.10 Pyrosequencing

Once the dispensation order for each sequencing assay was generated by the Q-CpG software, the various assays were assigned to specific wells on a 96-well plate (which corresponds to the layout of the PSQ96 low read plate, in which a well will contain a given single stranded PCR product annealed to its respective sequencing primer). After the layout of a plate to undergo pyrosequencing had been finalised, the required volumes for each PyroGold™ reagent (Qiagen; Manchester, UK) were calculated (namely the enzyme and substrate mixes, as well as each individual nucleotide). These were consequently added to the appropriate well of the pyrosequencing cartridge.

Pyrosequencing was started once the low read plate (containing the single stranded PCR product annealed to its sequencing primer) was placed in the PSQ96 ID machine (Qiagen; Manchester, UK) along with the loaded pyrosequencing cartridge.

2.3.11 Analysis of pyrosequencing results

Once the pyrosequencing run was completed, the 'CpG statistics' file was downloaded from the Q-CpG software. This data file contains the ratio of C / T incorporation (and therefore methylation) at each CpG dinucleotide analysed presented as a percentage; 100% indicates a completely methylated cytosine (in which no thymine was incorporated), whereas 0% indicates a completely unmethylated and therefore fully converted cytosine residue in which only thymine was incorporated into the nascent oligonucleotide.

The methylation status of a given CpG dinucleotide is presented as a percentage. Although a given cytosine residue in a CpG dinucleotide may or may not be methylated in an all-or-none fashion on a single DNA molecule, the PCR product being sequenced had been generated by amplifying a region of interest in which the template DNA comprised a pool

of DNA obtained from a population of cells; there may be variation in the methylation status at a specific CpG dinucleotide within the cell population. Therefore, the percentage reflects the proportion of DNA molecules in the pool of DNA used as template for the PCR reaction that were methylated at the CpG dinucleotide in question.

For each experiment performed in this project (in which dexamethasone and / or 5-azacytidine was administered to preadipocytes with the methylation status of genomic DNA being consequently analysed by pyrosequencing), the methylation status of a given CpG dinucleotide was calculated by averaging the methylation percentage at each analysed position across 3 – 4 experiments (i.e. n = 3 / 4 for each CpG dinucleotide). Data were only included in the calculations if generated in a pyrosequencing reaction that had passed the internal quality control stage, with each pyrogram being inspected visually to check for any anomalies.

2.4 Statistical analysis

All data (normalised gene expression and CpG methylation) are presented as the mean ± standard error of mean (SEM). Statistical analyses were performed using SPSS (version 20), with a *P* value < 0.05 being considered statistically significant.

2.4.1 Analysis of gene expression in the differentiation time-course

Gene expression analyses which compared abdominal and gluteal tissue for each gender were performed separately. Data were analysed using a repeated measures analysis of variance (ANOVA) test in which depot and time-point were independent variables.

2.4.2 Analysis of gene expression in response to dexamethasone and / or 5-azacytidine

Gene expression analyses which compared abdominal and gluteal tissue for each gender were performed separately. Data were analysed using a two-way ANOVA test in which depot and drug treatment were independent variables.

2.4.3 Analysis of CpG methylation status

The methylation status of a given CpG was calculated by averaging the data from 3 - 4 experiments. Inter-depot differences of the methylation status of a particular genomic region within a cell line were analysed using a T-test.

3 Results

Results

3.1 Selection of candidate genes

Two substantial datasets comprising the gene expression and DNA methylation profiles of abdominal and gluteal subcutaneous adipose tissue had been generated prior to the current project. These data were used to guide the selection of candidate genes suitable for further investigation. Global gene expression profiles were analysed using total RNA extracted from whole subcutaneous abdominal and gluteal adipose tissue biopsies taken from 30 females and 40 males (n=70) aged between 39 – 56 whose BMI ranged from 20.7 – 45.5 using Affymetrix HGU133 Plus 2 arrays (Affymetrix; Santa Clara, USA).

To complement the microarray study, a differential methylation hybridisation (DMH) array (Epigenomics AG; Berlin, Germany) was performed in DNA extracted from paired subcutaneous abdominal - subcutaneous gluteal whole adipose tissue biopsies from 12 females. This was supplemented with DNA from a further 28 subcutaneous abdominal biopsies (20 males, 8 females). The DMH array contained probes to detect 430 differentially methylated genes, 13,500 CpG rich promoter regions and 13,650 CpG rich regions in gene bodies.

These studies identified differentially expressed genes as well as differentially methylated genomic regions between these two subcutaneous adipose depots. A combined dataset was also generated, in which correlations between methylation and the expression of genes located in close proximity (i.e. within 250 kb) to probes on the DMH array were calculated.

Several highly differentially expressed and / or methylated genes were identified from these datasets and taken to the next stage of selection. Certain selection criteria had to be

met for a gene to be eligible for further study. Given that DNA methylation in the regulation of depot-specific gene expression was a key focus of this project, a gene was only included if an upstream CpG island was located within 1 kb of the gene using the UCSC genome browser. Once this criterion was met, a literature search was performed; genes were only included if they were considered potentially relevant to WAT physiology. The final list of candidate genes identified for further study is outlined in table 3.1.

Table 3.1 Background information on selected candidate genes

Gene ID	Expression pattern	*P*-value	Methylation pattern *	*P*-value	Comments
TBX5	High in Abd	$3.1x10^{-6}$	High in Abd	$7x10^{-7}$	Developmental regulator
TBX15	High in Glut	$5.2x10^{-6}$	High in Abd	$3.2x10^{-6}$	GWAS hit for body fat distribution (WHR)
COMP	High in Glut	$3.5x10^{-6}$	N/A	N/A	Extracellular matrix protein
HOXA5	High in Abd	$2.9x10^{-18}$	N/A	N/A	Depot-specific expression retained *in vitro*
SIM1	N/A	N/A	High in Glut	$8.6x10^{-6}$	Variants associated with severe obesity.
HOTAIR	High in Glut	$3.8x10^{-18}$	N/A	N/A	Most differentially expressed gene identified
ISL1	N/A	N/A	High in Glut	$2x10^{-7}$	Developmental regulator
RSPO3	High in Abd	$4.8x10^{-12}$	N/A	N/A	GWAS hit for body fat distribution (WHR)

* This data refers to the gene closest to a differentially methylated **probe**; the genes themselves were ***not*** differentially methylated.

To investigate the nature of these candidate genes, two paired preadipocyte cell lines comprising immortalised subcutaneous abdominal and gluteal preadipocytes derived from an individual male and another from an individual female were used. For simplicity these cell lines will be referred to as ‘male’ and ‘female’ abdominal / gluteal preadipocytes. However, their characteristics should ***not*** be interpreted as representative of either gender.

These cell lines are a useful and valid model of preadipocytes as they exhibit a faster proliferation rate and also retain their ability to differentiate (Darimont, C. *et al* 2003).

3.2 Depot-specific gene expression in subcutaneous preadipocyte cell lines

The expression pattern of the candidate genes selected for further investigation was analysed in untreated subcutaneous abdominal and gluteal preadipocytes from both male and female cell lines, with the data presented in figure 3.1.

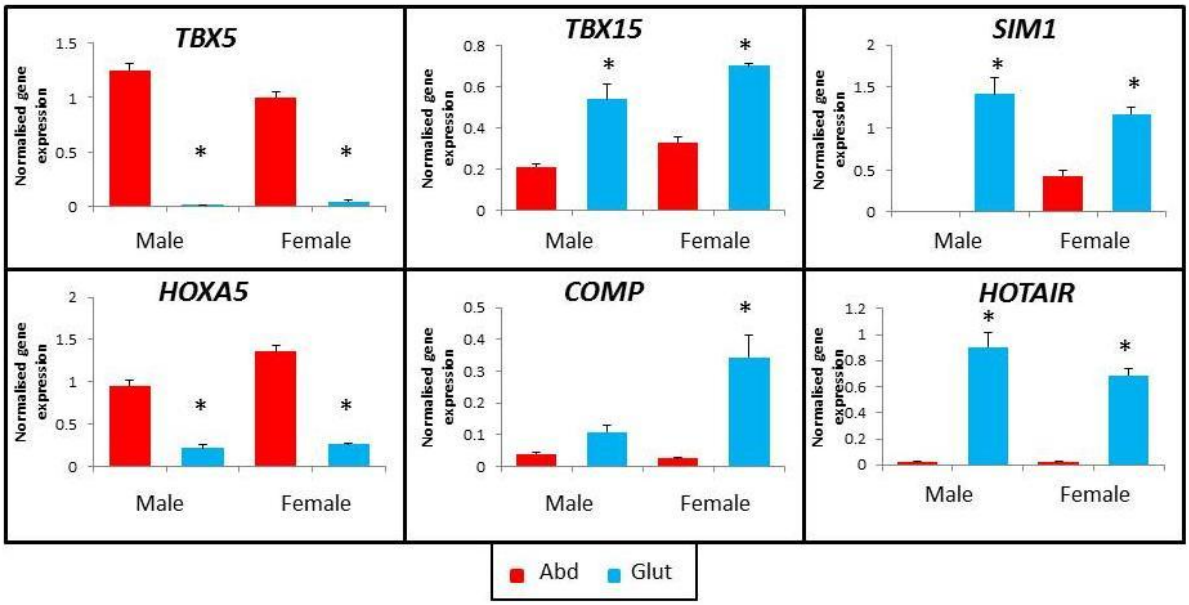

Figure 3.1 - *Depot-specific gene expression profiles exhibited by two paired preadipocyte cell lines.* The basal expression of candidate genes was analysed in untreated abdominal (Abd) and gluteal (Glut) preadipocytes from both male and female cell lines. Expression was normalised to *18s* and *PPIA*. Data are presented as mean ± SEM of male (n=6) and female (n=5) preadipocyte cell lines and were analysed using a two-way ANOVA. * indicates $P<0.05$ compared to abdominal tissue of the same sex.

It is evident that the depot-specific expression pattern of each candidate gene is the same in both untreated preadipocytes from male and female cell lines. Furthermore, the observed expression patterns replicated and verified the microarray data used during the selection of these candidate genes. Indeed, *TBX5* and *HOXA5* were highly expressed in abdominal preadipocytes, whereas *TBX15*, *HOTAIR*, and *COMP* were more highly expressed in gluteal preadipocytes (albeit the higher expression of *COMP* in male gluteal preadipocytes

did not reach significance). *SIM1* was also included for analysis as it was associated with a highly differentially methylated locus on the DMH array; gene expression analysis indicated it was expressed in a depot-specific manner, being more highly expressed in gluteal preadipocytes.

The expression data for several other genes that initially met the inclusion criteria for further study has not been shown. Firstly, although the microarray data indicated that ***RSPO3*** is more highly expressed in abdominal tissue, its' expression could not be detected using cDNA diluted 1/40. For this reason, the *RSPO3* data is not shown and the gene was not included in further studies. Secondly, data from the microarray and DMH array suggested that ***ISL1*** is located within 250 kb of a highly differentially methylated locus between abdominal and gluteal depots and that its expression was positively correlated with methylation. However, its expression was also undetectable when using cDNA at a dilution of 1/40, so the data has not been shown and this gene was not studied any further.

Therefore, data generated by the microarray investigation was replicated and verified in two paired preadipocyte cell lines. Together these data support the notion that preadipocytes exhibit depot-specific gene expression profiles that can be retained during *in vitro* culture, even after immortalisation.

3.3 Differentiation of subcutaneous abdominal and gluteal preadipocyte cell lines

In addition to analysing the depot-specific basal expression of the various candidate genes in untreated male and female preadipocytes, their pattern of expression during adipogenesis was also studied. Abdominal and gluteal preadipocytes from both cell lines were cultured in differentiation medium for 14 days, with samples taken for gene expression analysis on days 0, 2, 4, 7, and 14. For the first four days, the PPARγ agonist troglitazone and IBMX were also added to the differentiation medium.

To ensure that proper differentiation occurred, the expression of several adipogenic markers was analysed and the accumulation of lipid was assessed visually. This data is presented in figure 3.2. Overall, the expression of the adipogenic markers *PPARγ* (*PPARG*), *fatty acid synthase* (*FASN*), and *leptin* changed significantly during the 14 day time course, as shown in figure 3.2A. Gene expression typically increased at day 4 or 7.

Leptin expression started to increase at day 7 and peaked by day 14 in both cell lines (albeit non-significantly in male preadipocytes), which agrees with it being a late marker of adipogenesis. Although the expression profile of *PPARG* exhibited by the male preadipocytes was characteristic of an archetypal adipogenic gene, this was not the case for all markers analysed. For instance, *FASN* expression peaked at day 7 but this level of expression was not maintained until day 14 in male preadipocytes and female abdominal cells. Increased *PPARG* expression was also not maintained in female preadipocytes.

Despite these expression patterns, proper adipogenesis *did* occur in both male and female cell lines, as mature adipocytes from both depots accumulated substantial amounts of lipid by day 14. Images of male preadipocytes at day 0 and lipid-laden adipocytes at day 14 are provided as a representative example in figure 3.2B.

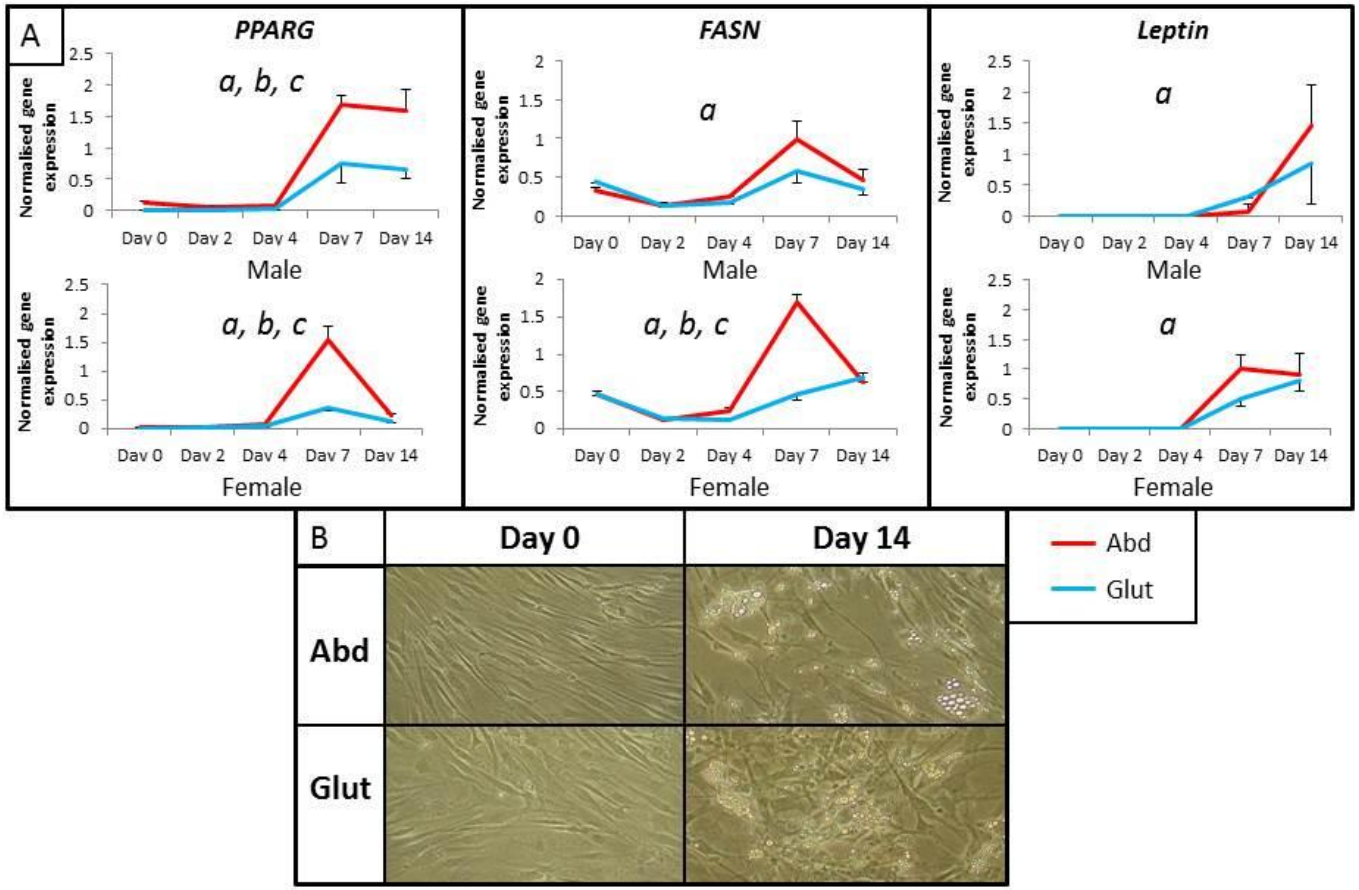

Figure 3.2 – *Expression of adipogenic markers and accumulation of lipid over a 14 day differentiation time course.* **A** – Expression of certain markers of adipogenesis was analysed in abdominal (Abd) and gluteal (Glut) preadipocytes from both male and female cell lines during a 14 day differentiation time course. Samples were collected on days 0, 2, 4, 7, and 14. Gene expression was normalised to *18s* and *UBC*. Data are presented as mean ± SEM of male (n=4) and female (n=3) preadipocyte cell lines and were analysed using repeated measured ANOVA. *a* indicates time $p<0.05$; *b* indicates depot $p<0.05$; and *c* indicates interaction $p<0.05$. **B** – A representative image of cells at days 0 and 14 is provided using photographs of abdominal and gluteal preadipocytes from the male cell line as an example.

After establishing that adipogenesis had occurred, the expression profile of the various candidate genes over the differentiation time course was analysed; data is presented in figure 3.3. It was reassuring to find that the same depot-specific expression profiles for a given gene were observed in both male and female preadipocyte cell lines.

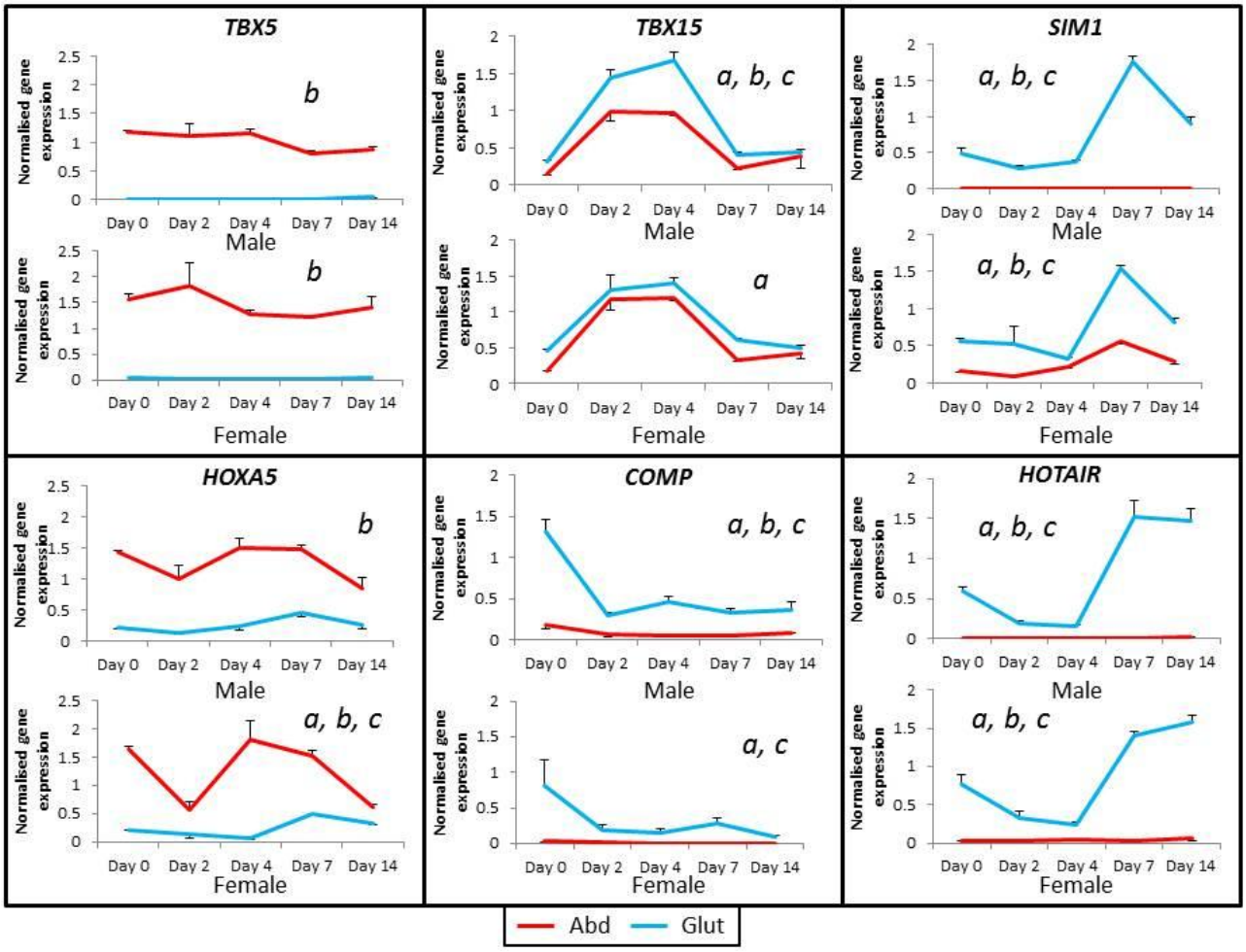

Figure 3.3 – *Expression of candidate genes over a 14 day adipogenic time course.* The expression of the candidate genes was analysed in abdominal (Abd) and gluteal (Glut) preadipocytes from both male and female cell lines during a 14 day differentiation time course. Gene expression was normalised to *18s* and *UBC*. Data are presented as mean ± SEM of male (n=4) and female (n=3) preadipocyte cell lines and were analysed using repeated measures ANOVA. *a* indicates time $p<0.05$; *b* indicates depot $p<0.05$; and *c* indicates interaction $p<0.05$.

The expression of *TBX5* within each depot did not change significantly during adipogenesis. Instead, the striking depot-specific expression pattern observed at baseline was simply maintained for the 14 days, during which time the significantly higher abdominal *TBX5* expression remained high in both cell lines.

TBX15 expression changed significantly over the 14 day time course and broadly followed the same pattern of expression in both male and female cell lines. It appeared to increase in both depots from day 0, and peak between days 2 and 4. By day 7, however, its expression returned to baseline in both abdominal and gluteal adipocytes. The higher expression of *TBX15* in gluteal preadipocytes persisted throughout adipogenesis, although this depot-specific difference in expression only reached significance in male cells. A significant interaction between depot and time was only detected in male cells, likely due to the more exaggerated pattern of *TBX15* expression by gluteal preadipocytes.

The striking depot-specific expression pattern of *SIM1* persisted during adipogenesis in both cell lines. Its expression pattern also changed significantly over the 14 day time course in both male and female cells. Gluteal *SIM1* expression remained at basal levels until day 4, at which point it increased significantly and peaked at day 7 before returning to baseline by day 14. A significant interaction between time and depot was also detected in both cell lines.

The marked depot difference in *HOXA5* expression was detected in both male and female cells throughout the differentiation time course. Its expression followed a broadly similar pattern in both cell lines, although this pattern was more exaggerated and reached significance only in female preadipocytes. Abdominal *HOXA5* expression appeared to decrease between days 0 and 2 but then recovered to baseline level by day 4. This level

was maintained until day 7 but declined by day 14. Furthermore, a significant interaction between depot and time was also detected in female cells.

COMP expression changed significantly over the differentiation time course in both male and female cells. Indeed, the higher gluteal expression detected at day 0 (albeit non-significantly in female cells) decreased upon the induction of adipogenesis, with this lower level of expression being maintained for the remaining duration of the differentiation time course. In contrast, the already-low level of *COMP* expression in abdominal preadipocytes did not appear to change during adipogenesis. A significant interaction between depot and time was detected in both cell lines.

A striking depot-specific difference in *HOTAIR* expression was observed in both male and female cells, which was accompanied by significant changes in its pattern of expression during adipogenesis too. Indeed, the high expression of *HOTAIR* in gluteal preadipocytes at day 0 was followed by a decline until day 4, at which point its expression increased substantially, where it even surpassed its already-high baseline level by day 14. A significant interaction between depot and time was also detected in both cell lines.

Overall, the various candidate genes maintained their depot-specific gene expression profiles during adipogenesis. Furthermore, each candidate gene followed its own distinct pattern of expression during the 14 day differentiation time course. Significant interactions between depot and time were identified for several genes (most notably *SIM1*, *COMP*, and *HOTAIR*), suggesting they may be involved in depot-specific regulation of adipogenesis.

3.4 Depot-specific DNA methylation profiles in subcutaneous preadipocyte cell lines

In addition to depot-specific gene expression, data from the DMH array had identified many differentially methylated genomic regions between subcutaneous abdominal and gluteal adipose tissue. Furthermore, correlations between methylation and the expression of certain genes located within 250 kb of the methylated loci had been identified in the combined dataset. *TBX5*, *TBX15*, and *SIM1* were among the top hits in this combined dataset and were subject to further study in which the DNA methylation profile of CpG islands associated with these genes was analysed using bisulfite-pyrosequencing. A CpG island overlapping the *COMP* promoter was also analysed but the data is not presented or discussed as this investigation was not completed due to time constraints.

3.4.1 Differential methylation of *TBX5*

TBX5 is highly expressed in abdominal tissue (see figure 3.1). In the combined dataset, the expression of *TBX5* was found to positively correlate with DNA methylation. Data from the DMH array suggested a locus 36 kb upstream of this gene was highly methylated in subcutaneous abdominal adipose tissue; this locus resided in an upstream CpG island. In preparation for bisulfite-pyrosequencing, most of this CpG island was amplified as two separate PCR products (*TBX5*_1 and *TBX5*_2) – see figure 3.4A.

Upon bisulfite-pyrosequencing these PCR products, it was found that the amplified genomic region from abdominal preadipocytes of both male and female cell lines was heavily methylated (figure 3.4B). In comparison, this amplified genomic region from gluteal preadipocytes was essentially unmethylated in both cell lines. These findings verified the data gathered in the DMH array.

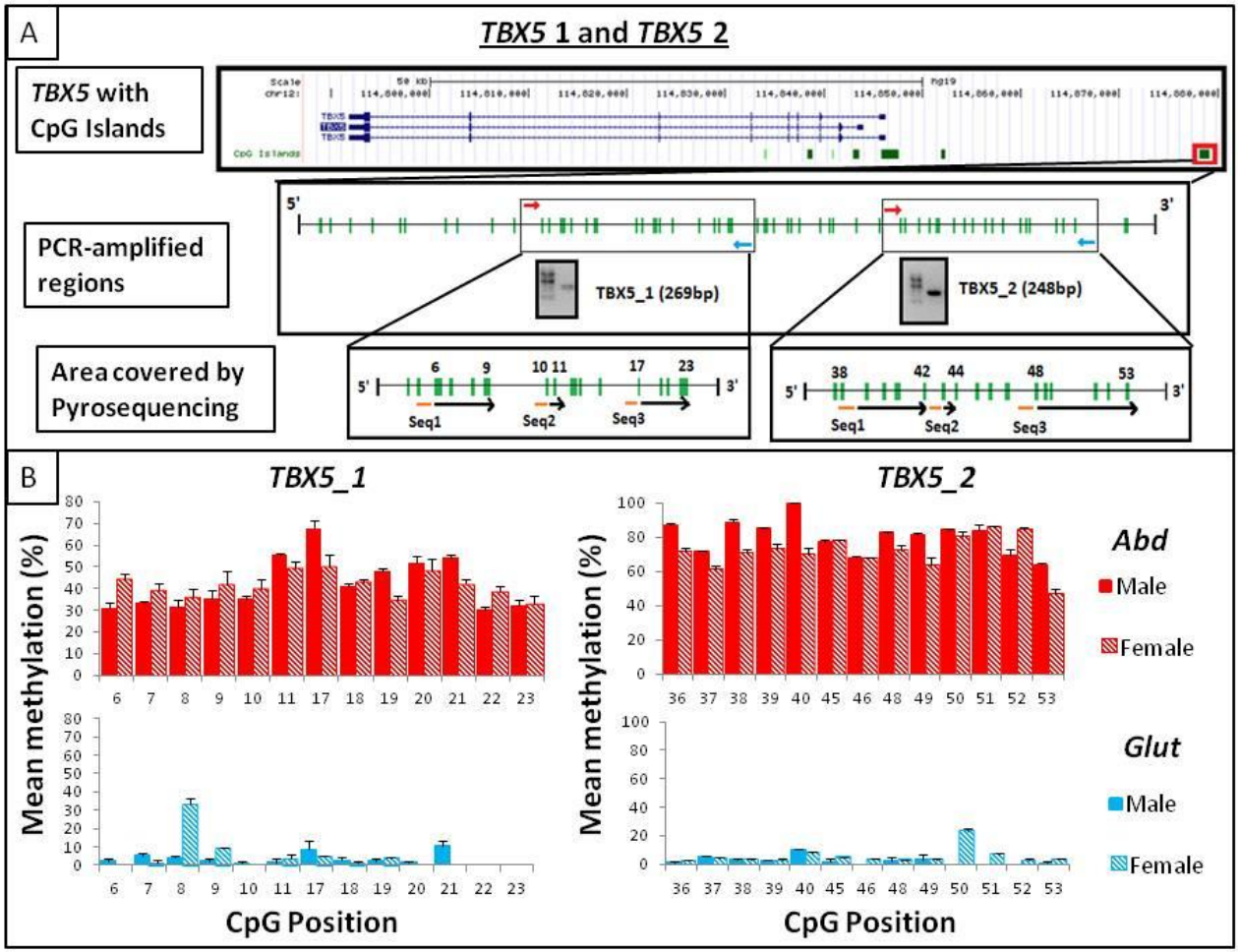

Figure 3.4 – *DNA methylation profile of the CpG island 36 kb away from TBX5.* **A** – The green box highlighted in red indicates the CpG island associated with *TBX5* expression from the DMH array. Most of this CpG island was analysed by amplifying two separate regions (*TBX5*_1 and *TBX5*_2); each PCR product was pyrosequenced separately using three sequencing primers. **B** – The mean methylation status of each region of the *TBX5* CpG island was analysed in untreated abdominal and gluteal preadipocytes from the male (n=4) and female (n=3) cell lines. In agreement with the DMH data, this genomic region from abdominal preadipocytes in both male and female cell lines was hypermethylated, whereas that from gluteal preadipocytes was essentially unmethylated. Data is presented as mean ± SEM.

Although the DMH array data was replicated and verified, the positive correlation between DNA methylation and gene expression does not fit with the general consensus that this epigenetic mark exerts transcriptionally repressive effects. As a result of this, *TBX5* was subject to further bioinformatic analysis, during which a CpG island that overlaps its promoter was identified. As the methylation status of promoter regions can influence the transcriptional activity of the associated gene (Deaton, A. *et al* 2011), a portion of this CpG island was also amplified (as *TBX5*_5) and analysed using bisulfite-pyrosequencing (see figure 3.5A). Note that the anti-sense strand was amplified and analysed.

Interestingly, the DNA methylation pattern for this CpG island was the opposite to that observed for the region identified by the DMH array (figure 3.4B). Indeed, this amplified genomic region from gluteal preadipocytes from both cell lines was significantly hypermethylated in comparison to that from abdominal preadipocytes of the same cell line (figures 3.5B and 3.5C). This pattern of DNA methylation fits with the depot-specific pattern of *TBX5* expression, in which *TBX5* is more highly expressed in abdominal tissue where its promoter CpG island is relatively hypomethylated.

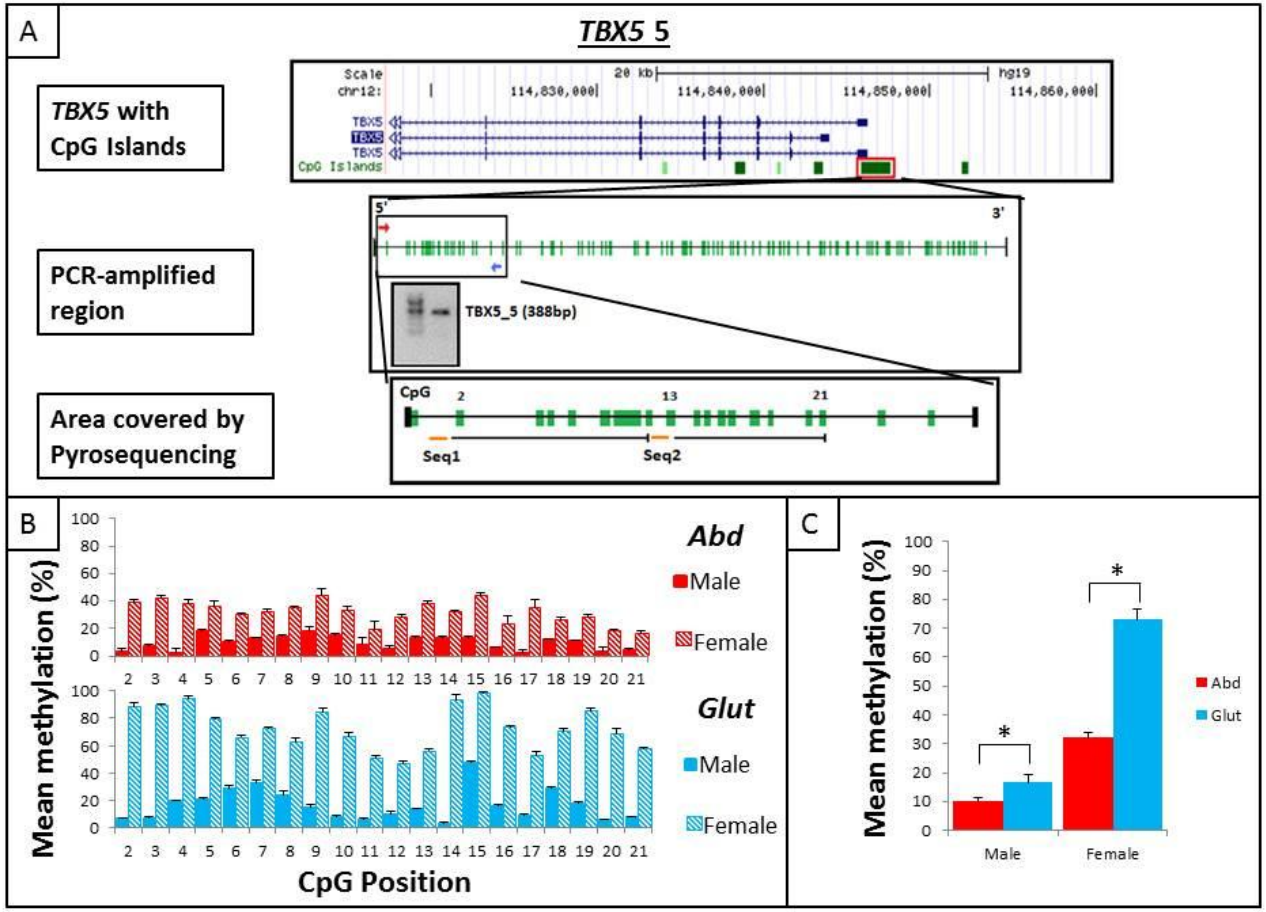

Figure 3.5 – *DNA methylation profile of CpG island located at TBX5 promoter.* **A** – A section of the CpG island present at the promoter of *TBX5* gene (highlighted by the red box) was amplified as a single PCR product (*TBX5*_5) which was later pyrosequenced using two sequencing primers. **B** – The methylation status of the amplified CpG island region was analysed in untreated abdominal and gluteal preadipocytes from both male (n=4) and female (n=3) cell lines. **C** – The mean methylation (%) of the entire PCR product in both abdominal and gluteal preadipocytes of the male and female cell lines is presented. Data is presented as mean ± SEM and the inter-depot difference within a cell line was analysed using a T-test. * indicates $P<0.05$.

3.4.2 Differential methylation of *TBX15*

The DMH array identified a highly differentially methylated locus within the *TBX15* promoter, with the expression of *TBX15* being found to negatively correlate with methylation in the combined dataset. Bioinformatic analysis of the differentially methylated locus highlighted it is surrounded by numerous CpG islands. The CpG island which contained the differentially methylated locus and also overlapped the *TBX15* promoter was amplified as a single PCR product and analysed using bisulfite-pyrosequencing (figure 3.6A). Note that the anti-sense strand was amplified and analysed.

A striking pattern of differential methylation was observed; the amplified genomic region from abdominal preadipocytes of both male and female cell lines was significantly hypermethylated, whereas the same region was essentially unmethylated in gluteal preadipocytes (figures 3.6B and C). This pattern of DNA methylation also agrees with the negative correlation between DNA methylation and *TBX15* expression calculated in the combined dataset. Indeed, *TBX15* is more highly expressed in gluteal preadipocytes in both cell lines, with this promoter CpG island being hypomethylated.

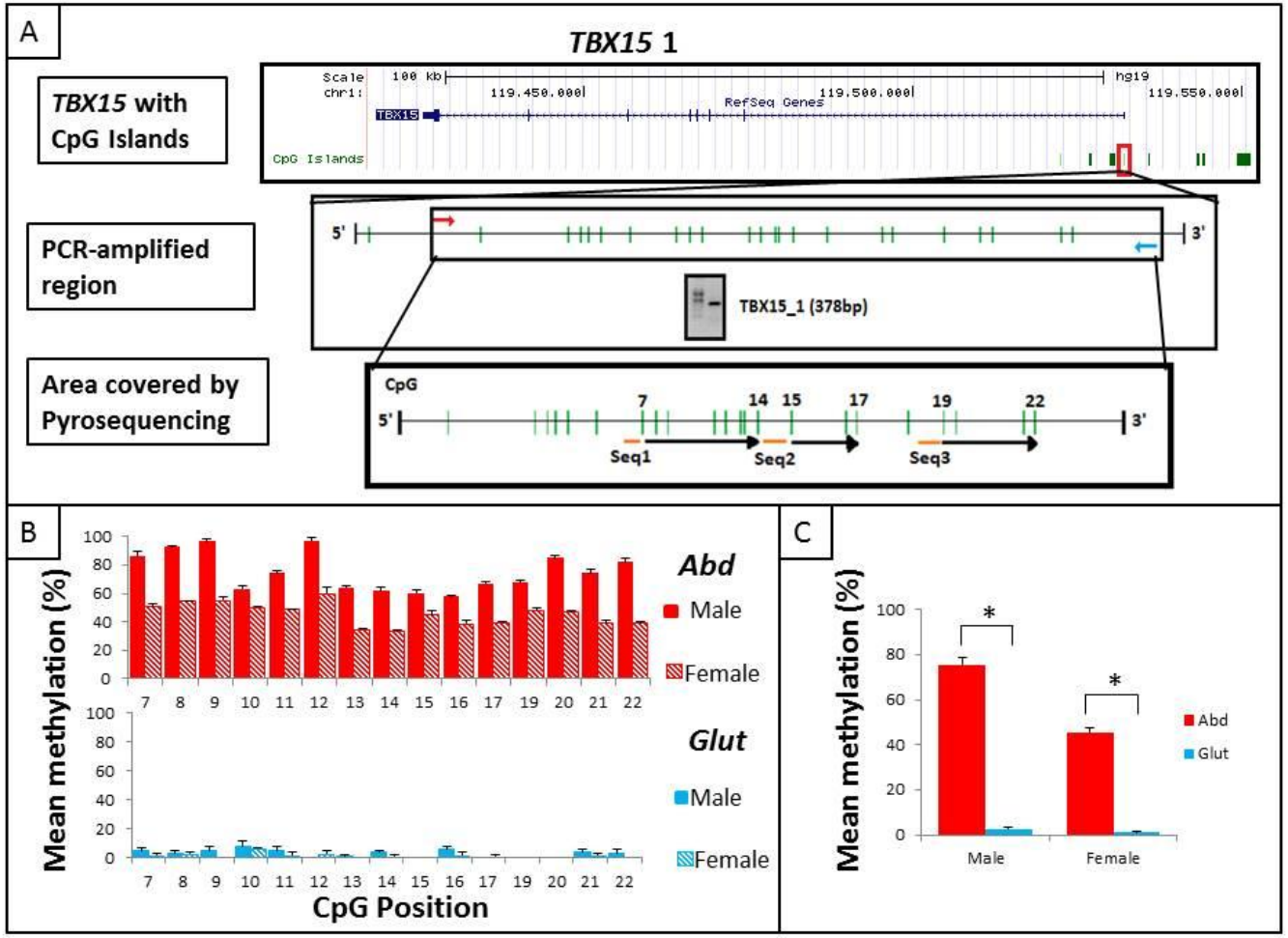

Figure 3.6 – *DNA methylation profile of CpG island at TBX15 promoter.* **A** – The CpG island closest to the *TBX15* promoter (highlighted by the red box) was amplified as a single PCR product (*TBX15*_1) and was pyrosequenced using three sequencing primers. **B** - The methylation status of the amplified CpG island region was analysed in untreated abdominal and gluteal preadipocytes from both male (n=4) and female (n=3) cell lines. **C** - The mean methylation (%) of the entire PCR product from abdominal and gluteal preadipocytes of both cell lines is presented. Data is presented as mean ± SEM and the inter-depot difference within a cell line was analysed using a T-test. * indicates $P<0.05$.

3.4.3 Differential methylation of *SIM1*

At this stage, the DMH data had been replicated and verified after bisulfite-pyrosequencing of two regions identified by the array in two paired preadipocyte cell lines. *SIM1* was located within 250 kb of another differentially methylated locus identified in the DMH array, with the combined dataset indicating that *SIM1* expression was positively correlated with DNA methylation (much like the data for *TBX5*).

Bioinformatic analysis of the differentially methylated locus identified by the DMH array indicated it was 3 kb away from *SIM1*. It was also found that the area surrounding the *SIM1* promoter is populated by a cluster of CpG islands. After considering the findings from the investigation of *TBX5* (figures 3.4 and 3.5), the decision was made to analyse the methylation status of the CpG island closest to the *SIM1* promoter (~500 bp upstream) due to its potential importance in regulating transcription (see figure 3.7A). Note that the anti-sense strand was amplified and analysed.

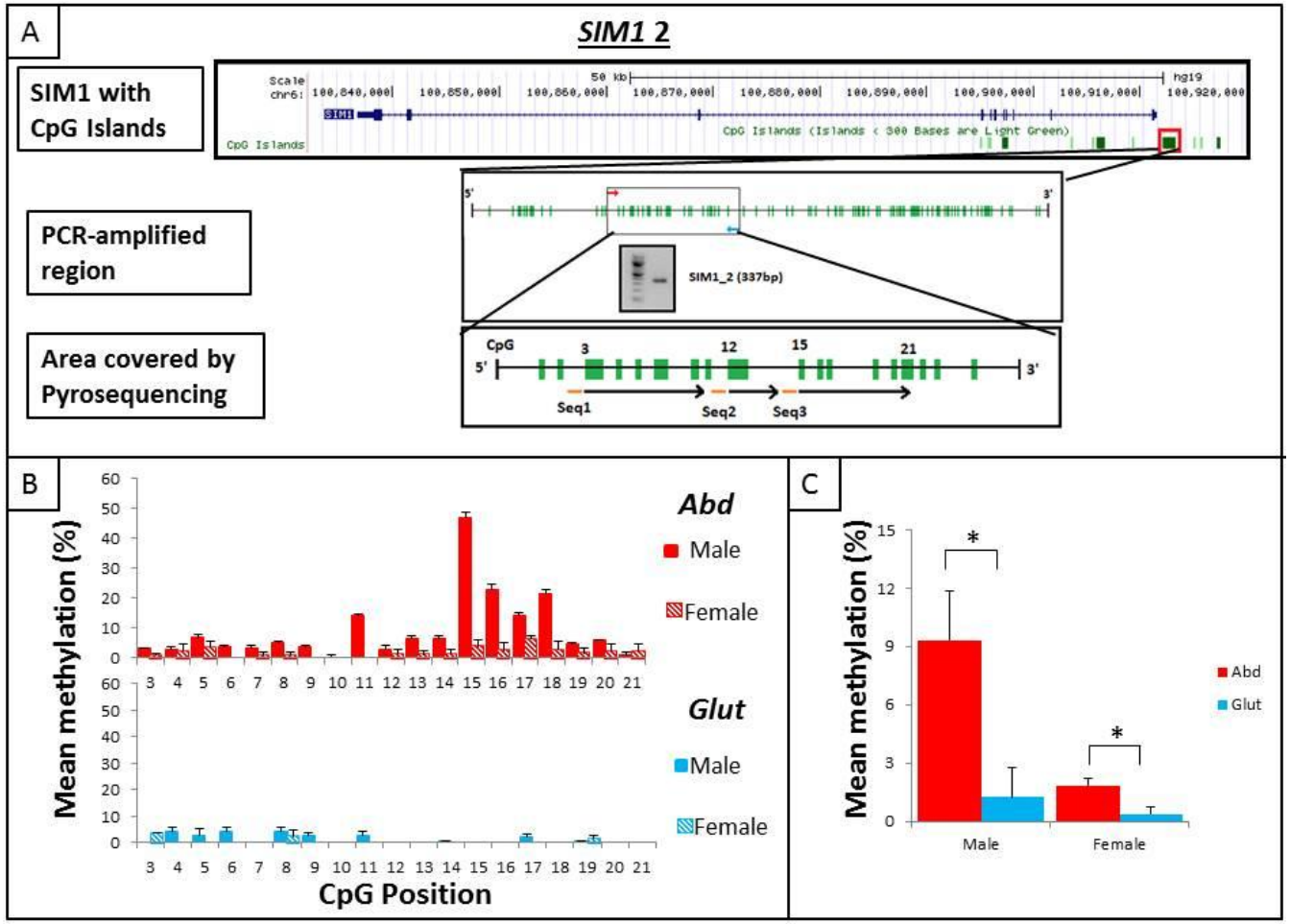

Figure 3.7 – *DNA methylation status of CpG island at SIM1 promoter.* **A** – The CpG island closest to the promoter of the *SIM1* gene (highlighted by the red box) was amplified as a single PCR product (*SIM1*_1) and was pyrosequenced using three sequencing primers. **B** - The methylation status of the amplified CpG island region was analysed in untreated abdominal and gluteal preadipocytes from both male and female cell lines. **C** - The mean methylation (%) of the entire PCR product in both abdominal and gluteal preadipocytes of the male and female cell lines is presented. Data is presented as mean ± SEM and the inter-depot difference within a cell line was analysed using a T-test. * indicates $P<0.05$.

It was found that this amplified genomic region is significantly hypermethylated in abdominal preadipocytes of both cell lines, whereas the same region was essentially unmethylated in gluteal preadipocytes (figure 3.7B and C). This pattern of methylation is opposite to that detected by the DMH array, but it does agree with the depot-specific expression pattern of *SIM1*. Indeed, *SIM1* is more highly expressed in gluteal preadipocytes where the CpG island closest to its promoter is relatively hypomethylated.

Overall, the DMH array data had been replicated and verified for both *TBX5* and *TBX15*, with such data supporting the existence of depot-specific DNA methylation profiles in subcutaneous abdominal and gluteal preadipocytes. Furthermore, it is clear that there is far greater complexity in terms of the relationships between the methylation status of specific genomic regions and the expression of their associated genes than the combined dataset would initially lead one to believe. Indeed, this point was exemplified by further investigation of genomic regions more 'biologically relevant' to the regulation of *TBX5* and *SIM1* expression distinct from the initial DMH array 'hit', both of which originally exhibited a potentially paradoxical positive relationship between DNA methylation and expression.

3.5 Regulation of gene expression by DNA methylation

After depot-specific gene expression and DNA methylation profiles in two paired preadipocyte cell lines had been observed, this begged the question of whether the depot-specific gene expression was regulated by DNA methylation. To investigate this, the expression of the candidate genes was analysed in abdominal and gluteal preadipocytes from both cell lines after they had been incubated with the DNA demethylating agent 5-azacytidine for 48 hr. The data are presented in figure 3.8.

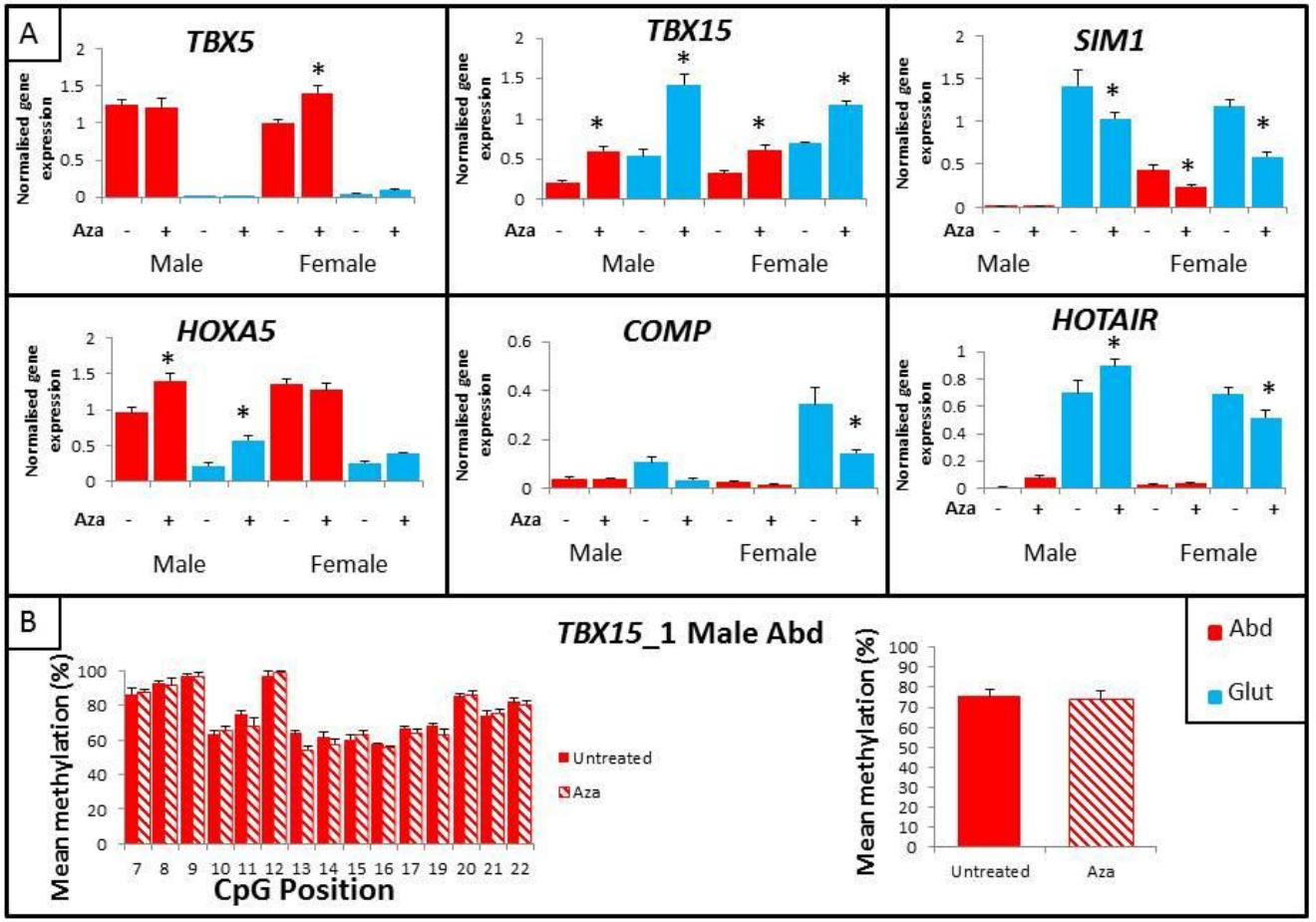

Figure 3.8 – *Gene expression in preadipocyte cell lines after 5-azacytidine treatment.* **A** – The expression of candidate genes in response to incubation with 15µM 5-azacytidine (Aza) for 48 hr was analysed in abdominal (Abd) and gluteal (Glut) preadipocytes from both male and female cell lines. Gene expression was normalised to *18s* and *PPIA*. Data are presented as mean ± SEM of male (n=6) and female (n=5) preadipocyte cell lines and were analysed using a two-way ANOVA. * indicates $P<0.05$ compared to untreated preadipocytes from the same depot of the same cell line. **B** – The methylation profile and mean methylation of *TBX15*_1 in untreated and treated male abdominal preadipocytes has been provided as a representative example. Data presented as mean ± SEM (n=4) and the inter-depot difference was analysed using a T-test. * indicates $P<0.05$.

Numerous gene- and cell line-specific effects were observed after treating male and female preadipocytes with 5-azacytidine (figure 3.8A). In terms of gene–specific effects, 5-azacytidine significantly increased *TBX15* expression in abdominal and gluteal preadipocytes from both male and female cell lines. Remarkably, this treatment increased *TBX15* expression approximately 2 – 3 fold.

Conversely, the same drug treatment significantly decreased *SIM1* expression in the male and female gluteal preadipocytes. Consistent with its effect in gluteal preadipocytes, 5-azacytidine also reduced *SIM1* expression in female abdominal preadipocytes, whereas no effect was detected in male abdominal preadipocytes; note that *SIM1* expression was undetectable in these cells when using cDNA at 1/40 dilution (figure 3.1). 5-azacytidine also decreased the expression of *COMP* in gluteal preadipocytes in both cell lines, although this only reached significance in female cells.

Several cell line-specific effects were also observed; 5-azacytidine treatment significantly increased *HOXA5* expression in male abdominal and gluteal preadipocytes, but no effect was observed in female cells. Furthermore, although the near-undetectable expression of *TBX5* in gluteal preadipocytes from both male and female cell lines was unaffected by 5-azacytidine, its expression was increased significantly only in female abdominal preadipocytes. Finally, although 5-azacytidine treatment had no effect on *HOTAIR* expression in abdominal preadipocytes, it had opposing effects in gluteal preadipocytes. Indeed, it increased the expression of *HOTAIR* in male cells but decreased it in female gluteal cells, although the magnitude of this effect was fairly small (~30%).

As the expression of several candidate genes located within 250 kb of differentially methylated genomic loci (i.e. *TBX5*, *TBX15*, and *SIM1*) was found to be sensitive to 5-

azacytidine treatment, the methylation status of the associated (and previously studied) genomic regions was also analysed. Interestingly, no significant change in the methylation status of any genomic regions was observed in DNA from abdominal or gluteal preadipocytes of either cell line after drug treatment. The methylation status of *TBX15*_1 is provided as a representative example in figure 3.8B, with the mean methylation of the entire amplicon shown in figure 3.8C.

Therefore, the expression of certain genes (*TBX15* and *SIM1*) was found to change in response to 5-azacytidine treatment in both male and female cell lines, which suggests their expression is regulated by DNA methylation. However, accompanying changes in DNA methylation were not observed upon bisulfite-pyrosequencing of specific genomic regions previously found to exhibit depot-specific methylation profiles that correlated with the expression of their associated genes.

3.6 Regulation of gene expression by glucocorticoids

Glucocorticoids play an important role in determining body fat distribution (see section 1.6.2) and are also capable of modulating DNA methylation status (see section 1.7.7). Given this, the expression of the candidate genes was analysed in abdominal and gluteal preadipocytes of both cell lines treated with the synthetic glucocorticoid dexamethasone for 48 hr. The data are presented in figure 3.9.

Much like 5-azacytidine, dexamethasone was found to exert gene- and cell line-specific effects. *COMP* displayed the most notable response to dexamethasone, as its expression was robustly induced in a dose-dependent fashion in abdominal and gluteal preadipocytes from both cell lines (see figure 3.9A).

Dexamethasone significantly down-regulated the expression of *TBX5* in male and female abdominal preadipocytes but had no effect in gluteal cells. However, this effect was not dose-dependent as the same reduced level of expression was achieved with 10nM dexamethasone (data not shown). Conversely, dexamethasone significantly increased gluteal expression of *HOTAIR* in both male and female preadipocytes, but had no effect in abdominal cells. Much like *TBX5*, this effect on *HOTAIR* expression was not dose-dependent.

TBX15 expression was completely refractory to dexamethasone at all doses tested in both cell lines. *SIM1* expression in gluteal preadipocytes was decreased by dexamethasone, although significance was only reached in male cells. In addition to these gene-specific effects, dexamethasone also exerted some cell line-specific effects. For instance, dexamethasone significantly decreased *HOXA5* expression in female abdominal preadipocytes but had no effect in male preadipocytes from either depot.

No significant change in the methylation status of any previously studied genomic region associated with *TBX5* or *SIM1* was observed after dexamethasone treatment, despite the expression of these genes being responsive to this drug. The methylation status of *TBX5*_1 is provided as a representative example in figure 3.9B, with the mean methylation of the entire amplicon presented in figure 3.9C.

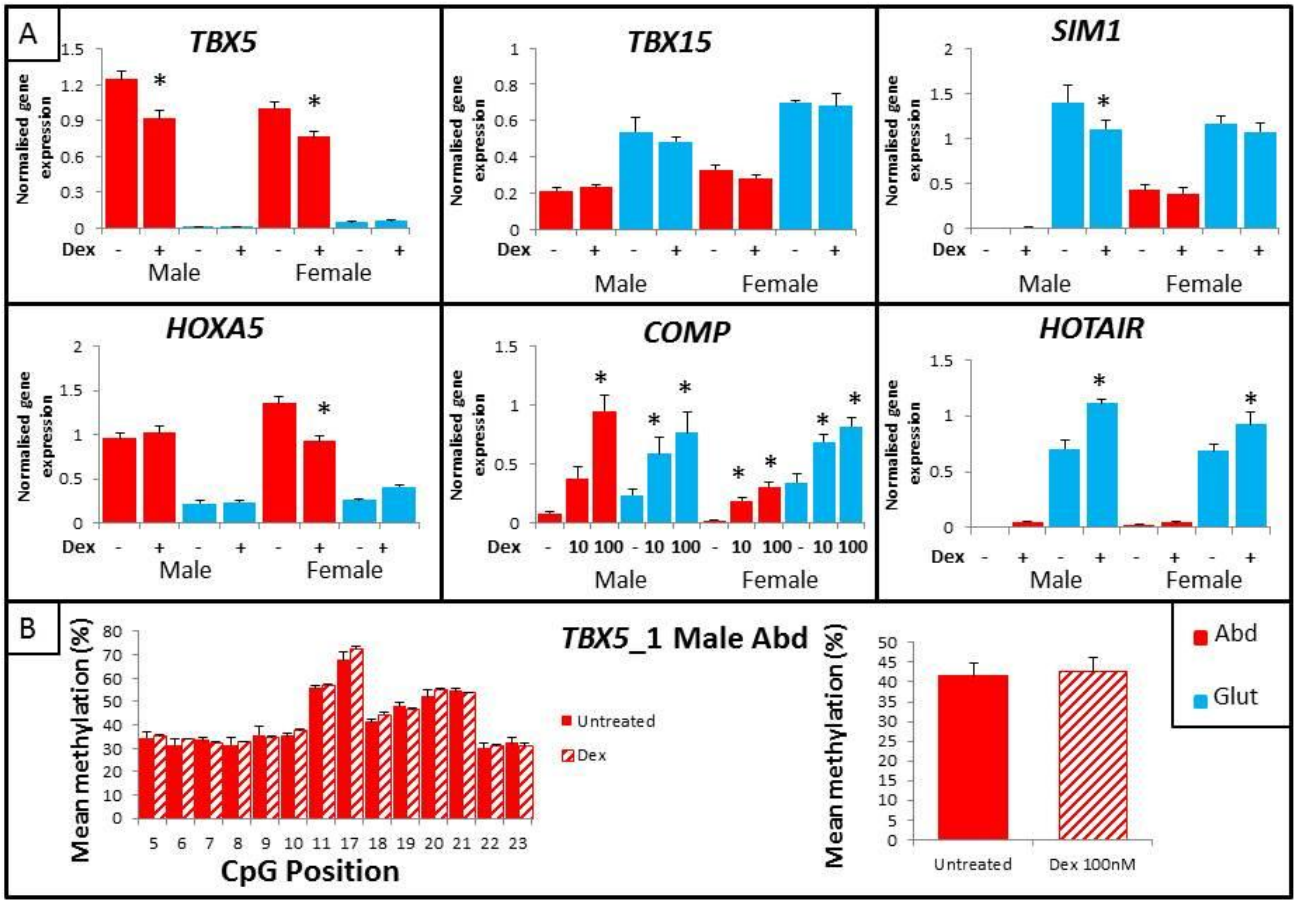

Figure 3.9 – *Gene expression in preadipocyte cell lines after dexamethasone treatment.* **A** – The expression of candidate genes was analysed in abdominal (Abd) and gluteal (Glut) preadipocytes from both male and female cell lines treated with 100nM dexamethasone (Dex) for 48 hr (unless stated otherwise). Expression was normalised to *18s* and *PPIA* in female cells but *18s* and *UBC* in male cells. Data are presented as mean ± SEM of male (n=6) and female (n=5) preadipocyte cell lines and were analysed using a two-way ANOVA. * indicates $P<0.05$ compared to untreated preadipocytes from the same depot of the same cell line. **B** – The methylation profile and mean methylation status of *TBX5*_1 in male abdominal preadipocytes has been provided as a representative example. Data is presented as mean ± SEM and the inter-depot difference was analysed using a T-test. * indicates $P<0.05$.

Overall, dexamethasone was found to modulate the expression of differentially expressed candidate genes within abdominal and gluteal preadipocytes from two cell lines, which is potentially interesting given the influence of glucocorticoids over body fat distribution. Of all the genes analysed, *COMP* exhibited the most robust and distinct response to dexamethasone treatment.

The effect of dexamethasone on *HOTAIR* expression suggests that glucocorticoids may modulate gene expression in subcutaneous preadipocytes in a depot-specific manner. Finally, although dexamethasone altered the expression of *TBX5* and *SIM1*, no change in the methylation status of any previously analysed genomic regions associated with these genes was observed.

3.7 Dexamethasone-mediated induction of *COMP* expression may involve DNA methylation

After finding that the expression of certain candidate genes responded to 5-azacytidine and dexamethasone in isolation, this begged the question of whether the effect of dexamethasone was mediated by DNA methylation. To investigate this, abdominal and gluteal preadipocytes from both cell lines were incubated with 100nM dexamethasone and 15μM 5-azacytidine for 48 hr before gene expression was analysed. *COMP* displayed the most remarkable response to this combination treatment of all candidate genes analysed, with this effect being observed in both cell lines. For these reasons, its data is presented in figure 3.10.

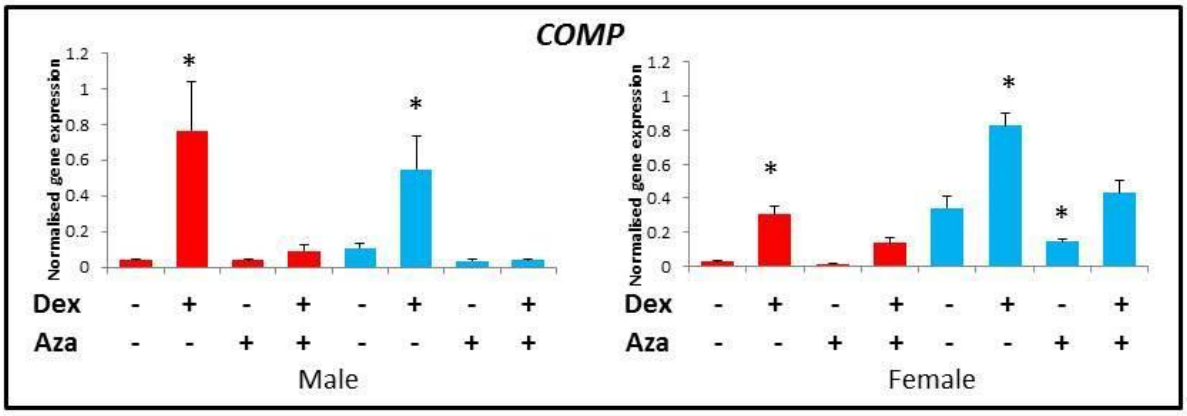

Figure 3.10 - *COMP expression in response to co-administration of dexamethasone and 5-azacytidine.* The expression of *COMP* was analysed after abdominal and gluteal preadipocytes from both male and female cell lines were incubated with a combination of 100nM dexamethasone (Dex) and 15µM 5-azacytidine (Aza) for 48 hr. Gene expression was normalised to *18s* and *PPIA*. Abdominal data are presented in red, Gluteal in Blue. Data are presented as mean ± SEM of male (n=6) and female (n=5) preadipocyte cell lines and were analysed using a two-way ANOVA. * indicates $P<0.05$ compared to untreated preadipocytes from the same depot of the same sex.

As shown in figure 3.9A, dexamethasone was found to strongly induce the expression of *COMP* in a dose-dependent fashion in both abdominal and gluteal preadipocytes of both cell types. Furthermore, 5-azacytidine was found to reduce its expression in gluteal preadipocytes, although this only reached significance in the female cell line (see figure 3.8A). Remarkably, upon co-administration of these drugs to preadipocytes from both cell lines it appears that the dexamethasone-mediated induction of COMP expression is completely abrogated by the presence of 5-azacytidine. This thereby suggests that dexamethasone-mediated stimulation of *COMP* expression involves DNA methylation.

4 Discussion

Discussion

There is a mounting body of evidence indicating adipose tissue is not homogenous. Indeed, different WAT depots have been found to exhibit both distinct functional characteristics and gene expression profiles. Given this, it follows that body fat distribution is being increasingly recognised as an important determinant of metabolic health, with a substantial amount of data associating lower body fat accumulation (i.e. within the gluteofemoral depot) with a reduced risk of developing metabolic disease, principally T2DM.

Overall, data from this project supports the notion that different WAT depots should be treated as distinct 'mini-organs', but goes further by providing evidence that epigenetic mechanisms, specifically DNA methylation, are likely involved in regulating depot-specific gene expression in human subcutaneous preadipocytes. Another important outcome has been the identification of several novel genes that may contribute to adipose function in a depot-specific manner.

4.1 Depot-specific gene expression in subcutaneous abdominal and gluteal preadipocyte cell lines

The initial aim of this project was to analyse the depot-specific gene expression of a select number of candidate genes previously identified in a microarray study as being differentially expressed between subcutaneous abdominal and gluteal whole adipose tissue. The microarray results were replicated and therefore verified in two paired preadipocyte cell lines (figure 3.1), so several points can be made. Firstly, these subcutaneous WAT depots exhibit distinct gene expression profiles, a finding which agrees with other work (Karastergiou, K. *et al* 2013). However, the experiments conducted using preadipocyte cell lines provided some cell type-specificity which was lacking in the microarray study (as whole tissue was used) with that data indicating it is

preadipocytes (at least) that differentially express certain genes. Secondly, the depot-specific gene expression profiles persisted in both preadipocyte cell lines for several generations, even after immortalisation, which also agrees with previous work (Tchkonia, T. *et al* 2006). This data also supports the notion that (subcutaneous) preadipocytes possess a heritable 'intrinsic memory' of their anatomical origin.

4.2 Depot-specific DNA methylation in subcutaneous abdominal and gluteal preadipocyte cell lines

Another aim was to analyse depot-specific DNA methylation patterns at specific loci which had been found to be differentially methylated between subcutaneous abdominal and gluteal whole adipose tissue in a DMH array using bisulfite-pyrosequencing. The regions of interest had been associated with the expression of certain genes in a combined dataset which identified correlations between the microarray and DMH data. The DMH array data was replicated and validated at the *TBX5*- and *TBX15*-associated loci in both preadipocyte cell lines (figures 3.4 and 3.6 respectively). Given this, it was confirmed that abdominal and gluteal subcutaneous WAT display depot-specific DNA methylation profiles, with preadipocytes comprising at least one cell type exhibiting these patterns.

Much like the regional gene expression profiles, these depot-specific DNA methylation profiles persisted in both preadipocyte cell lines for several generations, even after immortalisation. At this stage, it follows that the gene expression and bisulfite-pyrosequencing results reported in the preadipocyte cell lines warrant validation in primary preadipocytes. However, it is also apparent that the transformation process has not perturbed the basal gene expression or DNA methylation profiles of the candidate genes analysed (at least), as there is agreement between data from the various arrays which used

primary tissue and that from experiments which used the cell lines, suggesting the latter were an acceptable model of the former.

During the bisulfite-pyrosequencing analysis, an important issue was encountered. Essentially, the expression of certain genes (e.g. *TBX5* and *SIM1*) had been found to (paradoxically) correlate positively with methylation in the combined dataset, but upon analysis of a genomic region within a CpG island closer to the promoter of each gene (as opposed to the more distal DMH 'hit') the expected relationship was uncovered. Indeed, increased methylation was identified in gluteal tissue for *TBX5* and abdominal tissue for *SIM1* (figures 3.4 and 3.7 respectively), which agreed with reduced expression of such genes in these depots. This data suggests that DNA methylation patterns of genomic regions closest to a gene's promoter (and on the sense strand) are more likely to be involved in regulatory control over its expression than more distal regions.

It is important to note that no substantial differences in the basal expression or DNA methylation patterns were observed between the preadipocyte cell lines. Given that one paired cell line was from an individual male and the other from an individual female, it is possible that any sex-dependent differences may arise from the local microenvironment experienced *in vivo* and not be intrinsic to preadipocytes, as suggested previously (Tchoukalova, Y. D. *et al* 2010).

To explore the role of DNA methylation in the expression of the various candidate genes in the preadipocyte cell lines, the demethylating agent 5-azacytidine was used as a screening tool. *TBX15* exhibited the most robust response to drug treatment, with its expression increasing in both depots in both cell lines, whilst *SIM1* expression was decreased in gluteal cells in both cell lines (figure 3.8). Together, this suggests that DNA

methylation is involved in regulating depot-specific gene expression, albeit in a gene-specific fashion.

Unfortunately, there are several limitations to this aspect of the project. First of all, 5-azacytidine activity was not assessed directly, so it is not clear whether DNA demethylation actually occurred, especially as no alterations in DNA methylation status were observed in any genomic region analysed. This issue could be addressed by using bisulfite-pyrosequencing to analyse the methylation status of a transposable unit present throughout the genome to provide a representative measure of global methylation; LINE-1 elements have been used for this previously (Hollenbach, P W. *et al* 2010).

As no changes in methylation status at a specific genomic region were observed, no mechanistic link between 5-azacytidine action, DNA methylation, and gene expression has been uncovered. Using *TBX15* as an example, this probably means the region chosen for bisulfite-pyrosequencing was evidently not sensitive to 5-azacytidine and is unlikely to be a regulatory site. Perhaps analysing the methylation status of a more extended part of the promoter sequence itself (on the sense strand), irrespective of whether it contains a CpG island, would be more successful in terms of identifying 5-azacytidine-sensitive CpG sites.

It is possible that the analysed CpG sites were demethylated by 5-azacytidine but were re-methylated by a local repressor complex during cell division, which has been proposed before (Hagemann, S. *et al* 2011). However, this is unlikely as mRNA molecules are generally considered to be turned over fairly rapidly, so re-methylation would theoretically cause any change in gene expression to return to baseline before the cells were harvested. As changes in gene expression were observed though, the lack of observed changes in DNA methylation probably reflect the nature of the regions analysed.

As the sensitivity of a CpG site to drug-induced demethylation may be influenced by the underlying chromatin structure (Hagemann, S. *et al* 2011), it is important to consider that only a single epigenetic mark has been analysed in this project, namely DNA methylation. Other technologies, like chromatin-immunoprecipitation (Ch-IP), could be used in future studies to analyse histone modifications or transcription factor binding, for example, in conjunction with bisulfite-pyrosequencing. This would mean a more complete picture of the epigenetic 'code' at a specific genomic region of interest can be obtained, which would also make any associated gene expression data more meaningful.

It is interesting that 5-azacytidine treatment was found to decrease *SIM1* expression, as this is a potentially paradoxical finding. This may suggest that *SIM1* is potentially regulated by a 5-azacytidine-sensitive silencing element which may have been demethylated and subsequently activated. Such an element may reside within the promoter, with the altered methylation status of a CpG site within the binding site of a transcription factor potentially favouring repression or inhibiting activation. Evidently this finding warrants further investigation.

A complicating factor is that several cell line-specific responses to 5-azacytidine treatment were observed. It is unclear whether these were due to individual differences in each cell line and / or a consequence of cellular transformation. Indeed, it is possible that transformation altered the epigenetic profile of the preadipocytes such that these cell lines may only be suitable for studying certain genes like *TBX15* which exhibited a robust, cell line-independent response to drug treatment.

4.3 Regional variation in adipogenesis

To complement the investigation of depot-specific gene expression in preadipocytes, the pattern of expression for several candidate genes during adipogenesis was also analysed. As discussed in section 3.3 and shown in figure 3.2, abdominal and gluteal preadipocytes of both cell lines differentiated over a 14 day time course, during which time they underwent morphological changes and accumulated lipid. However, the pattern of adipogenic marker expression was not ideal as their increased expression was generally not maintained until day 14. However, these cell lines were generated fairly recently and the differentiation technique is still being optimised. The tendency towards loss of expression of the adipogenic markers is most likely due to the fact that the differentiation medium was not supplemented with lipid rather than the cells themselves being a poor model for studying this process (Pinnick, K. - personal communication). To reiterate though, despite the expression patterns, the preadipocytes underwent adipogenesis and accumulated lipid.

The adipogenic markers chosen did not show any consistent regional variation in their expression pattern. In marked contrast, however, the expression of several candidate genes (particularly *SIM1*, *HOTAIR*, and *COMP*) displayed both regional and temporal variation during adipogenesis. Together, it is possible that the 'adipose phenotype' is conferred by the expression of core adipogenic genes, while the depot-specific properties of WAT emerge from regional variation in the expression of other genes (which may modify the core adipogenic process).

4.3.1 *HOTAIR* and *SIM1*

To support this idea of regional variation in adipogenesis, several candidate genes already found to be differentially expressed in preadipocytes exhibited both temporal and depot-specific variation during differentiation. One striking example concerned *HOTAIR*, which is a long non-coding RNA transcribed from the *HOX-C* cluster on chromosome 12 that can recruit Polycomb repressor complex 2 to suppress gene expression from the *HOX-D* cluster on chromosome 2 (Rinn, J. L. *et al* 2007).

HOTAIR was the most highly differentially expressed gene identified in the microarray, and was essentially confined to gluteal preadipocytes only. Abdominal *HOTAIR* expression remained undetectable during the 14 day time course. However, in gluteal preadipocytes its expression decreased briefly before it increased remarkably after day 4 to a level surpassing its already high baseline. It peaked at day 7 with this level being maintained until day 14. Given this, *HOTAIR* could be a *bona fide* gluteal-specific regulator of adipogenesis, and it would certainly be interesting to identify at least one of its targets.

SIM1 may represent another gluteal-specific regulator of adipogenesis. Interestingly, its expression remained at baseline until day 4, at which point it increased and peaked at day 7 before starting to return to baseline by day 14. It is unclear whether its expression would return to baseline in the mature adipocyte with sufficient time or remain at an above-baseline plateau.

SIM1 encodes the human homologue of the *Drosophila melanogaster* single-minded (*SIM*) gene, which is a transcription factor classically associated with neurogenesis, particularly within the hypothalamus. The relevance of *SIM1* to adiposity and metabolic health was first identified in a young female patient who presented with severe obesity and

hyperphagia; molecular genetic analysis indicated that a chromosomal translocation had disrupted *SIM1*, rendering her haploinsufficient (Holder, J. L. *et al* 1999).

This phenotype has been replicated in heterozygous *SIM1* knockout mice (Michaud, J. L. *et al* 2001), although it appears this hyperphagic, obese phenotype is driven by perturbation of *SIM1* expressing neurons in the paraventricular nucleus of the hypothalamus (Xi, D. *et al* 2011). Conversely, overexpression of *SIM1* in these neurons reduces food intake (Yang, C. *et al* 2006). In addition, loss-of-function *SIM1* mutations have been associated with obesity (Ramachandrappa, S. *et al* 2013; Bonnefond, A. *et al* 2013). The distinct expression profile of *SIM1* in preadipocytes and during adipogenesis suggests it may represent a novel regulator of (gluteal subcutaneous) adipose function and that its role in metabolism may extend beyond neuronal development.

What is interesting about the timing of both *HOTAIR* and *SIM1* is that their expression peaks just as the lipid droplet starts to form (which typically occurs around day 7). This timing implicates these genes in adipogenesis and evidently warrants further investigation. This could involve silencing either of these genes in preadipocytes before analysing the morphology and phenotype of such cells after an adipogenic time course.

4.3.2 *COMP*

COMP may represent another novel gluteal-specific adipogenic regulator in addition to *HOTAIR* and *SIM1*. *COMP* encodes a homo-pentameric, non-collagenous extracellular matrix glycoprotein. Each subunit contains an epidermal growth-factor-like and calcium binding (thrombospondin-like) domain (Chen, H. *et al* 1999). Mutations in this gene have been associated with the dwarfing condition pseudoachrondroplasia, which is characterised by disproportionate short stature, abnormal joints, and osteoarthritis, and the related condition of multiple epiphyseal dysplasia; these phenotypes reflect the expression of

COMP in cartilage, tendons and ligaments (Thur, J. *et al* 2001; Posey, K. *et al* 2004). Given this expression pattern, *COMP* has not previously been implicated in adipose physiology.

COMP is particularly fascinating as although it shows depot-specific expression in preadipocytes (although this did not reach significance in the male cell line), dexamethasone was found to robustly increase its expression in a dose-dependent fashion in both male and female abdominal and gluteal preadipocytes (figure 3.9). It was therefore surprising to find that upon induction of adipogenesis, *COMP* expression in abdominal preadipocytes did not change whereas it was decreased by ~70 - 80% in gluteal cells given that the differentiation medium contained 1µM dexamethasone.

Given this, it is possible that the reduction in *COMP* expression is a permissive step that allows adipogenesis to commence, which thereby suggests *COMP* is anti-adipogenic. This is interesting as glucocorticoids are pro-adipogenic in conjunction with other hormones (Hauner, H. *et al* 1989), but evidently may induce the expression of an anti-adipogenic gene when administered in isolation. It would be interesting to see whether *COMP* over-expression in preadipocytes, or even exposure to exogenous COMP, inhibits adipogenesis. Identification of one of the physiological regulators of *COMP* would be useful. For example, if weight gain *in vivo* reduced *COMP* expression, this could permit hyperplasia in the gluteal depot and facilitate metabolically-favourable lower body fat accumulation. Perturbation of *COMP* expression (or its regulatory mechanisms) could drive 'ectopic' upper body fat accumulation and promote the pathogenesis of metabolic disease.

The other reason why *COMP* is particularly interesting is that although its expression was induced dose-dependently by dexamethasone, this effect was blocked by the presence of 5-azacytidine (figure 3.10). This suggests that glucocorticoid-mediated stimulation of *COMP*

expression involves DNA methylation, which could prevent the binding of a methylation-sensitive activating transcription factor or recruit a repressive complex (either could be investigated using Ch-IP), or a repressive element could be methylated and silenced. Either way, due to this striking effect, identifying the genomic locus involved and analysing its DNA methylation status in response to dexamethasone and / or 5-azacytidine treatment is a priority. A large (~3.4 kb) CpG island spans the promoter of *COMP*, so this would represent a logical region to initially analyse.

In addition to this, it would also be useful to identify the molecule(s) in the differentiation medium responsible for down-regulating *COMP* expression. This could involve co-administration experiments involving dexamethasone and specific components of the differentiation medium to see if the effect of dexamethasone and 5-azacytidine can be replicated. If PPARγ agonists were responsible (which are administered for the first four days), this may provide a mechanism partly explaining how these drugs direct the preferential expansion of (lower body) subcutaneous WAT depots in patients being treated for metabolic disease (Mori, Y. *et al* 1999).

Overall, *COMP* is arguably one of the more interesting candidate genes identified in this project as it may represent a novel regulator of depot-specific adipogenesis whose expression is regulated by DNA methylation. This is perhaps enhanced as it is not a transcription factor but a component of the extracellular matrix, a structure which plays a highly important but often unappreciated role in adipose tissue physiology (Divoux, A. *et al* 2011).

4.3.3 *TBX5* and *HOXA5*

The pattern of *TBX5* and *HOXA5* expression suggest they may represent regulators of abdominal WAT. *TBX5* expression did not really change during adipogenesis in either depot, but it is possible that it may contribute to the generation and maintenance of an 'abdominal' phenotype. Indeed, *TBX5* is a developmental regulator of the T-box domain-containing family of transcription factors. It has been reported that *TBX5* may regulate target gene expression by interacting with a co-activator which can recruit histone modifying enzymes (Murakami, M. *et al* 2005). *TBX5* has not previously been associated with adipose function. Instead, mutations in this gene precipitate Holt-Oram syndrome, an autosomal dominant disorder characterised by upper limb and cardiac malformations (Packham, E. A. *et al* 2002).

Although a genomic region associated with *TBX5* was identified as highly differentially methylated between depots in the DMH array, its expression was not significantly altered by 5-azacytidine. This suggests DNA methylation is probably not the primary mechanism regulating its expression. The functional relevance of dexamethasone reducing *TBX5* expression by ~ 30% is not clear either, although it is probably not biologically important given the fairly small magnitude of change.

The increased expression of *HOXA5* in abdominal preadipocytes agrees with previous work (Karastergiou, K. *et al* 2013). There is some data to suggest that its expression did change during adipogenesis (most notably a decrease from days 0 to 2 followed by a recovery at day 4), although this pattern was more exaggerated in the female cell line. This lack of clarity coupled with the fairly indistinct expression pattern (which does not completely agree with other findings in primary tissue – see Karastergiou, K. *et al* 2013) makes it difficult to judge how important a role *HOXA5* plays in WAT function. In its

favour, however, *HOXA5* expression was found to be induced in subcutaneous abdominal WAT following dramatic weight loss after bariatric surgery (Dankel, S. N. *et al* 2010), which means it may respond to metabolic status. Furthermore, its expression in subcutaneous abdominal WAT has been positively correlated with both BMI and WHR (Gesta, S. *et al* 2006), suggesting it may contribute to both adiposity and body fat distribution.

4.3.4 *TBX15*

In contrast to the other candidate genes, *TBX15* may regulate adipogenesis in both abdominal and gluteal preadipocytes. *TBX15* expression was detectable in both depots, although it was more highly expressed in gluteal cells. This depot-specific expression pattern persisted during adipogenesis although significance was only reached in male cells. During differentiation, *TBX15* expression followed the same pattern in both male and female abdominal and gluteal preadipocytes. Its expression increased upon induction of differentiation (days 0 – 2), with this level being maintained until day 4, at which point it returned to baseline in both depots and remained there until day 14. Overall this suggests *TBX15* is only required for a defined phase early in adipogenesis (between days 0 – 4).

As this distinct expression pattern occurs in both depots, *TBX15* may represent a novel component of the core adipogenic machinery. However, it may also contribute to regional variation in adipogenesis. Indeed, the relative depot difference in expression was more exaggerated and reached significance in the male cell line during adipogenesis, suggesting *TBX15* may contribute more to gluteal adipogenesis, although its contribution to this process may not be as substantial as those made by *HOTAIR* or *SIM1*, for example.

In line with *TBX15* possibly contributing to regional variation in adipogenesis and body fat distribution, the single nucleotide polymorphism (SNP) rs984222 within the *TBX15*-

WARS2 locus on chromosome 1 has been significantly associated with WHR in a meta-analysis of studies investigating populations of European ancestry (Heid, I. *et al* 2010). This has since been replicated in a population of predominantly African ancestry (Liu, C. T. *et al* 2013). However, this SNP was not found to be significantly associated with BMI or subcutaneous or visceral fat area in a Japanese population (Hotta, K. *et al* 2013); note that WHR was not investigated in this study.

There are several studies investigating the functional role of *TBX15*, but the meaning of this data is unclear given that mouse tissue has been used. Within these studies there are contradictory reports; *TBX15* overexpression in 3T3-L1 cells has been found to inhibit adipogenesis (Gesta, S. *et al* 2011) whereas *TBX15* knockdown in primary mouse subcutaneous fat has been found to have the same effect (Gburcik, V. *et al* 2012). Furthermore, the regional expression patterns of *TBX15* in humans and mice seem to be different, with this being complicated by the fact that there is currently no consensus on the pattern of *TBX15* expression in humans (Gesta, S. *et al* 2006; Tam, C. S. *et al* 2011; and Schleinitz, D. *et al* 2013). Overall, it appears that *TBX15* probably contributes to (human) adipose tissue function and body fat distribution, but this is not currently backed by any meaningful mechanistic data.

4.4 Conclusion

In conclusion, data have been presented which support and complement the body of work suggesting different WAT depots are distinct and should be treated as separate mini-organs. In addition to confirming that human subcutaneous preadipocytes exhibit depot-specific gene expression profiles, evidence suggesting depot-specific DNA methylation (i.e. epigenetic) patterns also exist was presented. By using 5-azacytidine as a screening tool, it was also found that the expression of certain depot-specific genes may be regulated

by DNA methylation, although no specific genomic loci whose methylation status responded to drug treatment were located. However, by considering the bioinformatic approach used in the analysis of *TBX5* and *SIM1*, the potentially functional loci whose methylation status may be involved in regulating gene expression are possibly located within the promoter region; this knowledge will be useful for future studies.

The expression of several candidate genes was found to respond to glucocorticoid administration, which is potentially of interest given these hormones are important determinants of body fat distribution. Evidence suggesting glucocorticoids may mediate their effect on gene expression (i.e. *COMP*) via DNA methylation was also presented; this property of glucocorticoids has not been observed in adipose tissue previously.

Overall, this project has been a successful exploratory venture as a number of novel candidate genes not previously implicated in adipose tissue function have been identified which has opened several avenues for further investigation. Furthermore, these genes may contribute to regional variation in adipogenesis, a phenomenon which may drive the generation of depot-specific phenotypes in WAT and ultimately underlie the relationship between body fat distribution and metabolic health.

5 References

References

Adams, M.; Montague, C. T.; Prins, J. B.; Holder, J. C.; Smith, S. A.; Sanders, L.; Digby, J. E.; Sewter, C. P.; Lazar, M. A.; Chatterjee, V. K.; O'Rahilly, S., Activators of peroxisome proliferator-activated receptor gamma have depot-specific effects on human preadipocyte differentiation. *The Journal of clinical investigation* 1997, *100*, 3149-53.

Agarwal, A. K.; Arioglu, E.; De Almeida, S.; Akkoc, N.; Taylor, S. I.; Bowcock, A. M.; Barnes, R. I.; Garg, A., AGPAT2 is mutated in congenital generalized lipodystrophy linked to chromosome 9q34. *Nature genetics* 2002, *31*, 21-3.

Agarwal, A. K.; Garg, A., A novel heterozygous mutation in peroxisome proliferator-activated receptor-gamma gene in a patient with familial partial lipodystrophy. *The Journal of clinical endocrinology and metabolism* 2002, *87*, 408-11.

Alexander, R.; Lodish, H.; Sun, L., MicroRNAs in adipogenesis and as therapeutic targets for obesity. *Expert opinion on therapeutic targets* 2011, *15*, 623-36.

Allan, C. A.; Strauss, B. J.; Burger, H. G.; Forbes, E. A.; McLachlan, R. I., Testosterone therapy prevents gain in visceral adipose tissue and loss of skeletal muscle in nonobese aging men. *The Journal of clinical endocrinology and metabolism* 2008, *93*, 139-46.

Amir, R. E.; Van den Veyver, I. B.; Wan, M.; Tran, C. Q.; Francke, U.; Zoghbi, H. Y., Rett syndrome is caused by mutations in X-linked MECP2, encoding methyl-CpG-binding protein 2. *Nature genetics* 1999, *23*, 185-8.

Barnes, P. J., Mechanisms and resistance in glucocorticoid control of inflammation. *The Journal of steroid biochemistry and molecular biology* 2010, *120*, 76-85.

Barroso, I.; Gurnell, M.; Crowley, V. E.; Agostini, M.; Schwabe, J. W.; Soos, M. A.; Maslen, G. L.; Williams, T. D.; Lewis, H.; Schafer, A. J.; Chatterjee, V. K.; O'Rahilly, S., Dominant negative mutations in human PPARgamma associated with severe insulin resistance, diabetes mellitus and hypertension. *Nature* 1999, *402*, 880-3.

Beck, E.; Esser, N.; Paquot, N.; Scheen, A. J., Metabolically obese normal-weight individuals and metabolically healthy, but obese, subjects. *Revue medicale suisse* 2009, *5*, 1644-6, 1648-9.

Behrens, G. M., Cardiovascular risk and body-fat abnormalities in HIV-infected adults. *The New England journal of medicine* 2005, *352*, 1721-2; author reply 1721-2.

Bell, A. C.; Felsenfeld, G., Methylation of a CTCF-dependent boundary controls imprinted expression of the Igf2 gene. *Nature* 2000, *405*, 482-5.

Bernstein, B. E.; Meissner, A.; Lander, E. S., The mammalian epigenome. *Cell* 2007, *128*, 669-81.

Billon, N.; Iannarelli, P.; Monteiro, M. C.; Glavieux-Pardanaud, C.; Richardson, W. D.; Kessaris, N.; Dani, C.; Dupin, E., The generation of adipocytes by the neural crest. *Development (Cambridge, England)* 2007, *134*, 2283-92.

Binder, E. B., The role of FKBP5, a co-chaperone of the glucocorticoid receptor in the pathogenesis and therapy of affective and anxiety disorders. *Psychoneuroendocrinology* 2009, *34 Suppl 1*, S186-95.

Bird, A. P.; Wolffe, A. P., Methylation-induced repression--belts, braces, and chromatin. *Cell* 1999, *99*, 451-4.

Bird, A., DNA methylation patterns and epigenetic memory. *Genes & development* 2002, *16*, 6-21.

Blum, W.; Garzon, R.; Klisovic, R. B.; Schwind, S.; Walker, A.; Geyer, S.; Liu, S.; Havelange, V.; Becker, H.; Schaaf, L.; Mickle, J.; Devine, H.; Kefauver, C.; Devine, S. M.; Chan, K. K.; Heerema, N. A.; Bloomfield, C. D.; Grever, M. R.; Byrd, J. C.; Villalona-Calero, M.; Croce, C. M.; Marcucci, G., Clinical response and miR-29b predictive significance in older AML patients treated with a 10-day schedule of decitabine. *Proceedings of the National Academy of Sciences of the United States of America* 2010, *107*, 7473-8.

Blumer, R. M.; van Vonderen, M. G.; Sutinen, J.; Hassink, E.; Ackermans, M.; van Agtmael, M. A.; Yki-Jarvinen, H.; Danner, S. A.; Reiss, P.; Sauerwein, H. P., Zidovudine/lamivudine contributes to insulin resistance within 3 months of starting combination antiretroviral therapy. *AIDS (London, England)* 2008, *22*, 227-36.

Boguslavsky, R. L.; Stewart, C. L.; Worman, H. J., Nuclear lamin A inhibits adipocyte differentiation: implications for Dunnigan-type familial partial lipodystrophy. *Human molecular genetics* 2006, *15*, 653-63.

Bonnefond, A.; Raimondo, A.; Stutzmann, F.; Ghoussaini, M.; Ramachandrappa, S.; Bersten, D. C.; Durand, E.; Vatin, V.; Balkau, B.; Lantieri, O.; Raverdy, V.; Pattou, F.; Van Hul, W.; Van Gaal, L.; Peet, D. J.; Weill, J.; Miller, J. L.; Horber, F.; Goldstone, A. P.; Driscoll, D. J.; Bruning, J. B.; Meyre, D.; Whitelaw, M. L.; Froguel, P., Loss-of-function mutations in SIM1 contribute to obesity and Prader-Willi-like features. *The Journal of clinical investigation* 2013, *123*, 3037-41.

Boquest, A. C.; Noer, A.; Collas, P., Epigenetic programming of mesenchymal stem cells from human adipose tissue. *Stem cell reviews* 2006, *2*, 319-29.

Borengasser, S. J.; Zhong, Y.; Kang, P.; Lindsey, F.; Ronis, M. J.; Badger, T. M.; Gomez-Acevedo, H.; Shankar, K., Maternal Obesity Enhances White Adipose Tissue Differentiation and Alters Genome-Scale DNA Methylation in Male Rat Offspring. *Endocrinology*, 2013, *154*, 4113-25.

Boutet, E.; El Mourabit, H.; Prot, M.; Nemani, M.; Khallouf, E.; Colard, O.; Maurice, M.; Durand-Schneider, A. M.; Chretien, Y.; Gres, S.; Wolf, C.; Saulnier-Blache, J. S.; Capeau, J.; Magre, J., Seipin deficiency alters fatty acid Delta9 desaturation and lipid droplet formation in Berardinelli-Seip congenital lipodystrophy. *Biochimie* 2009, *91*, 796-803.

Bowers, R. R.; Kim, J. W.; Otto, T. C.; Lane, M. D., Stable stem cell commitment to the adipocyte lineage by inhibition of DNA methylation: role of the BMP-4 gene. *Proceedings of the National Academy of Sciences of the United States of America* 2006, *103*, 13022-7.

Bowers, R. R.; Lane, M. D., Wnt signaling and adipocyte lineage commitment. *Cell cycle (Georgetown, Tex.)* 2008, *7*, 1191-6.

Brasaemle, D. L., Thematic review series: adipocyte biology. The perilipin family of structural lipid droplet proteins: stabilization of lipid droplets and control of lipolysis. *Journal of lipid research* 2007, *48*, 2547-59.

Buckingham, J. C., Glucocorticoids: exemplars of multi-tasking. *British journal of pharmacology* 2006, *147 Suppl 1*, S258-68.

Buemann, B.; Sorensen, T. I.; Pedersen, O.; Black, E.; Holst, C.; Toubro, S.; Echwald, S.; Holst, J. J.; Rasmussen, C.; Astrup, A., Lower-body fat mass as an independent marker of insulin sensitivity--the role of adiponectin. *International journal of obesity* 2005, *29*, 624-31.

Camhi, S. M.; Bray, G. A.; Bouchard, C.; Greenway, F. L.; Johnson, W. D.; Newton, R. L.; Ravussin, E.; Ryan, D. H.; Smith, S. R.; Katzmarzyk, P. T., The relationship of waist circumference and BMI to visceral, subcutaneous, and total body fat: sex and race differences. *Obesity* 2011, *19*, 402-8.

Canoy, D.; Luben, R.; Welch, A.; Bingham, S.; Wareham, N.; Day, N.; Khaw, K. T., Fat distribution, body mass index and blood pressure in 22,090 men and women in the Norfolk cohort of the European Prospective Investigation into Cancer and Nutrition (EPIC-Norfolk) study. *Journal of hypertension* 2004, *22*, 2067-74.

Canoy, D.; Boekholdt, S. M.; Wareham, N.; Luben, R.; Welch, A.; Bingham, S.; Buchan, I.; Day, N.; Khaw, K. T., Body fat distribution and risk of coronary heart disease in men and women in the European Prospective Investigation Into Cancer and Nutrition in Norfolk cohort: a population-based prospective study. *Circulation* 2007, *116*, 2933-43.

Cao, H.; Hegele, R. A., Nuclear lamin A/C R482Q mutation in canadian kindreds with Dunnigan-type familial partial lipodystrophy. *Human molecular genetics* 2000, *9*, 109-12.
Caserta, F.; Tchkonia, T.; Civelek, V. N.; Prentki, M.; Brown, N. F.; McGarry, J. D.; Forse, R. A.; Corkey, B. E.; Hamilton, J. A.; Kirkland, J. L., Fat depot origin affects fatty acid handling in cultured rat and human preadipocytes. *American journal of physiology. Endocrinology and metabolism* 2001, *280*, E238-47.

Chen, H.; Deere, M.; Hecht, J. T.; Lawler, J., Cartilage oligomeric matrix protein is a calcium-binding protein, and a mutation in its type 3 repeats causes conformational changes. *The Journal of biological chemistry* 2000, *275*, 26538-44.

Cifarelli, R. A.; Conconi, M. T.; Marmo, R.; Di Liddo, R.; Dininno, C.; Ferraro, S.; Cellini, F.; Parnigotto, P., 5-Azacytidine makes human preadipocytes able to differentiate into mesoderm-derived cell lineages. *Stem cells and development* 2012, *21*, 76-85.

Cinti, S., The adipose organ: morphological perspectives of adipose tissues. *The Proceedings of the Nutrition Society* 2001, *60*, 319-28.

Coleman, D. L., Effects of parabiosis of obese with diabetes and normal mice. *Diabetologia* 1973, *9*, 294-298.

Coleman, R. A.; Lee, D. P., Enzymes of triacylglycerol synthesis and their regulation. *Progress in lipid research* 2004, *43*, 134-76.

Collins, J. M.; Neville, M. J.; Pinnick, K. E.; Hodson, L.; Ruyter, B.; van Dijk, T. H.; Reijngoud, D. J.; Fielding, M. D.; Frayn, K. N., De novo lipogenesis in the differentiating human adipocyte can provide all fatty acids necessary for maturation. *Journal of lipid research* 2011, *52*, 1683-92.

Coppack, S. W.; Frayn, K. N.; Humphreys, S. M.; Dhar, H.; Hockaday, T. D., Effects of insulin on human adipose tissue metabolism in vivo. *Clinical science (London, England : 1979)* 1989, *77*, 663-70.

Dankel, S. N.; Fadnes, D. J.; Stavrum, A. K.; Stansberg, C.; Holdhus, R.; Hoang, T.; Veum, V. L.; Christensen, B. J.; Vage, V.; Sagen, J. V.; Steen, V. M.; Mellgren, G., Switch from stress response to homeobox transcription factors in adipose tissue after profound fat loss. *PloS one* 2010, *5*, e11033.

Darimont, C.; Mace, K., Immortalization of human preadipocytes. *Biochimie* 2003, *85*, 1231-3.

Deaton, A. M.; Bird, A., CpG islands and the regulation of transcription. *Genes & development* 2011, *25*, 1010-22.

Delaval, K.; Wagschal, A.; Feil, R., Epigenetic deregulation of imprinting in congenital diseases of aberrant growth. *BioEssays : news and reviews in molecular, cellular and developmental biology* 2006, *28*, 453-9.

Dieudonne, M. N.; Pecquery, R.; Boumediene, A.; Leneveu, M. C.; Giudicelli, Y., Androgen receptors in human preadipocytes and adipocytes: regional specificities and regulation by sex steroids. *The American journal of physiology* 1998, *274*, C1645-52.

Divoux, A.; Clement, K., Architecture and the extracellular matrix: the still unappreciated components of the adipose tissue. *Obesity reviews : an official journal of the International Association for the Study of Obesity* 2011, *12*, e494-503.

Dixon, J. B., The effect of obesity on health outcomes. *Molecular Cellular Endocrinology* 2010, *316(2)*, 104-108.

Dowling, H. J.; Fried, S. K.; Pi-Sunyer, F. X., Insulin resistance in adipocytes of obese women: effects of body fat distribution and race. *Metabolism: clinical and experimental* 1995, *44*, 987-95.

Drong, A. W.; Nicholson, G.; Hedman, A. K.; Meduri, E.; Grundberg, E.; Small, K. S.; Shin, S. Y.; Bell, J. T.; Karpe, F.; Soranzo, N.; Spector, T. D.; McCarthy, M. I.; Deloukas, P.; Rantalainen, M.; Lindgren, C. M., The presence of methylation quantitative trait loci indicates a direct genetic influence on the level of DNA methylation in adipose tissue. *PloS one* 2013, *8*, e55923.

El Hadri, K.; Glorian, M.; Monsempes, C.; Dieudonne, M. N.; Pecquery, R.; Giudicelli, Y.; Andreani, M.; Dugail, I.; Feve, B., In vitro suppression of the lipogenic pathway by the nonnucleoside reverse transcriptase inhibitor efavirenz in 3T3 and human preadipocytes or adipocytes. *The Journal of biological chemistry* 2004, *279*, 15130-41.

Elberg, G.; Gimble, J. M.; Tsai, S. Y., Modulation of the murine peroxisome proliferator-activated receptor gamma 2 promoter activity by CCAAT/enhancer-binding proteins. *The Journal of biological chemistry* 2000, *275*, 27815-22.

Elbers, J. M.; Asscheman, H.; Seidell, J. C.; Gooren, L. J., Effects of sex steroid hormones on regional fat depots as assessed by magnetic resonance imaging in transsexuals. *The American journal of physiology* 1999, *276*, E317-25.

Farmer, S. R., Transcriptional control of adipocyte formation. *Cell metabolism* 2006, *4*, 263-73.

Feinberg, A. P., Phenotypic plasticity and the epigenetics of human disease. *Nature* 2007, *447*, 433-40.

Finkelstein, E. A.; Khavjou, O. A.; Thompson, H.; Trogdon, J. G.; Pan, L.; Sherry, B.; Dietz, W., Obesity and Severe Obesity Forecasts Through 2030. *American Journal of Preventive Medicine* 2012, *42*, 563-570.

Fiorenza, C. G.; Chou, S. H.; Mantzoros, C. S., Lipodystrophy: pathophysiology and advances in treatment. *Nature reviews. Endocrinology* 2011, *7*, 137-50.

Frayn, K. N.; Shadid, S.; Hamlani, R.; Humphreys, S. M.; Clark, M. L.; Fielding, B. A.; Boland, O.; Coppack, S. W., Regulation of fatty acid movement in human adipose tissue in the postabsorptive-to-postprandial transition. *The American journal of physiology* 1994, *266*, E308-17.

Frayn, K. N.; Coppack, S. W.; Fielding, B. A.; Humphreys, S. M., Coordinated regulation of hormone-sensitive lipase and lipoprotein lipase in human adipose tissue in vivo: implications for the control of fat storage and fat mobilization. *Advances in enzyme regulation* 1995, *35*, 163-78.

Frayn, K. N., Visceral fat and insulin resistance--causative or correlative? *The British journal of nutrition* 2000, *83 Suppl 1*, S71-7.

Frayn, K., Adipose tissue as a buffer for daily lipid flux. *Diabetologia* 2002, *45*, 1201-1210.

Frayn, K. N.; Karpe, F.; Fielding, B. A.; Macdonald, I. A.; Coppack, S. W., Integrative physiology of human adipose tissue. *International journal of obesity and related metabolic disorders : journal of the International Association for the Study of Obesity* 2003, *27*, 875-88.

Friedman, R. C.; Farh, K. K.; Burge, C. B.; Bartel, D. P., Most mammalian mRNAs are conserved targets of microRNAs. *Genome research* 2009, *19*, 92-105.

Frommer, M.; McDonald, L. E.; Millar, D. S.; Collis, C. M.; Watt, F.; Grigg, G. W.; Molloy, P. L.; Paul, C. L., A genomic sequencing protocol that yields a positive display of 5-methylcytosine residues in individual DNA strands. *Proceedings of the National Academy of Sciences of the United States of America* 1992, *89*, 1827-31.

Fujiki, K.; Kano, F.; Shiota, K.; Murata, M., Expression of the peroxisome proliferator activated receptor gamma gene is repressed by DNA methylation in visceral adipose tissue of mouse models of diabetes. *BMC biology* 2009, *7*, 38.

Fuks, F., DNA methylation and histone modifications: teaming up to silence genes. *Current opinion in genetics & development* 2005, *15*, 490-5.

Funada, J.; Dennis, A. L.; Roberts, R.; Karpe, F.; Frayn, K. N., Regulation of subcutaneous adipose tissue blood flow is related to measures of vascular and autonomic function. *Clinical science (London, England : 1979)* 2010, *119*, 313-22.

Galic, S.; Oakhill, J. S.; Steinberg, G. R., Adipose tissue as an endocrine organ. *Mol Cell Endocrinol* 2010, *316*, 129-39.

110. Gallagher, D.; Visser, M.; Sepulveda, D.; Pierson, R. N.; Harris, T.; Heymsfield, S. B., How useful is body mass index for comparison of body fatness across age, sex, and ethnic groups? *American journal of epidemiology* 1996, *143*, 228-39.

Garg, A., Acquired and inherited lipodystrophies. *The New England journal of medicine* 2004, *350*, 1220-34.

Gburcik, V.; Cawthorn, W. P.; Nedergaard, J.; Timmons, J. A.; Cannon, B., An essential role for Tbx15 in the differentiation of brown and "brite" but not white adipocytes. *American journal of physiology. Endocrinology and metabolism* 2012, *303*, E1053-60.

Gesta, S.; Bluher, M.; Yamamoto, Y.; Norris, A. W.; Berndt, J.; Kralisch, S.; Boucher, J.; Lewis, C.; Kahn, C. R., Evidence for a role of developmental genes in the origin of obesity and body fat distribution. *Proceedings of the National Academy of Sciences of the United States of America* 2006, *103*, 6676-81.

Gesta, S.; Tseng, Y. H.; Kahn, C. R., Developmental origin of fat: tracking obesity to its source. *Cell* 2007, *131*, 242-56.

Gesta, S.; Bezy, O.; Mori, M. A.; Macotela, Y.; Lee, K. Y.; Kahn, C. R., Mesodermal developmental gene Tbx15 impairs adipocyte differentiation and mitochondrial respiration. *Proceedings of the National Academy of Sciences of the United States of America* 2011, *108*, 2771-6.

Goll, M. G.; Bestor, T. H., Eukaryotic cytosine methyltransferases. *Annual review of biochemistry* 2005, *74*, 481-514.

124.

Grodin, J. M.; Siiteri, P. K.; MacDonald, P. C., Source of estrogen production in postmenopausal women. *The Journal of clinical endocrinology and metabolism* 1973, *36*, 207-14.

Guo, Z.; Johnson, C. M.; Jensen, M. D., Regional lipolytic responses to isoproterenol in women. *The American journal of physiology* 1997, *273*, E108-12.

Gupta, R. K.; Arany, Z.; Seale, P.; Mepani, R. J.; Ye, L.; Conroe, H. M.; Roby, Y. A.; Kulaga, H.; Reed, R. R.; Spiegelman, B. M., Transcriptional control of preadipocyte determination by Zfp423. *Nature* 2010, *464*, 619-23.

Gupta, R. K.; Mepani, R. J.; Kleiner, S.; Lo, J. C.; Khandekar, M. J.; Cohen, P.; Frontini, A.; Bhowmick, D. C.; Ye, L.; Cinti, S.; Spiegelman, B. M., Zfp423 expression identifies committed preadipocytes and localizes to adipose endothelial and perivascular cells. *Cell metabolism* 2012, *15*, 230-9.

Hagemann, S.; Heil, O.; Lyko, F.; Brueckner, B., Azacytidine and decitabine induce gene-specific and non-random DNA demethylation in human cancer cell lines. *PloS one* 2011, *6*, e17388.

Hassan, M.; Latif, N.; Yacoub, M., Adipose tissue: friend or foe? *Nature Reviews Cardiology* 2012, *9*, 689-702.

Hauner, H.; Wabitsch, M.; Pfeiffer, E. F., Differentiation of adipocyte precursor cells from obese and nonobese adult women and from different adipose tissue sites. *Hormone and metabolic research. Supplement series* 1988, *19*, 35-9.

Hauner, H.; Entenmann, G.; Wabitsch, M.; Gaillard, D.; Ailhaud, G.; Negrel, R.; Pfeiffer, E. F., Promoting effect of glucocorticoids on the differentiation of human adipocyte precursor cells cultured in a chemically defined medium. *The Journal of clinical investigation* 1989, *84*, 1663-70.

Hauner, H.; Skurk, T.; Wabitsch, M., Cultures of human adipose precursor cells. *Methods in molecular biology (Clifton, N.J.)* 2001, *155*, 239-47.

Hebebrand, J.; Hinney, A.; Knoll, N.; Volckmar, A. L.; Scherag, A., Molecular genetic aspects of weight regulation. *Deutsches Arzteblatt international* 2013, *110*, 338-44.

Heerwagen, M. J.; Miller, M. R.; Barbour, L. A.; Friedman, J. E., Maternal obesity and fetal metabolic programming: a fertile epigenetic soil. *American journal of physiology. Regulatory, integrative and comparative physiology* 2010, *299*, R711-22.

Hegele, R. A.; Cao, H.; Frankowski, C.; Mathews, S. T.; Leff, T., PPARG F388L, a transactivation-deficient mutant, in familial partial lipodystrophy. *Diabetes* 2002, *51*, 3586-90.

Heid, I. M.; Jackson, A. U.; Randall, J. C.; Winkler, T. W.; Qi, L.; Steinthorsdottir, V.; Thorleifsson, G.; Zillikens, M. C.; Speliotes, E. K.; Magi, R.; Workalemahu, T.; White, C. C.; Bouatia-Naji, N.; Harris, T. B.; Berndt, S. I.; Ingelsson, E.; Willer, C. J.; Weedon, M. N.; Luan, J.; Vedantam, S.; Esko, T.; Kilpelainen, T. O.; Kutalik, Z.; Li, S.; Monda, K. L.; Dixon, A. L.; Holmes, C. C.; Kaplan, L. M.; Liang, L.; Min, J. L.; Moffatt, M. F.; Molony, C.; Nicholson, G.; Schadt, E. E.; Zondervan, K. T.; Feitosa, M. F.; Ferreira, T.; Lango Allen, H.; Weyant, R. J.; Wheeler, E.; Wood, A. R.; Estrada, K.; Goddard, M. E.; Lettre, G.; Mangino, M.; Nyholt, D. R.; Purcell, S.; Smith, A. V.; Visscher, P. M.; Yang, J.; McCarroll, S. A.; Nemesh, J.; Voight, B. F.; Absher, D.; Amin, N.; Aspelund, T.; Coin, L.;

Glazer, N. L.; Hayward, C.; Heard-Costa, N. L.; Hottenga, J. J.; Johansson, A.; Johnson, T.; Kaakinen, M.; Kapur, K.; Ketkar, S.; Knowles, J. W.; Kraft, P.; Kraja, A. T.; Lamina, C.; Leitzmann, M. F.; McKnight, B.; Morris, A. P.; Ong, K. K.; Perry, J. R.; Peters, M. J.; Polasek, O.; Prokopenko, I.; Rayner, N. W.; Ripatti, S.; Rivadeneira, F.; Robertson, N. R.; Sanna, S.; Sovio, U.; Surakka, I.; Teumer, A.; van Wingerden, S.; Vitart, V.; Zhao, J. H.; Cavalcanti-Proenca, C.; Chines, P. S.; Fisher, E.; Kulzer, J. R.; Lecoeur, C.; Narisu, N.; Sandholt, C.; Scott, L. J.; Silander, K.; Stark, K.; Tammesoo, M. L.; Teslovich, T. M.; Timpson, N. J.; Watanabe, R. M.; Welch, R.; Chasman, D. I.; Cooper, M. N.; Jansson, J. O.; Kettunen, J.; Lawrence, R. W.; Pellikka, N.; Perola, M.; Vandenput, L.; Alavere, H.; Almgren, P.; Atwood, L. D.; Bennett, A. J.; Biffar, R.; Bonnycastle, L. L.; Bornstein, S. R.; Buchanan, T. A.; Campbell, H.; Day, I. N.; Dei, M.; Dorr, M.; Elliott, P.; Erdos, M. R.; Eriksson, J. G.; Freimer, N. B.; Fu, M.; Gaget, S.; Geus, E. J.; Gjesing, A. P.; Grallert, H.; Grassler, J.; Groves, C. J.; Guiducci, C.; Hartikainen, A. L.; Hassanali, N.; Havulinna, A. S.; Herzig, K. H.; Hicks, A. A.; Hui, J.; Igl, W.; Jousilahti, P.; Jula, A.; Kajantie, E.; Kinnunen, L.; Kolcic, I.; Koskinen, S.; Kovacs, P.; Kroemer, H. K.; Krzelj, V.; Kuusisto, J.; Kvaloy, K.; Laitinen, J.; Lantieri, O.; Lathrop, G. M.; Lokki, M. L.; Luben, R. N.; Ludwig, B.; McArdle, W. L.; McCarthy, A.; Morken, M. A.; Nelis, M.; Neville, M. J.; Pare, G.; Parker, A. N.; Peden, J. F.; Pichler, I.; Pietilainen, K. H.; Platou, C. G.; Pouta, A.; Ridderstrale, M.; Samani, N. J.; Saramies, J.; Sinisalo, J.; Smit, J. H.; Strawbridge, R. J.; Stringham, H. M.; Swift, A. J.; Teder-Laving, M.; Thomson, B.; Usala, G.; van Meurs, J. B.; van Ommen, G. J.; Vatin, V.; Volpato, C. B.; Wallaschofski, H.; Walters, G. B.; Widen, E.; Wild, S. H.; Willemsen, G.; Witte, D. R.; Zgaga, L.; Zitting, P.; Beilby, J. P.; James, A. L.; Kahonen, M.; Lehtimaki, T.; Nieminen, M. S.; Ohlsson, C.; Palmer, L. J.; Raitakari, O.; Ridker, P. M.; Stumvoll, M.; Tonjes, A.; Viikari, J.; Balkau, B.; Ben-Shlomo, Y.; Bergman, R. N.; Boeing, H.; Smith, G. D.; Ebrahim, S.; Froguel, P.; Hansen, T.; Hengstenberg, C.; Hveem, K.; Isomaa, B.; Jorgensen, T.; Karpe, F.; Khaw, K. T.; Laakso, M.; Lawlor, D. A.; Marre, M.; Meitinger, T.; Metspalu, A.; Midthjell, K.; Pedersen, O.; Salomaa, V.; Schwarz, P. E.; Tuomi, T.; Tuomilehto, J.; Valle, T. T.; Wareham, N. J.; Arnold, A. M.; Beckmann, J. S.; Bergmann, S.; Boerwinkle, E.; Boomsma, D. I.; Caulfield, M. J.; Collins, F. S.; Eiriksdottir, G.; Gudnason, V.; Gyllensten, U.; Hamsten, A.; Hattersley, A. T.; Hofman, A.; Hu, F. B.; Illig, T.; Iribarren, C.; Jarvelin, M. R.; Kao, W. H.; Kaprio, J.; Launer, L. J.; Munroe, P. B.; Oostra, B.; Penninx, B. W.; Pramstaller, P. P.; Psaty, B. M.; Quertermous, T.; Rissanen, A.; Rudan, I.; Shuldiner, A. R.; Soranzo, N.; Spector, T. D.; Syvanen, A. C.; Uda, M.; Uitterlinden, A.; Volzke, H.; Vollenweider, P.; Wilson, J. F.; Witteman, J. C.; Wright, A. F.; Abecasis, G. R.; Boehnke, M.; Borecki, I. B.; Deloukas, P.; Frayling, T. M.; Groop, L. C.; Haritunians, T.; Hunter, D. J.; Kaplan, R. C.; North, K. E.; O'Connell, J. R.; Peltonen, L.; Schlessinger, D.; Strachan, D. P.; Hirschhorn, J. N.; Assimes, T. L.; Wichmann, H. E.; Thorsteinsdottir, U.; van Duijn, C. M.; Stefansson, K.; Cupples, L. A.; Loos, R. J.; Barroso, I.; McCarthy, M. I.; Fox, C. S.; Mohlke, K. L.; Lindgren, C. M., Meta-analysis identifies 13 new loci associated with waist-hip ratio and reveals sexual dimorphism in the genetic basis of fat distribution. *Nature genetics* 2010, *42*, 949-60.

Hellman, A.; Chess, A., Gene body-specific methylation on the active X chromosome. *Science* 2007, *315*, 1141-3.

Hocking, S. L.; Wu, L. E.; Guilhaus, M.; Chisholm, D. J.; James, D. E., Intrinsic depot-specific differences in the secretome of adipose tissue, preadipocytes, and adipose tissue-derived microvascular endothelial cells. *Diabetes* 2010, *59*, 3008-16.

Holder, J. L., Jr.; Butte, N. F.; Zinn, A. R., Profound obesity associated with a balanced translocation that disrupts the SIM1 gene. *Human molecular genetics* 2000, *9*, 101-8.

Hollenbach, P. W.; Nguyen, A. N.; Brady, H.; Williams, M.; Ning, Y.; Richard, N.; Krushel, L.; Aukerman, S. L.; Heise, C.; MacBeth, K. J., A comparison of azacitidine and decitabine activities in acute myeloid leukemia cell lines. *PloS one* 2010, *5*, e9001.

Hollenberg, C. H.; Raben, M. S.; Astwood, E. B., The lipolytic response to corticotropin. *Endocrinology* 1961, *68*, 589-598.

Hollis, G.; Huber, R., 11beta-Hydroxysteroid dehydrogenase type 1 inhibition in type 2 diabetes mellitus. *Diabetes, obesity & metabolism* 2011, *13*, 1-6.

Horowitz, J. F.; Klein, S., Whole body and abdominal lipolytic sensitivity to epinephrine is suppressed in upper body obese women. *American journal of physiology. Endocrinology and metabolism* 2000, *278*, E1144-52.

Hotta, K.; Kitamoto, A.; Kitamoto, T.; Mizusawa, S.; Teranishi, H.; So, R.; Matsuo, T.; Nakata, Y.; Hyogo, H.; Ochi, H.; Nakamura, T.; Kamohara, S.; Miyatake, N.; Kotani, K.; Itoh, N.; Mineo, I.; Wada, J.; Yoneda, M.; Nakajima, A.; Funahashi, T.; Miyazaki, S.; Tokunaga, K.; Masuzaki, H.; Ueno, T.; Chayama, K.; Hamaguchi, K.; Yamada, K.; Hanafusa, T.; Oikawa, S.; Sakata, T.; Tanaka, K.; Matsuzawa, Y.; Nakao, K.; Sekine, A., Replication study of 15 recently published Loci for body fat distribution in the Japanese population. *Journal of atherosclerosis and thrombosis* 2013, *20*, 336-50.

Hou, X.; Lu, J.; Weng, J.; Ji, L.; Shan, Z.; Liu, J.; Tian, H.; Ji, Q.; Zhu, D.; Ge, J.; Lin, L.; Chen, L.; Guo, X.; Zhao, Z.; Li, Q.; Zhou, Z.; Shan, G.; Yang, Z.; Yang, W.; Jia, W., Impact of waist circumference and body mass index on risk of cardiometabolic disorder and cardiovascular disease in Chinese adults: a national diabetes and metabolic disorders survey. *PloS one* 2013, *8*, e57319.

Huang, Y.; Sitwala, K.; Bronstein, J.; Sanders, D.; Dandekar, M.; Collins, C.; Robertson, G.; MacDonald, J.; Cezard, T.; Bilenky, M.; Thiessen, N.; Zhao, Y.; Zeng, T.; Hirst, M.; Hero, A.; Jones, S.; Hess, J. L., Identification and characterization of Hoxa9 binding sites in hematopoietic cells. *Blood* 2012, *119*, 388-98.

Illingworth, R.; Kerr, A.; Desousa, D.; Jorgensen, H.; Ellis, P.; Stalker, J.; Jackson, D.; Clee, C.; Plumb, R.; Rogers, J.; Humphray, S.; Cox, T.; Langford, C.; Bird, A., A novel CpG island set identifies tissue-specific methylation at developmental gene loci. *PLoS biology* 2008, *6*, e22.

Illingworth, R. S.; Bird, A. P., CpG islands--'a rough guide'. *FEBS letters* 2009, *583*, 1713-20.

Intine, R. V.; Sarras, M. P., Jr., Metabolic memory and chronic diabetes complications: potential role for epigenetic mechanisms. *Current diabetes reports* 2012, *12*, 551-9.

Issa, J. P., Optimizing therapy with methylation inhibitors in myelodysplastic syndromes: dose, duration, and patient selection. *Nature clinical practice. Oncology* 2005, *2 Suppl 1*, S24-9.

Jackson, A. S.; Pollock, M. L., Generalized equations for predicting body density of men. *The British journal of nutrition* 1978, *40*, 497-504.

Jackson, A. S.; Pollock, M. L.; Ward, A., Generalized equations for predicting body density of women. *Medicine and science in sports and exercise* 1980, *12*, 175-81.

Jackson, A. S.; Stanforth, P. R.; Gagnon, J.; Rankinen, T.; Leon, A. S.; Rao, D. C.; Skinner, J. S.; Bouchard, C.; Wilmore, J. H., The effect of sex, age and race on estimating percentage body fat from body mass index: The Heritage Family Study. *International journal of obesity and related metabolic disorders : journal of the International Association for the Study of Obesity* 2002, *26*, 789-96.

Jensen, M. A.; Fukushima, M.; Davis, R. W., DMSO and betaine greatly improve amplification of GC-rich constructs in de novo synthesis. *PloS one* 2010, *5*, e11024.

Joe, A. W.; Yi, L.; Even, Y.; Vogl, A. W.; Rossi, F. M., Depot-specific differences in adipogenic progenitor abundance and proliferative response to high-fat diet. *Stem cells (Dayton, Ohio)* 2009, *27*, 2563-70.

Jones, P. A.; Taylor, S. M., Cellular differentiation, cytidine analogs and DNA methylation. *Cell* 1980, *20*, 85-93.

Jones, P. A., Functions of DNA methylation: islands, start sites, gene bodies and beyond. *Nature reviews. Genetics* 2012, *13*, 484-92.

Kagoshima, M.; Wilcke, T.; Ito, K.; Tsaprouni, L.; Barnes, P. J.; Punchard, N.; Adcock, I. M., Glucocorticoid-mediated transrepression is regulated by histone acetylation and DNA methylation. *European journal of pharmacology* 2001, *429*, 327-34.

Kanda, H., S.; Tateya, Y.; Tamori, K.; Kotani, K.; Hiasa, R.; Kitazawa, S.; Kitazawa, H.; Miyachi, S.; Maeda, K.; Egashira and M. Kasuga., MCP-1 contributes to macrophage infiltration into adipose tissue, insulin resistance, and hepatic steatosis in obesity. *Journal of Clinical Investigation* 2006, *116(6)*, 1494-1505.

Karastergiou, K.; Smith, S. R.; Greenberg, A. S.; Fried, S. K., Sex differences in human adipose tissues - the biology of pear shape. *Biology of sex differences* 2012, *3*, 13.

Karastergiou, K.; Fried, S. K.; Xie, H.; Lee, M. J.; Divoux, A.; Rosencrantz, M. A.; Chang, R. J.; Smith, S. R., Distinct developmental signatures of human abdominal and gluteal subcutaneous adipose tissue depots. *The Journal of clinical endocrinology and metabolism* 2013, *98*, 362-71.

Kelly, T.; Yang, W.; Chen, C. S.; Reynolds, K.; He, J., Global burden of obesity in 2005 and projections to 2030. *International journal of obesity* 2008, *32*, 1431-7.

Kershaw, E. E.; Morton, N. M.; Dhillon, H.; Ramage, L.; Seckl, J. R.; Flier, J. S., Adipocyte-specific glucocorticoid inactivation protects against diet-induced obesity. *Diabetes* 2005, *54*, 1023-31.

Kim, T. H.; Abdullaev, Z. K.; Smith, A. D.; Ching, K. A.; Loukinov, D. I.; Green, R. D.; Zhang, M. Q.; Lobanenkov, V. V.; Ren, B., Analysis of the vertebrate insulator protein CTCF-binding sites in the human genome. *Cell* 2007, *128*, 1231-45.

King, H.; Aubert, R. E.; Herman, W. H., Global Burden of Diabetes, 1995–2025: Prevalence, numerical estimates, and projections. *Diabetes Care* 1998, *21*, 1414-1431.

Kirkland, J. L.; Hollenberg, C. H.; Gillon, W.; Kindler, S., Effect of hypophysectomy on rat preadipocyte replication and differentiation. *Endocrinology* 1992, *131*, 2769-73.

Klose, R. J.; Bird, A. P., Genomic DNA methylation: the mark and its mediators. *Trends in biochemical sciences* 2006, *31*, 89-97.

Kloting, N.; Berthold, S.; Kovacs, P.; Schon, M. R.; Fasshauer, M.; Ruschke, K.; Stumvoll, M.; Bluher, M., MicroRNA expression in human omental and subcutaneous adipose tissue. *PloS one* 2009, *4*, e4699.

Kotelevtsev, Y.; Holmes, M. C.; Burchell, A.; Houston, P. M.; Schmoll, D.; Jamieson, P.; Best, R.; Brown, R.; Edwards, C. R. W.; Seckl, J. R.; Mullins, J. J., 11β-Hydroxysteroid dehydrogenase type 1 knockout mice show attenuated glucocorticoid-inducible responses and resist hyperglycemia on obesity or stress. *Proceedings of the National Academy of Sciences* 1997, *94*, 14924-14929.

Koutsari, C.; Snozek, C. L.; Jensen, M. D., Plasma NEFA storage in adipose tissue in the postprandial state: sex-related and regional differences. *Diabetologia* 2008, *51*, 2041-8.

Lacasa, D.; Garcia, E.; Agli, B.; Giudicelli, Y., Control of rat preadipocyte adipose conversion by ovarian status: regional specificity and possible involvement of the mitogen-activated protein kinase-dependent and c-fos signaling pathways. *Endocrinology* 1997, *138*, 2729-34.

Langenberg, C.; Sharp, S. J.; Schulze, M. B.; Rolandsson, O.; Overvad, K.; Forouhi, N. G.; Spranger, J.; Drogan, D.; Huerta, J. M.; Arriola, L.; de Lauzon-Guillan, B.; Tormo, M. J.; Ardanaz, E.; Balkau, B.; Beulens, J. W.; Boeing, H.; Bueno-de-Mesquita, H. B.; Clavel-Chapelon, F.; Crowe, F. L.; Franks, P. W.; Gonzalez, C. A.; Grioni, S.; Halkjaer, J.; Hallmans, G.; Kaaks, R.; Kerrison, N. D.; Key, T. J.; Khaw, K. T.; Mattiello, A.; Nilsson, P.; Norat, T.; Palla, L.; Palli, D.; Panico, S.; Quiros, J. R.; Romaguera, D.; Romieu, I.; Sacerdote, C.; Sanchez, M. J.; Slimani, N.; Sluijs, I.; Spijkerman, A. M.; Teucher, B.; Tjonneland, A.; Tumino, R.; van der, A. D.; van der Schouw, Y. T.; Feskens, E. J.; Riboli, E.; Wareham, N. J., Long-term risk of incident type 2 diabetes and measures of overall and regional obesity: the EPIC-InterAct case-cohort study. *PLoS medicine* 2012, *9*, e1001230.

Laurent, L.; Wong, E.; Li, G.; Huynh, T.; Tsirigos, A.; Ong, C. T.; Low, H. M.; Kin Sung, K. W.; Rigoutsos, I.; Loring, J.; Wei, C. L., Dynamic changes in the human methylome during differentiation. *Genome research* 2010, *20*, 320-31.

Lee, J. H.; Skalnik, D. G., CpG-binding protein (CXXC finger protein 1) is a component of the mammalian Set1 histone H3-Lys4 methyltransferase complex, the analogue of the yeast Set1/COMPASS complex. *The Journal of biological chemistry* 2005, *280*, 41725-31.

Lee, S. Y.; Gallagher, D., Assessment methods in human body composition. *Current opinion in clinical nutrition and metabolic care* 2008, *11*, 566-72.

Lee, R. S.; Tamashiro, K. L.; Yang, X.; Purcell, R. H.; Harvey, A.; Willour, V. L.; Huo, Y.; Rongione, M.; Wand, G. S.; Potash, J. B., Chronic corticosterone exposure increases expression and decreases deoxyribonucleic acid methylation of Fkbp5 in mice. *Endocrinology* 2010, *151*, 4332-43.

Lee, R. S.; Tamashiro, K. L.; Yang, X.; Purcell, R. H.; Huo, Y.; Rongione, M.; Potash, J. B.; Wand, G. S., A measure of glucocorticoid load provided by DNA methylation of Fkbp5 in mice. *Psychopharmacology* 2011, *218*, 303-12.

Lee, M. J.; Pramyothin, P.; Karastergiou, K.; Fried, S. K., Deconstructing the roles of glucocorticoids in adipose tissue biology and the development of central obesity. *Biochimica et biophysica acta* 2013, Epub ahead of print.

Lemieux, I., Energy partitioning in gluteal-femoral fat: does the metabolic fate of triglycerides affect coronary heart disease risk? *Arteriosclerosis, thrombosis, and vascular biology* 2004, *24*, 795-7.

Lim, L. P.; Lau, N. C.; Garrett-Engele, P.; Grimson, A.; Schelter, J. M.; Castle, J.; Bartel, D. P.; Linsley, P. S.; Johnson, J. M., Microarray analysis shows that some microRNAs downregulate large numbers of target mRNAs. *Nature* 2005, *433*, 769-73.

Lindgren, C. M.; Heid, I. M.; Randall, J. C.; Lamina, C.; Steinthorsdottir, V.; Qi, L.; Speliotes, E. K.; Thorleifsson, G.; Willer, C. J.; Herrera, B. M.; Jackson, A. U.; Lim, N.; Scheet, P.; Soranzo, N.; Amin, N.; Aulchenko, Y. S.; Chambers, J. C.; Drong, A.; Luan, J.; Lyon, H. N.; Rivadeneira, F.; Sanna, S.; Timpson, N. J.; Zillikens, M. C.; Zhao, J. H.; Almgren, P.; Bandinelli, S.; Bennett, A. J.; Bergman, R. N.; Bonnycastle, L. L.; Bumpstead, S. J.; Chanock, S. J.; Cherkas, L.; Chines, P.; Coin, L.; Cooper, C.; Crawford, G.; Doering, A.; Dominiczak, A.; Doney, A. S.; Ebrahim, S.; Elliott, P.; Erdos, M. R.; Estrada, K.; Ferrucci, L.; Fischer, G.; Forouhi, N. G.; Gieger, C.; Grallert, H.; Groves, C. J.; Grundy, S.; Guiducci, C.; Hadley, D.; Hamsten, A.; Havulinna, A. S.; Hofman, A.; Holle, R.; Holloway, J. W.; Illig, T.; Isomaa, B.; Jacobs, L. C.; Jameson, K.; Jousilahti, P.; Karpe, F.; Kuusisto, J.; Laitinen, J.; Lathrop, G. M.; Lawlor, D. A.; Mangino, M.; McArdle, W. L.; Meitinger, T.; Morken, M. A.; Morris, A. P.; Munroe, P.; Narisu, N.; Nordstrom, A.; Nordstrom, P.; Oostra, B. A.; Palmer, C. N.; Payne, F.; Peden, J. F.; Prokopenko, I.; Renstrom, F.; Ruokonen, A.; Salomaa, V.; Sandhu, M. S.; Scott, L. J.; Scuteri, A.; Silander, K.; Song, K.; Yuan, X.; Stringham, H. M.; Swift, A. J.; Tuomi, T.; Uda, M.; Vollenweider, P.; Waeber, G.; Wallace, C.; Walters, G. B.; Weedon, M. N.; Witteman, J. C.; Zhang, C.; Zhang, W.; Caulfield, M. J.; Collins, F. S.; Davey Smith, G.; Day, I. N.; Franks, P. W.; Hattersley, A. T.; Hu, F. B.; Jarvelin, M. R.; Kong, A.; Kooner, J. S.; Laakso, M.; Lakatta, E.; Mooser, V.; Morris, A. D.; Peltonen, L.; Samani, N. J.; Spector, T. D.; Strachan, D. P.; Tanaka, T.; Tuomilehto, J.; Uitterlinden, A. G.; van Duijn, C. M.; Wareham, N. J.; Hugh, W.; Waterworth, D. M.; Boehnke, M.; Deloukas, P.; Groop, L.; Hunter, D. J.; Thorsteinsdottir, U.; Schlessinger, D.; Wichmann, H. E.; Frayling, T. M.; Abecasis, G. R.; Hirschhorn, J. N.; Loos, R. J.; Stefansson, K.; Mohlke, K. L.; Barroso, I.; McCarthy, M. I., Genome-wide association scan meta-analysis identifies three Loci influencing adiposity and fat distribution. *PLoS genetics* 2009, *5*, e1000508.

Lister, R.; Pelizzola, M.; Dowen, R. H.; Hawkins, R. D.; Hon, G.; Tonti-Filippini, J.; Nery, J. R.; Lee, L.; Ye, Z.; Ngo, Q. M.; Edsall, L.; Antosiewicz-Bourget, J.; Stewart, R.; Ruotti, V.; Millar, A. H.; Thomson, J. A.; Ren, B.; Ecker, J. R., Human DNA methylomes at base resolution show widespread epigenomic differences. *Nature* 2009, *462*, 315-22.

Liu, C. T.; Monda, K. L.; Taylor, K. C.; Lange, L.; Demerath, E. W.; Palmas, W.; Wojczynski, M. K.; Ellis, J. C.; Vitolins, M. Z.; Liu, S.; Papanicolaou, G. J.; Irvin, M. R.; Xue, L.; Griffin, P. J.; Nalls, M. A.; Adeyemo, A.; Liu, J.; Li, G.; Ruiz-Narvaez, E. A.; Chen, W. M.; Chen, F.; Henderson, B. E.; Millikan, R. C.; Ambrosone, C. B.; Strom, S. S.; Guo, X.; Andrews, J. S.; Sun, Y. V.; Mosley, T. H.; Yanek, L. R.; Shriner, D.; Haritunians,

T.; Rotter, J. I.; Speliotes, E. K.; Smith, M.; Rosenberg, L.; Mychaleckyj, J.; Nayak, U.; Spruill, I.; Garvey, W. T.; Pettaway, C.; Nyante, S.; Bandera, E. V.; Britton, A. F.; Zonderman, A. B.; Rasmussen-Torvik, L. J.; Chen, Y. D.; Ding, J.; Lohman, K.; Kritchevsky, S. B.; Zhao, W.; Peyser, P. A.; Kardia, S. L.; Kabagambe, E.; Broeckel, U.; Chen, G.; Zhou, J.; Wassertheil-Smoller, S.; Neuhouser, M. L.; Rampersaud, E.; Psaty, B.; Kooperberg, C.; Manson, J. E.; Kuller, L. H.; Ochs-Balcom, H. M.; Johnson, K. C.; Sucheston, L.; Ordovas, J. M.; Palmer, J. R.; Haiman, C. A.; McKnight, B.; Howard, B. V.; Becker, D. M.; Bielak, L. F.; Liu, Y.; Allison, M. A.; Grant, S. F.; Burke, G. L.; Patel, S. R.; Schreiner, P. J.; Borecki, I. B.; Evans, M. K.; Taylor, H.; Sale, M. M.; Howard, V.; Carlson, C. S.; Rotimi, C. N.; Cushman, M.; Harris, T. B.; Reiner, A. P.; Cupples, L. A.; North, K. E.; Fox, C. S., Genome-wide association of body fat distribution in african ancestry populations suggests new Loci. *PLoS genetics* 2013, *9*, e1003681.

Long, H. K.; Blackledge, N. P.; Klose, R. J., ZF-CxxC domain-containing proteins, CpG islands and the chromatin connection. *Biochemical Society transactions* 2013, *41*, 727-40.

Lovejoy, J. C., C. M. Champagne, L. de Jonge, H. Xie and S. R. Smith. Increased visceral fat and decreased energy expenditure during the menopausal transition. *International Journal of Obesity (Lond)* 2008, *32(6)*, 949-958

Maeda, N.; Shimomura, I.; Kishida, K.; Nishizawa, H.; Matsuda, M.; Nagaretani, H.; Furuyama, N.; Kondo, H.; Takahashi, M.; Arita, Y.; Komuro, R.; Ouchi, N.; Kihara, S.; Tochino, Y.; Okutomi, K.; Horie, M.; Takeda, S.; Aoyama, T.; Funahashi, T.; Matsuzawa, Y., Diet-induced insulin resistance in mice lacking adiponectin/ACRP30. *Nature medicine* 2002, *8*, 731-7.

Magre, J.; Delepine, M.; Khallouf, E.; Gedde-Dahl, T., Jr.; Van Maldergem, L.; Sobel, E.; Papp, J.; Meier, M.; Megarbane, A.; Bachy, A.; Verloes, A.; d'Abronzo, F. H.; Seemanova, E.; Assan, R.; Baudic, N.; Bourut, C.; Czernichow, P.; Huet, F.; Grigorescu, F.; de Kerdanet, M.; Lacombe, D.; Labrune, P.; Lanza, M.; Loret, H.; Matsuda, F.; Navarro, J.; Nivelon-Chevalier, A.; Polak, M.; Robert, J. J.; Tric, P.; Tubiana-Rufi, N.; Vigouroux, C.; Weissenbach, J.; Savasta, S.; Maassen, J. A.; Trygstad, O.; Bogalho, P.; Freitas, P.; Medina, J. L.; Bonnicci, F.; Joffe, B. I.; Loyson, G.; Panz, V. R.; Raal, F. J.; O'Rahilly, S.; Stephenson, T.; Kahn, C. R.; Lathrop, M.; Capeau, J., Identification of the gene altered in Berardinelli-Seip congenital lipodystrophy on chromosome 11q13. *Nature genetics* 2001, *28*, 365-70.

Mancini, D. N.; Singh, S. M.; Archer, T. K.; Rodenhiser, D. I., Site-specific DNA methylation in the neurofibromatosis (NF1) promoter interferes with binding of CREB and SP1 transcription factors. *Oncogene* 1999, *18*, 4108-19.

Manolopoulos, K. N.; Karpe, F.; Frayn, K. N., Gluteofemoral body fat as a determinant of metabolic health. *International journal of obesity* 2010, *34*, 949-59.

Manolopoulos, K. N.; Karpe, F.; Frayn, K. N., Marked resistance of femoral adipose tissue blood flow and lipolysis to adrenaline in vivo. *Diabetologia* 2012, *55*, 3029-37.

Mariman, E. C.; Wang, P., Adipocyte extracellular matrix composition, dynamics and role in obesity. *Cellular and molecular life sciences : CMLS* 2010, *67*, 1277-92.
Martin, M. L.; Jensen, M. D., Effects of body fat distribution on regional lipolysis in obesity. *The Journal of clinical investigation* 1991, *88*, 609-13.

Masuzaki, H.; Paterson, J.; Shinyama, H.; Morton, N. M.; Mullins, J. J.; Seckl, J. R.; Flier, J. S., A transgenic model of visceral obesity and the metabolic syndrome. *Science* 2001, *294*, 2166-70.

Maunakea, A. K.; Nagarajan, R. P.; Bilenky, M.; Ballinger, T. J.; D'Souza, C.; Fouse, S. D.; Johnson, B. E.; Hong, C.; Nielsen, C.; Zhao, Y.; Turecki, G.; Delaney, A.; Varhol, R.; Thiessen, N.; Shchors, K.; Heine, V. M.; Rowitch, D. H.; Xing, X.; Fiore, C.; Schillebeeckx, M.; Jones, S. J.; Haussler, D.; Marra, M. A.; Hirst, M.; Wang, T.; Costello, J. F., Conserved role of intragenic DNA methylation in regulating alternative promoters. *Nature* 2010, *466*, 253-7.

Maynard, L. M.; Wisemandle, W.; Roche, A. F.; Chumlea, W. C.; Guo, S. S.; Siervogel, R. M., Childhood body composition in relation to body mass index. *Pediatrics* 2001, *107*, 344-50.

Mazess, R. B.; Barden, H. S.; Bisek, J. P.; Hanson, J., Dual-energy x-ray absorptiometry for total-body and regional bone-mineral and soft-tissue composition. *American Journal of Clinical Nutrition* 1990, *51*, 1106-12.

McGuinness, O. P., Point-counterpoint: Interleukin-6 does/does not have a beneficial role in insulin sensitivity and glucose homeostasis. *Journal of applied physiology (Bethesda, Md. : 1985)* 2007, *102*, 823; author reply 825.

McQuaid, S. E.; Humphreys, S. M.; Hodson, L.; Fielding, B. A.; Karpe, F.; Frayn, K. N., Femoral adipose tissue may accumulate the fat that has been recycled as VLDL and nonesterified fatty acids. *Diabetes* 2010, *59*, 2465-73.

Meisinger, C.; Doring, A.; Thorand, B.; Heier, M.; Lowel, H., Body fat distribution and risk of type 2 diabetes in the general population: are there differences between men and women? The MONICA/KORA Augsburg cohort study. *Am J Clin Nutr* 2006, *84*, 483-9.

Meseguer, A.; Puche, C.; Cabero, A., Sex steroid biosynthesis in white adipose tissue. *Hormone and metabolic research = Hormon- und Stoffwechselforschung = Hormones et metabolisme* 2002, *34*, 731-6.

Michaud, J. L.; Boucher, F.; Melnyk, A.; Gauthier, F.; Goshu, E.; Levy, E.; Mitchell, G. A.; Himms-Hagen, J.; Fan, C. M., Sim1 haploinsufficiency causes hyperphagia, obesity and reduction of the paraventricular nucleus of the hypothalamus. *Human molecular genetics* 2001, *10*, 1465-73.

Mills, G. W.; Avery, P. J.; McCarthy, M. I.; Hattersley, A. T.; Levy, J. C.; Hitman, G. A.; Sampson, M.; Walker, M., Heritability estimates for beta cell function and features of the insulin resistance syndrome in UK families with an increased susceptibility to type 2 diabetes. *Diabetologia* 2004, *47*, 732-8.

Mori, Y.; Murakawa, Y.; Okada, K.; Horikoshi, H.; Yokoyama, J.; Tajima, N.; Ikeda, Y., Effect of troglitazone on body fat distribution in type 2 diabetic patients. *Diabetes Care* 1999, *22*, 908-12.

Murakami, M.; Nakagawa, M.; Olson, E. N.; Nakagawa, O., A WW domain protein TAZ is a critical coactivator for TBX5, a transcription factor implicated in Holt-Oram syndrome. *Proceedings of the National Academy of Sciences of the United States of America* 2005, *102*, 18034-9.

Neville, M. J.; Collins, J. M.; Gloyn, A. L.; McCarthy, M. I.; Karpe, F., Comprehensive human adipose tissue mRNA and microRNA endogenous control selection for quantitative real-time-PCR normalization. *Obesity* 2011, *19*, 888-92.

Ouchi, N.; Higuchi, A.; Ohashi, K.; Oshima, Y.; Gokce, N.; Shibata, R.; Akasaki, Y.; Shimono, A.; Walsh, K., Sfrp5 is an anti-inflammatory adipokine that modulates metabolic dysfunction in obesity. *Science* 2010, *329*, 454-7.

Pacenti, M.; Barzon, L.; Favaretto, F.; Fincati, K.; Romano, S.; Milan, G.; Vettor, R.; Palu, G., Microarray analysis during adipogenesis identifies new genes altered by antiretroviral drugs. *AIDS (London, England)* 2006, *20*, 1691-705.

Packham, E. A.; Brook, J. D., T-box genes in human disorders. *Human molecular genetics* 2003, *12 Spec No 1*, R37-44.

Park, B. O.; Ahrends, R.; Teruel, M. N., Consecutive positive feedback loops create a bistable switch that controls preadipocyte-to-adipocyte conversion. *Cell reports* 2012, *2*, 976-90.

Payne, V. A.; Grimsey, N.; Tuthill, A.; Virtue, S.; Gray, S. L.; Dalla Nora, E.; Semple, R. K.; O'Rahilly, S.; Rochford, J. J., The human lipodystrophy gene BSCL2/seipin may be essential for normal adipocyte differentiation. *Diabetes* 2008, *57*, 2055-60.

Peckett, A. J.; Wright, D. C.; Riddell, M. C., The effects of glucocorticoids on adipose tissue lipid metabolism. *Metabolism: clinical and experimental* 2011, *60*, 1500-10.

Pereira, C. D.; Azevedo, I.; Monteiro, R.; Martins, M. J., 11beta-Hydroxysteroid dehydrogenase type 1: relevance of its modulation in the pathophysiology of obesity, the metabolic syndrome and type 2 diabetes mellitus. *Diabetes, obesity & metabolism* 2012, *14*, 869-81.

Pfaffl, M. W., A new mathematical model for relative quantification in real-time RT-PCR. *Nucleic acids research* 2001, *29*, e45.

Poissonnet, C. M.; Burdi, A. R.; Garn, S. M., The chronology of adipose tissue appearance and distribution in the human fetus. *Early human development* 1984, *10*, 1-11.

Posey, K. L.; Hayes, E.; Haynes, R.; Hecht, J. T., Role of TSP-5/COMP in pseudoachondroplasia. *The international journal of biochemistry & cell biology* 2004, *36*, 1005-12.

Prokhortchouk, E.; Defossez, P. A., The cell biology of DNA methylation in mammals. *Biochimica et biophysica acta* 2008, *1783*, 2167-73.

Ramachandrappa, S.; Raimondo, A.; Cali, A. M.; Keogh, J. M.; Henning, E.; Saeed, S.; Thompson, A.; Garg, S.; Bochukova, E. G.; Brage, S.; Trowse, V.; Wheeler, E.; Sullivan, A. E.; Dattani, M.; Clayton, P. E.; Datta, V.; Bruning, J. B.; Wareham, N. J.; O'Rahilly, S.; Peet, D. J.; Barroso, I.; Whitelaw, M. L.; Farooqi, I. S., Rare variants in single-minded 1 (SIM1) are associated with severe obesity. *The Journal of clinical investigation* 2013, *123*, 3042-50.

Ramirez, M. E.; McMurry, M. P.; Wiebke, G. A.; Felten, K. J.; Ren, K.; Meikle, A. W.; Iverius, P. H., Evidence for sex steroid inhibition of lipoprotein lipase in men: comparison of abdominal and femoral adipose tissue. *Metabolism: clinical and experimental* 1997, *46*, 179-85.

Rando, O. J., Combinatorial complexity in chromatin structure and function: revisiting the histone code. *Current opinion in genetics & development* 2012, *22*, 148-55.

Raucci, R.; Rusolo, F.; Sharma, A.; Colonna, G.; Castello, G.; Costantini, S., Functional and structural features of adipokine family. *Cytokine* 2013, *61*, 1-14.

Rehrer, C. W.; Karimpour-Fard, A.; Hernandez, T. L.; Law, C. K.; Stob, N. R.; Hunter, L. E.; Eckel, R. H., Regional differences in subcutaneous adipose tissue gene expression. *Obesity* 2012, *20*, 2168-73.

Rideout, W. M., 3rd; Coetzee, G. A.; Olumi, A. F.; Jones, P. A., 5-Methylcytosine as an endogenous mutagen in the human LDL receptor and p53 genes. *Science* 1990, *249*, 1288-90.

Rinn, J. L.; Kertesz, M.; Wang, J. K.; Squazzo, S. L.; Xu, X.; Brugmann, S. A.; Goodnough, L. H.; Helms, J. A.; Farnham, P. J.; Segal, E.; Chang, H. Y., Functional demarcation of active and silent chromatin domains in human HOX loci by noncoding RNAs. *Cell* 2007, *129*, 1311-23.

Rizack, M. A., An Epinephrine-sensitive Lipolytic Activity in Adipose Tissue. *Journal of Biological Chemistry* 1961, *236*, 657-662.

Rockall, A. G.; Sohaib, S. A.; Evans, D.; Kaltsas, G.; Isidori, A. M.; Monson, J. P.; Besser, G. M.; Grossman, A. B.; Reznek, R. H., Computed tomography assessment of fat distribution in male and female patients with Cushing's syndrome. *European journal of endocrinology / European Federation of Endocrine Societies* 2003, *149*, 561-7.

Rodeheffer, M. S.; Birsoy, K.; Friedman, J. M., Identification of white adipocyte progenitor cells in vivo. *Cell* 2008, *135*, 240-9.

Romao, J. M.; Jin, W.; Dodson, M. V.; Hausman, G. J.; Moore, S. S.; Guan, L. L., MicroRNA regulation in mammalian adipogenesis. *Experimental biology and medicine (Maywood, N.J.)* 2011, *236*, 997-1004.

Ronaghi, M., Pyrosequencing sheds light on DNA sequencing. *Genome research* 2001, *11*, 3-11.

Ronn, T.; Volkov, P.; Davegardh, C.; Dayeh, T.; Hall, E.; Olsson, A. H.; Nilsson, E.; Tornberg, A.; Dekker Nitert, M.; Eriksson, K. F.; Jones, H. A.; Groop, L.; Ling, C., A six months exercise intervention influences the genome-wide DNA methylation pattern in human adipose tissue. *PLoS genetics* 2013, *9*, e1003572.

Rose, K. M.; Newman, B.; Mayer-Davis, E. J.; Selby, J. V., Genetic and behavioral determinants of waist-hip ratio and waist circumference in women twins. *Obesity research* 1998, *6*, 383-92.

Rosen, B. S.; Cook, K. S.; Yaglom, J.; Groves, D. L.; Volanakis, J. E.; Damm, D.; White, T.; Spiegelman, B. M., Adipsin and complement factor D activity: an immune-related defect in obesity. *Science* 1989, *244*, 1483-7.

Rosen, E. D.; Sarraf, P.; Troy, A. E.; Bradwin, G.; Moore, K.; Milstone, D. S.; Spiegelman, B. M.; Mortensen, R. M., PPAR gamma is required for the differentiation of adipose tissue in vivo and in vitro. *Molecular cell* 1999, *4*, 611-7.

Rosen, E. D.; Hsu, C. H.; Wang, X.; Sakai, S.; Freeman, M. W.; Gonzalez, F. J.; Spiegelman, B. M., C/EBPalpha induces adipogenesis through PPARgamma: a unified pathway. *Genes & development* 2002, *16*, 22-6.

Rosen, E. D.; MacDougald, O. A., Adipocyte differentiation from the inside out. *Nature reviews. Molecular cell biology* 2006, *7*, 885-96.

Ross, S. E.; Hemati, N.; Longo, K. A.; Bennett, C. N.; Lucas, P. C.; Erickson, R. L.; MacDougald, O. A., Inhibition of adipogenesis by Wnt signaling. *Science* 2000, *289*, 950-3.

Sakamoto, H.; Kogo, Y.; Ohgane, J.; Hattori, N.; Yagi, S.; Tanaka, S.; Shiota, K., Sequential changes in genome-wide DNA methylation status during adipocyte differentiation. *Biochemical and biophysical research communications* 2008, *366*, 360-6.

Santi, D. V.; Norment, A.; Garrett, C. E., Covalent bond formation between a DNA-cytosine methyltransferase and DNA containing 5-azacytosine. *Proceedings of the National Academy of Sciences of the United States of America* 1984, *81*, 6993-7.

Savage, D. B.; Tan, G. D.; Acerini, C. L.; Jebb, S. A.; Agostini, M.; Gurnell, M.; Williams, R. L.; Umpleby, A. M.; Thomas, E. L.; Bell, J. D.; Dixon, A. K.; Dunne, F.; Boiani, R.; Cinti, S.; Vidal-Puig, A.; Karpe, F.; Chatterjee, V. K.; O'Rahilly, S., Human metabolic syndrome resulting from dominant-negative mutations in the nuclear receptor peroxisome proliferator-activated receptor-gamma. *Diabetes* 2003, *52*, 910-7.

Saxonov, S.; Berg, P.; Brutlag, D. L., A genome-wide analysis of CpG dinucleotides in the human genome distinguishes two distinct classes of promoters. *Proceedings of the National Academy of Sciences of the United States of America* 2006, *103*, 1412-7.

Scammell, J. G.; Denny, W. B.; Valentine, D. L.; Smith, D. F., Overexpression of the FK506-binding immunophilin FKBP51 is the common cause of glucocorticoid resistance in three New World primates. *General and comparative endocrinology* 2001, *124*, 152-65.

Schleinitz, D.; Kloting, N.; Lindgren, C. M.; Breitfeld, J.; Dietrich, A.; Schon, M. R.; Lohmann, T.; Dressler, M.; Stumvoll, M.; McCarthy, M. I.; Bluher, M.; Kovacs, P., Fat depot-specific mRNA expression of novel loci associated with waist-hip ratio. *International journal of obesity* 2013, Epub ahead of print.

Schreiner, P. J.; Terry, J. G.; Evans, G. W.; Hinson, W. H.; Crouse, J. R., 3rd; Heiss, G., Sex-specific associations of magnetic resonance imaging-derived intra-abdominal and subcutaneous fat areas with conventional anthropometric indices. The Atherosclerosis Risk in Communities Study. *American journal of epidemiology* 1996, *144*, 335-45.

Seidell, J. C.; Perusse, L.; Despres, J. P.; Bouchard, C., Waist and hip circumferences have independent and opposite effects on cardiovascular disease risk factors: the Quebec Family Study. *Am J Clin Nutr* 2001, *74*, 315-21.

Seki, Y.; Williams, L.; Vuguin, P. M.; Charron, M. J., Minireview: Epigenetic programming of diabetes and obesity: animal models. *Endocrinology* 2012, *153*, 1031-8.

Selby, J. V.; Newman, B.; Quesenberry, C. P., Jr.; Fabsitz, R. R.; Carmelli, D.; Meaney, F. J.; Slemenda, C., Genetic and behavioral influences on body fat distribution. *International Journal of Obesity* 1990, *14*, 593-602.

Sharma, D.; Bhave, S.; Gregg, E.; Uht, R., Dexamethasone induces a putative repressor complex and chromatin modifications in the CRH promoter. *Molecular endocrinology (Baltimore, Md.)* 2013, *27*, 1142-52.

Shlay, J. C.; Sharma, S.; Peng, G.; Gibert, C. L.; Grunfeld, C., The effect of individual antiretroviral drugs on body composition in HIV-infected persons initiating highly active antiretroviral therapy. *Journal of acquired immune deficiency syndromes (1999)* 2009, *51*, 298-304.

Siiteri, P. K., Adipose tissue as a source of hormones. *The American Journal of Clinical Nutrition* 1987, *45*, 277-82.

Simha, V.; Garg, A., Phenotypic heterogeneity in body fat distribution in patients with congenital generalized lipodystrophy caused by mutations in the AGPAT2 or seipin genes. *The Journal of clinical endocrinology and metabolism* 2003, *88*, 5433-7.

Snijder, M. B.; Dekker, J. M.; Visser, M.; Bouter, L. M.; Stehouwer, C. D.; Kostense, P. J.; Yudkin, J. S.; Heine, R. J.; Nijpels, G.; Seidell, J. C., Associations of hip and thigh circumferences independent of waist circumference with the incidence of type 2 diabetes: the Hoorn Study. *American Journal of Clinical Nutrition* 2003, *77*, 1192-7.

Snijder, M. B.; Zimmet, P. Z.; Visser, M.; Dekker, J. M.; Seidell, J. C.; Shaw, J. E., Independent and opposite associations of waist and hip circumferences with diabetes, hypertension and dyslipidemia: the AusDiab Study. *International journal of obesity and related metabolic disorder: journal of the International Association for the Study of Obesity* 2004, *28*, 402-9.

Snijder, M. B.; Visser, M.; Dekker, J. M.; Goodpaster, B. H.; Harris, T. B.; Kritchevsky, S. B.; De Rekeneire, N.; Kanaya, A. M.; Newman, A. B.; Tylavsky, F. A.; Seidell, J. C., Low subcutaneous thigh fat is a risk factor for unfavourable glucose and lipid levels, independently of high abdominal fat. The Health ABC Study. *Diabetologia* 2005, *48*, 301-8.

Souren, N. Y.; Paulussen, A. D.; Loos, R. J.; Gielen, M.; Beunen, G.; Fagard, R.; Derom, C.; Vlietinck, R.; Zeegers, M. P., Anthropometry, carbohydrate and lipid metabolism in the East Flanders Prospective Twin Survey: heritabilities. *Diabetologia* 2007, *50*, 2107-16.

Spalding, K. L.; Arner, E.; Westermark, P. O.; Bernard, S.; Buchholz, B. A.; Bergmann, O.; Blomqvist, L.; Hoffstedt, J.; Naslund, E.; Britton, T.; Concha, H.; Hassan, M.; Ryden, M.; Frisen, J.; Arner, P., Dynamics of fat cell turnover in humans. *Nature* 2008, *453*, 783-7.

Speckman, R. A.; Garg, A.; Du, F.; Bennett, L.; Veile, R.; Arioglu, E.; Taylor, S. I.; Lovett, M.; Bowcock, A. M., Mutational and haplotype analyses of families with familial partial lipodystrophy (Dunnigan variety) reveal recurrent missense mutations in the globular C-terminal domain of lamin A/C. *American journal of human genetics* 2000, *66*, 1192-8.

Szymanski, K. M.; Binns, D.; Bartz, R.; Grishin, N. V.; Li, W. P.; Agarwal, A. K.; Garg, A.; Anderson, R. G.; Goodman, J. M., The lipodystrophy protein seipin is found at endoplasmic reticulum lipid droplet junctions and is important for droplet morphology. *Proceedings of the National Academy of Sciences of the United States of America* 2007, *104*, 20890-5.

Taksali, S. E.; Caprio, S.; Dziura, J.; Dufour, S.; Cali, A. M.; Goodman, T. R.; Papademetris, X.; Burgert, T. S.; Pierpont, B. M.; Savoye, M.; Shaw, M.; Seyal, A. A.; Weiss, R., High visceral and low abdominal subcutaneous fat stores in the obese adolescent: a determinant of an adverse metabolic phenotype. *Diabetes* 2008, *57*, 367-71.

Tam, C. S.; Heilbronn, L. K.; Henegar, C.; Wong, M.; Cowell, C. T.; Cowley, M. J.; Kaplan, W.; Clement, K.; Baur, L. A., An early inflammatory gene profile in visceral adipose tissue in children. *International journal of pediatric obesity : IJPO : an official journal of the International Association for the Study of Obesity* 2011, *6*, e360-3.

Tamori, Y.; Masugi, J.; Nishino, N.; Kasuga, M., Role of peroxisome proliferator-activated receptor-gamma in maintenance of the characteristics of mature 3T3-L1 adipocytes. *Diabetes* 2002, *51*, 2045-55.

Tan, G. D.; Goossens, G. H.; Humphreys, S. M.; Vidal, H.; Karpe, F., Upper and lower body adipose tissue function: a direct comparison of fat mobilization in humans. *Obesity research* 2004, *12*, 114-8.

Tang, Q. Q.; Lane, M. D., Activation and centromeric localization of CCAAT/enhancer-binding proteins during the mitotic clonal expansion of adipocyte differentiation. *Genes & development* 1999, *13*, 2231-41.

Tang, W.; Zeve, D.; Suh, J. M.; Bosnakovski, D.; Kyba, M.; Hammer, R. E.; Tallquist, M. D.; Graff, J. M., White fat progenitor cells reside in the adipose vasculature. *Science* 2008, *322*, 583-6.

Tang, Q. Q.; Lane, M. D., Adipogenesis: from stem cell to adipocyte. *Annual review of biochemistry* 2012, *81*, 715-36.

Tchkonia, T.; Giorgadze, N.; Pirtskhalava, T.; Tchoukalova, Y.; Karagiannides, I.; Forse, R. A.; DePonte, M.; Stevenson, M.; Guo, W.; Han, J.; Waloga, G.; Lash, T. L.; Jensen, M. D.; Kirkland, J. L., Fat depot origin affects adipogenesis in primary cultured and cloned human preadipocytes. *American journal of physiology. Regulatory, integrative and comparative physiology* 2002, *282*, R1286-96.

Tchkonia, T.; Tchoukalova, Y. D.; Giorgadze, N.; Pirtskhalava, T.; Karagiannides, I.; Forse, R. A.; Koo, A.; Stevenson, M.; Chinnappan, D.; Cartwright, A.; Jensen, M. D.; Kirkland, J. L., Abundance of two human preadipocyte subtypes with distinct capacities for replication, adipogenesis, and apoptosis varies among fat depots. *American journal of physiology. Endocrinology and metabolism* 2005, *288*, E267-77.

Tchkonia, T.; Giorgadze, N.; Pirtskhalava, T.; Thomou, T.; DePonte, M.; Koo, A.; Forse, R. A.; Chinnappan, D.; Martin-Ruiz, C.; von Zglinicki, T.; Kirkland, J. L., Fat depot-specific characteristics are retained in strains derived from single human preadipocytes. *Diabetes* 2006, *55*, 2571-8.

Tchkonia, T.; Lenburg, M.; Thomou, T.; Giorgadze, N.; Frampton, G.; Pirtskhalava, T.; Cartwright, A.; Cartwright, M.; Flanagan, J.; Karagiannides, I.; Gerry, N.; Forse, R. A.; Tchoukalova, Y.; Jensen, M. D.; Pothoulakis, C.; Kirkland, J. L., Identification of depot-specific human fat cell progenitors through distinct expression profiles and developmental gene patterns. *American journal of physiology. Endocrinology and metabolism* 2007, *292*, E298-307.

Tchkonia, T.; Thomou, T.; Zhu, Y.; Karagiannides, I.; Pothoulakis, C.; Jensen, M. D.; Kirkland, J. L., Mechanisms and metabolic implications of regional differences among fat depots. *Cell metabolism* 2013, *17*, 644-56.

Tchoukalova, Y. D.; Koutsari, C.; Votruba, S. B.; Tchkonia, T.; Giorgadze, N.; Thomou, T.; Kirkland, J. L.; Jensen, M. D., Sex- and depot-dependent differences in adipogenesis in normal-weight humans. *Obesity* 2010, *18*, 1875-80.

Tchoukalova, Y. D.; Votruba, S. B.; Tchkonia, T.; Giorgadze, N.; Kirkland, J. L.; Jensen, M. D., Regional differences in cellular mechanisms of adipose tissue gain with overfeeding. *Proceedings of the National Academy of Sciences of the United States of America* 2010, *107*, 18226-31.

Thomson, J. P.; Skene, P. J.; Selfridge, J.; Clouaire, T.; Guy, J.; Webb, S.; Kerr, A. R.; Deaton, A.; Andrews, R.; James, K. D.; Turner, D. J.; Illingworth, R.; Bird, A., CpG islands influence chromatin structure via the CpG-binding protein Cfp1. *Nature* 2010, *464*, 1082-6.

Thur, J.; Rosenberg, K.; Nitsche, D. P.; Pihlajamaa, T.; Ala-Kokko, L.; Heinegard, D.; Paulsson, M.; Maurer, P., Mutations in cartilage oligomeric matrix protein causing pseudoachondroplasia and multiple epiphyseal dysplasia affect binding of calcium and collagen I, II, and IX. *The Journal of biological chemistry* 2001, *276*, 6083-92.

Timchenko, N.; Wilson, D. R.; Taylor, L. R.; Abdelsayed, S.; Wilde, M.; Sawadogo, M.; Darlington, G. J., Autoregulation of the human C/EBP alpha gene by stimulation of upstream stimulatory factor binding. *Molecular and cellular biology* 1995, *15*, 1192-202.

Tomlinson, J. W.; Sinha, B.; Bujalska, I.; Hewison, M.; Stewart, P. M., Expression of 11beta-hydroxysteroid dehydrogenase type 1 in adipose tissue is not increased in human obesity. *The Journal of clinical endocrinology and metabolism* 2002, *87*, 5630-5.

Tontonoz, P.; Hu, E.; Spiegelman, B. M., Stimulation of adipogenesis in fibroblasts by PPAR gamma 2, a lipid-activated transcription factor. *Cell* 1994, *79*, 1147-56.

Tost, J.; Gut, I. G., DNA methylation analysis by pyrosequencing. *Nature protocols* 2007, *2*, 2265-75.

Toth, M. J.; Tchernof, A.; Sites, C. K.; Poehlman, E. T., Effect of menopausal status on body composition and abdominal fat distribution. *International journal of obesity and related metabolic disorders : journal of the International Association for the Study of Obesity* 2000, *24*, 226-31.

Tran, K. V.; Gealekman, O.; Frontini, A.; Zingaretti, M. C.; Morroni, M.; Giordano, A.; Smorlesi, A.; Perugini, J.; De Matteis, R.; Sbarbati, A.; Corvera, S.; Cinti, S., The vascular endothelium of the adipose tissue gives rise to both white and brown fat cells. *Cell metabolism* 2012, *15*, 222-9.

Trayhurn, P., Adipocyte biology. *Obesity reviews : an official journal of the International Association for the Study of Obesity* 2007, *8 Suppl 1*, 41-4.

Vague, J., Sexual differentiation. A determinant factor of the forms of obesity. 1947. *Obesity research* 1996, *4*, 201-3.

Vague, J., The degree of masculine differentiation of obesities: a factor determining predisposition to diabetes, atherosclerosis, gout, and uric calculous disease. 1956. *Nutrition (Burbank, Los Angeles County, Calif.)* 1999, *15*, 89-90; discussion 91.

Van Harmelen, V.; Rohrig, K.; Hauner, H., Comparison of proliferation and differentiation capacity of human adipocyte precursor cells from the omental and subcutaneous adipose tissue depot of obese subjects. *Metabolism: clinical and experimental* 2004, *53*, 632-7.

Wahrenberg, H.; Lonnqvist, F.; Arner, P., Mechanisms underlying regional differences in lipolysis in human adipose tissue. *The Journal of clinical investigation* 1989, *84*, 458-67.

Wang, J.; Thornton, J. C.; Kolesnik, S.; Pierson, R. N., Jr., Anthropometry in body composition. An overview. *Annals of the New York Academy of Sciences* 2000, *904*, 317-26.

Wang, M., Inhibitors of 11beta-hydroxysteroid dehydrogenase type 1 in antidiabetic therapy. *Handbook of experimental pharmacology* 2011, 127-46.

Watt, M. J.; Steinberg, G. R., Regulation and function of triacylglycerol lipases in cellular metabolism. *The Biochemical journal* 2008, *414*, 313-25.

Wells, J. C., Sexual dimorphism of body composition. *Best practice & research. Clinical endocrinology & metabolism* 2007, *21*, 415-30.

Whitlock, G.; Lewington, S.; Sherliker, P.; Clarke, R.; Emberson, J.; Halsey, J.; Qizilbash, N.; Collins, R.; Peto, R., Body-mass index and cause-specific mortality in 900 000 adults: collaborative analyses of 57 prospective studies. *Lancet* 2009, *373*, 1083-96.

Willett, W. C.; Dietz, W. H.; Colditz, G. A., Guidelines for Healthy Weight. *New England Journal of Medicine* 1999, *341*, 427-434.

Wochnik, G. M.; Ruegg, J.; Abel, G. A.; Schmidt, U.; Holsboer, F.; Rein, T., FK506-binding proteins 51 and 52 differentially regulate dynein interaction and nuclear translocation of the glucocorticoid receptor in mammalian cells. *The Journal of biological chemistry* 2005, *280*, 4609-16.

Xi, D.; Gandhi, N.; Lai, M.; Kublaoui, B. M., Ablation of Sim1 neurons causes obesity through hyperphagia and reduced energy expenditure. *PloS one* 2012, *7*, e36453.

Yamamoto, Y.; Gesta, S.; Lee, K. Y.; Tran, T. T.; Saadatirad, P.; Kahn, C. R., Adipose depots possess unique developmental gene signatures. *Obesity* 2010, *18*, 872-8.

Yang, C.; Gagnon, D.; Vachon, P.; Tremblay, A.; Levy, E.; Massie, B.; Michaud, J. L., Adenoviral-mediated modulation of Sim1 expression in the paraventricular nucleus affects food intake. *The Journal of neuroscience : the official journal of the Society for Neuroscience* 2006, *26*, 7116-20.

Yang, N.; Ray, D. W.; Matthews, L. C., Current concepts in glucocorticoid resistance. *Steroids* 2012, *77*, 1041-9.

Yang, Q. Y.; Liang, J. F.; Rogers, C. J.; Zhao, J. X.; Zhu, M. J.; Du, M., Maternal Obesity Induces Epigenetic Modifications to Facilitate Zfp423 Expression and Enhance Adipogenic Differentiation in Fetal Mice. *Diabetes* 2013.

Yekta, S.; Shih, I. H.; Bartel, D. P., MicroRNA-directed cleavage of HOXB8 mRNA. *Science* 2004, *304*, 594-6.

Yim, J. E.; Heshka, S.; Albu, J. B.; Heymsfield, S.; Gallagher, D., Femoral-gluteal subcutaneous and intermuscular adipose tissues have independent and opposing relationships with CVD risk. *Journal of applied physiology (Bethesda, Md. : 1985)* 2008, *104*, 700-7.

Yokomori, N.; Tawata, M.; Onaya, T., DNA demethylation during the differentiation of 3T3-L1 cells affects the expression of the mouse GLUT4 gene. *Diabetes* 1999, *48*, 685-90.

Yokomori, N.; Tawata, M.; Onaya, T., DNA demethylation modulates mouse leptin promoter activity during the differentiation of 3T3-L1 cells. *Diabetologia* 2002, *45*, 140-8.

Yusuf, S.; Hawken, S.; Ounpuu, S.; Bautista, L.; Franzosi, M. G.; Commerford, P.; Lang, C. C.; Rumboldt, Z.; Onen, C. L.; Lisheng, L.; Tanomsup, S.; Wangai, P., Jr.; Razak, F.; Sharma, A. M.; Anand, S. S., Obesity and the risk of myocardial infarction in 27,000 participants from 52 countries: a case-control study. *Lancet* 2005, *366*, 1640-9.

Zehentner, B. K.; Leser, U.; Burtscher, H., BMP-2 and sonic hedgehog have contrary effects on adipocyte-like differentiation of C3H10T1/2 cells. *DNA and cell biology* 2000, *19*, 275-81.

Zhang, Y.; Proenca, R.; Maffei, M.; Barone, M.; Leopold, L.; Friedman, J. M., Positional cloning of the mouse obese gene and its human homologue. *Nature* 1994, *372*, 425-432.

Zhang, J. W.; Klemm, D. J.; Vinson, C.; Lane, M. D., Role of CREB in transcriptional regulation of CCAAT/enhancer-binding protein beta gene during adipogenesis. *The Journal of biological chemistry* 2004, *279*, 4471-8.

Zhang, Q.; Ramlee, M. K.; Brunmeir, R.; Villanueva, C. J.; Halperin, D.; Xu, F., Dynamic and distinct histone modifications modulate the expression of key adipogenesis regulatory genes. *Cell cycle (Georgetown, Tex.)* 2012, *11*, 4310-22.

Zimmermann, R.; Strauss, J. G.; Haemmerle, G.; Schoiswohl, G.; Birner-Gruenberger, R.; Riederer, M.; Lass, A.; Neuberger, G.; Eisenhaber, F.; Hermetter, A.; Zechner, R., Fat mobilization in adipose tissue is promoted by adipose triglyceride lipase. *Science* 2004, *306*, 1383-6.

Zych, J.; Stimamiglio, M. A.; Senegaglia, A. C.; Brofman, P. R.; Dallagiovanna, B.; Goldenberg, S.; Correa, A., The epigenetic modifiers 5-aza-2'-deoxycytidine and trichostatin A influence adipocyte differentiation in human mesenchymal stem cells. *Brazilian journal of medical and biological research = Revista brasileira de pesquisas medicas e biologicas / Sociedade Brasileira de Biofisica ... [et al.]* 2013, *46*, 405-16.

Acknowledgements

I would like to extend my sincerest gratitude to Fredrik Karpe for his continued support and highly useful scientific insight that has helped steer and shape both this MSc project as well as the direction of future work. I am also incredibly grateful for the patience, knowledge, insight, and technical expertise provided by Katherine Pinnick throughout the duration of this project. I greatly anticipate continuing working with these two exceptional individuals during my DPhil project in the near future. I would also like to thank Marijana Todorcevic for performing the background work on the 5-azacytidine experiments, as well as the rest of the Oxlip laboratory for welcoming me into their ranks and making the working environment so tremendously enjoyable. Last but certainly not least, I'd like to thank my parents for their inexhaustible support of my studies which I greatly appreciate.